Receptors and neuronal modulation of circadian rhythm and sleep

By
Jinfei Ni

A dissertation submitted to the Johns Hopkins University in conformity with the requirement of the degree of Doctor of Philosophy

Baltimore, Maryland

April 2017

Abstract

Animal behavior is influenced by external environmental factors as well as internal physiological conditions. Environmental factors are usually detected by the sensory system and the information is further processed in the brain to modulate physiology and behavior. Light is the one of the most critical environmental factors and activates light receptor protein Rhodopsins, which are expressed in classical photoreceptors in the retina as well as other types of cells. Rhodopsin is involved in imaging forming function as well as other non-imaging forming function such as circadian entrainment. While the function of rhodopsin in the retina is well characterized, rhodopsin's function in the central nervous system is underinvestigated. In Chapter 2, we reported an uncharacterized rhodopsin, Rh7, in Drosophila. Rh7 functions as a extra-retina opsin. It is expressed in a subgroup of light sensitive circadian pacemaker neurons in the brain. Rh7 contributes to circadian photoentraiment through its function in the central pacemaker neurons. In chapter 4, we investigated the function of a retinal dehydrogenase (RDHB) in Drosophila vision. RDHB is required for *de novo* synthesis of 11-cis retinal as well as retinoid cycle.

Animal behavior is regulated by multiple neuronal circuits, which are activated by different sensory inputs and internal states. Sleep regulatory neurons in the brain sense internal sleep needs, assess multiple environmental cues and initiate physiological and behavioral processes associated with sleep. A comprehensive understanding of sleep neuronal networks lead to innovative approaches to improve sleep patterns, and recovery from sleep deprivation. In chaper 3, we identified two groups of sleep-promoting

neurons that connect the circadian system to the sleep center in the brain. These neurons use the neurotransmitter glutamate, and the neuropeptide Allatostatin A (AstA). One group of neurons (LPN) are *bona fide* circadian neurons, as they express the clock protein Timeless. Both of these neurons activate the Drosophila sleep center in the brain, the dFSB neurons. dFSB neurons receive inhibitory input from dopaminergic neurons at both dendritic and axonal terminals. The dFSB neurons are inhibitory neurons that down-regulates the activities of arousal neurons.

Acknowledgement

I shall take this opportunity to express my gratitude to my mentors, my colleagues, my friends and my family. Only with their supports and encouragement, it is possible to pursue my Ph.D.

First, I feel grateful for my Ph.D. advisor, Dr. Craig Montell. I joined Craig's lab directly when I joined Biological Chemistry Program at Hopkins in the summer of 2009. Craig bears contagious passion towards science that brings tremendous influence to the young generation, including me. His unique scientific physiology encourages young students think outside of box and pursue questions that interest them. Multiple times during our meeting, we not only discuss about progress of projects and future plans, but also he will pause and talk briefly about the thought process in his mind of why we should pursue the question in a particular manner. He would share with me valuable experiences of grant applications, and practice with me slide by slide when important presentations of mine come up. Last but not least, he mentorship cultivated a friendly, collaborative, progressive scientific community in the lab. It provides a nutritious environment for me to grow. In particular for my wife and me, we learned life-work balance from Craig and Denise. I shall express my thanks to Denise.

I shall also express my warm thanks to professors that served as my committee members. That includes Dr. Jeremy Nathans, Dr. King-Wai Yau, Dr. Mike Caterina and Dr. Xinzhong Dong. Jeremy is an iconic scientist and a great mentor for young scientist.

His class is fun of historical insights and it cultivated my own interest in pursue research questions in a historic perspective. Where is the question come from? How people studied previous? I also attended one of his public lectures about mentorship. The lessons I learned and kept deep in my mind is being proactive in seeking mentorship among all people surround you and understanding the mutual mentor-mentee relationship. I shall suggest anyone read my thesis think these two advises for a second. I enjoyed conversation with Dr. Yau about sensory physiology. He is a tower like figure in sensory transduction and would always bring rigorous discussions that stimulate my thoughts towards a deeper level. Mike and Xinzhong's phenomenal research in mammalian sensory biology stimulated my own interest in exploring this direction. I would also thank Dr. Chris Potter for reading my thesis and valuable advises during our joint labmeetings back in Hopkins.

I also thank faculties and administrations in both Hopkins and UC Santa Barbara. In particular, I thank program directors that recruited me and provide advices all the way to my graduation. In particular, I thank Dr. Natasha Zachara and Dr. Stephen Gould for their patient help to overcome the difficulties during graduation, especially when we are not physically in Baltimore.

I also thank my colleagues and friends in and outside of the Montell labs. Numerous names I would like to apologize not are able to list here. I started a joyful friendship with Dr. Marquis Walker and would last for long. I collaborated with Dr. Xiaoyue Wang, Dr.

Bradley Akitake, Dr. Zhengzheng Li, Dr. Yali Zhang and Dr. Weiwei Liu in the montell lab. I thank Lisa Baik and Dr. Todd Holmes at UCI for collaboration in my thesis project and wish Lisa good luck for her research.

I thank my undergraduate students. Mentoring them is a valuable experience I have. I enjoyed my friendship with Tyler and Ahmed. I am proud of the growing of Tyler as a young scientist and looking forward to their success in the future. Thanks to the mutual mentor-mentee relashition, I learned many from him. I want to thank Ahmed in picking me up at the LAX airport in the middle of night. I would never forget this experience.

Last but not least, I thank my wife for her support both at home and in the lab. I thank our parents for their support and help with the kids. I also thank my daughter Nia and my son Niall for all the joys they bring to us.

Table of contents

List of Figures

Chapter 2

Chapter 3

Chapter 4

Chapter 1: Introduction

1. Rhodopsin and phototransduction

1.1 Rhodopsin as photopigment in the animal kingdom

The majority of animals detect light through the photosensitive Rhodopsin. Functional Rhodopsin is composed of two moieties: a protein component called opsin, which is a prototypical G protein-coupled receptor (GPCR) and the vitamin-A derived retinoid chromophore[1]. In the dark state of mammalian rhodopsin, the chromophore is in the form of 11-cis-retinal. Upon light absorption, a photochemical reaction leads to isomerization of the chromophore (11-cis-retinal is converted to all-trans-retinal), which induces a conformational change of the GPCR[2-4].

The photochemical basis of vision has been demonstrated for almost 100 years. However, the first opsin gene was cloned only about 30 years ago[5-7]. Since then, thousands of opsins have been identified. All of them are thought to originate from a single common ancestor which dates back to *Cnidaria*[1]. Other types of light sensors in bacteria (bacterial rhodopsin) and Archaea (channel-rhodopsin) also use retinal derivatives as a chromophore, and they bear structural similarity to GPCR opsins. However, they rely on intrinsic ion channel or ion pump activities rather than intracellular signaling cascades in order to transmit light information to the cell[8]. Recent advances in the understanding of molecular and structural mechanisms of channel-rhodopsin have provided invaluable tools for optogenetic control of neuronal activity *in vivo*.

Opsins found in multi-cellular organisms are classified into two major groups— C-

opsins and R-opsins—according to the immediacy of their phylogenetic relationship. Furthermore, these two types of opsins are usually restricted separately into one of two distinct types of photoreceptor cells. C-opsins are expressed in ciliary photoreceptor cells while R-opsins are found in rhabdomeric photoreceptor cells[1]. These two types of photoreceptor cells have distinct structural features and signal transduction machineries. Ciliary photoreceptor cells use a cilia-based structure, which connects the two main anatomical units of the photoreceptor cell, the outersegment and innersegment. The outersegment contains all the molecular machinery necessary for phototransduction and is usually made of a corrugated membrane structure of discs membrane. This folding confers a large increase the surface area of photo-capturing tissue which results in tremendous signal amplification—in humans, only a couple of photons are required to stimulate phototransduction. Similar structural principles are used in rhabdomeric photoreceptor cells, in which phototransduction cascades occur in an actin based microvillar structure[2].

1.2 Two types of phototransduction cascades initiated by rhodopsin

Opsins are coupled to heterotrimeric G proteins. C-opsins and R-opsins initiate different signaling cascades downstream of their respective G-proteins. In C-opsin mediated phototransduction, a cyclic-nucleotide-based signaling motif is used to either open or close a cyclic-nucleotide gated ion channel, which results in change of membrane potential[1,9]. In R-opsin mediated phototransduction, the downstream effector of its associated G-protein is a phospholipase C (PLC)[10]. Activation of this phospholipase

C leads to the opening of cation channels belonging to the Transient Receptor Potential (TRP) channel superfamily[11,12]. Here, I provide a more detailed introduction of R-opsin (*Drosophila Melanogaster*) phototransduction mechanism, which is more relevant to the scope of this thesis.

1.3 Molecular mechanism of Drosophila phototranduction

Drosophila phototranduction has been studied for over 40 years and serves as a genetic paradigm for G protein signaling cascades which involve phosphoinositide motifs and TRP channels[2]. The compound eye is the major visual organ in Drosophila. It is composed of around 800 small reiterating basic units named ommatidia. Each ommatidium contains 20 cells, eight of which are photoreceptor cells (R cells). Six photoreceptor cells (R1-R6 cells) are anatomically fixed along the outer radius of the other two, encircling them[2]. Furthermore, these six cells all express the same R-Opsin, rhodopsin 1 (Rh1)[13]. However, the two inner photoreceptor cells (R7 and R8 cells) together express combinations of 4 other rhodopsins in one the following characteristic fashions, in any given ommatidium: Rh3 in R7 and Rh5 in R8 cells respectively or Rh4 in R7 and Rh6 in R8 cells respectively[2,14-16]. Since the outer photoreceptor cells express the same rhodopsin, they convey achromatic visual information to the brain. However, R7 and R8 cells express rhodopsins with different absorption spectrums. Therefore, inner photoreceptor cells provide certain aspects of chromatic visual information to the brain[17].

In principle, outer photoreceptor cells and inner photoreceptor cells employ the

same signaling cascade. Upon photo-isomerization of 11-cis-retinal, activated rhodopsin couples to the heterotrimeric G protein Gq[18], which activates Phospholipase C[10]. A single phospholipase coding gene (*norpA*) is required for phototransduction in the Drosophila compound eye, since in a *norpA* null allele background the photoreceptor cells are completely unresponsive to all types of light stimuli tested[10]. Two TRPC channels, TRP and TRPL are engaged downstream of PLC[11,12,19]. The TRP channel was the first cloned member of a large cation channel superfamily, Transient Receptor Potential channels[20]. Many TRP channels are involved in different modalities of sensory transduction, including vision, taste, olfaction, mechanosensation and temperature sensation[20]. Various models of how PLC activation leads to the opening of TRP and TRPL have been proposed. These include depletion of the inhibitory plasma membrane Phosphatidylinositol 4,5-bisphosphate, metabolites generated downstream of diacylglycerol catabolism, local acidification or mechanical force generated by change of the membrane curvature[21]. However, no consensus model has been agreed upon. One challenge in answering this question comes from the difficulty of expressing both the Rhodopsin and TRP channel, two key components of phototranduction, in heterologous cells[22].

1.4 Metabolism of the retinoid chromophore during de novo rhodopsin synthesis and the visual cycle

Upon light absorption, the chromophore is photo-isomerized from 11-cis-retinal to all-trans retinal. In mammals, the covalent bond between the opsin protein and the retinal

is unstable once the chromophore is photo-isomerized. Thus, all-*trans* retinal is released from rhodopsin upon light activation. Therefore, an enzymatic visual cycle is required for regenerating the 11-*cis* retinal and the functional rhodopsin.

A series of biochemical reactions take place in the rods/cones and the retinal pigment epithelium (RPE) cells to transport all-trans-retinal out of the photoreceptor cells into the RPE for further processing. For example, retinol dehydrogenases (RDHs), which are expressed in the RPE, are a family of short-chain dehydrogenases that play critical roles in the retinoid cycle. Mutations in RDHs cause photoreceptor degeneration.

In Drosophila, rhodopsin is a bistable photopigment. The chromophore is not detached from the protein upon light activation. Therefore, it was thought that an enzymatic visual cycle is dispensable for Drosophila to regenerate functional photopigment. However, long-term exposure to light leads to rhodopsin endocytosis and subsequent chromophore release from the opsin protein upon proteasome-mediated degradation. Under dietary condition that is deficient of retinoid, a visual cycle is required for synthesis new chromophore in adult flies.

1.5 Non-image forming vision is mediated by Rhodopsin

Rhodopsins also mediate phototransduction for non-image forming photoreception/vision. An example of Rhodopsin based non-image forming photoreception is mediated by melanopsin in the mammalian retina[23]. In the mammalian retina there exists a third class of photosensitive neurons that was discovered about 20 years ago. It is a specific class of retinal ganglion cells (RGC). Retinal ganglion cells are the only output neurons from

the retina to the brain. There are many classes of retinal ganglion cells responding to different patterns of light stimuli[23]. Most of them receive light-input from traditional photoreceptor cells, rods and cones, relayed by different groups of interneurons in the retina. However, around 1% of retinal ganglion cells are intrinsically light sensitive (hence the name intrinsically photosensitive RGC, or ipRGCs), due to their endogenous photopigment melanopsin. Melanopsin mediated phototransduction signaling cascades are starkly different from those employed by mammalian rods and cones[9,24,25]. It is more similar to the Drosophila phototransduction cascade in that it activates Phospholipase C beta and leads to the opening of TRP channels[25]. ipRGCs also receive input from rods and cones, although the detailed neuronal circuitry which relays light input from rods and cones to ipRGCs remains unclear[26-28]. ipRGC mediated light sensation accounts for various forms of non-image formation photoreception, including light entrainment of circadian clock, pupillary constriction and even mood regulation[29]. The axons of ipRGC project to brain regions that mediate these functions including: SCN, OPN, dLGN[23,29]. Strikingly, mutations in melanopsin affect but do not completely abolish non-image forming phototransduction, due to indirect light input from rods and cones[27]. However, when animals lose both melanopsin dependent light sensation and rod/cone mediated vision, non-image forming photoreception (including light entrainment of the circadian clock and pupillary constriction) is abolished[27].

Other forms of non-image forming photoreception mediated by rhodopsin have been demonstrated in various forms of photosensitive cells, including the horizontal cells in the retinas of fish, amphibians and birds, the pineal gland of birds and the lizard parietal eye[1].

mRNAs of a few opsins gene were detected in brains, testis, neutrophils and melanocytes. However, the functions of these opsins are not well defined, except for in the melanocytes. UV light activates melanocytes in the human skin through a Rhodopsin-Gq-PLC signaling cascade that opens a transient receptor potential channel called TRPA1. Calcium influx through the TRPA1 channel, together with the release of Calcium from intracellular Calcium store via an IP3R, leads to release of melanin. The photopigment in the melanocytes is retinal dependent, thus two rhodopsins have been proposed to function in the melanocyte: Rhodopsin and Melanopsin. Melanopsin is the logical candidate since it classically couples to a Gq-PLC signaling cascade, while Rhodopsin functions through CNG channels[30,31]. However, it is possible that Rhodopsin in the functions in the melanocyte by coupling to a non-canonical downstream signaling cascade.

2. Cellular and Molecular mechanisms of Circadian Rhythm

2.1 The Circadian system is an endogenous time-keeping machine

An animal's physiology and behavior are orchestrated by an endogenous time-keeping machinery termed circadian rhythm[32,33]. This internal biological clock endows animals to anticipate and adapt to the daily changes in the environment. The temporal compartmentalization of physiology and behavior imparts tremendous advantages in regulating physiology and behaviors that are critical to the animal survival. Many physiological processes such as metabolism, immunity, body temperature regulation and hormonal fluctuation are tightly regulated by internal clock. Circadian system also

regulates animal behavior, such as the sleep-rest cycle, foraging, mating and other complex social behavior[33].

Circadian system synchronizes animal's physiology and behavior to the daily fluctuation of environmental cues. These oscillating environmental signals, call zeitgeber are able set the phase of biological clock. The most dominate zeitgeber on early is the cycling of light/dark. The fluctuation of temperature can also entrain the circadian system. All these cues are cycling at a pace of 24 hours, due to the rotation of the earth. Therefore, circadian system runs at a periodicity appreciates 24 hours.

One important property of the circadian system is its ability to maintain oscillation under constant conditions. This indicates the circadian clock is composed of self-sustaining machinery that can drive recurring physiology and behavior independent of the environmental cues. Nevertheless, the circadian system can adjust its phase when animals are subject to a shifted day-night cycle. Another property of the circadian system is it can anticipate (or predict) the change of the oscillating environments. This allows animals to adjust its physiology for the upcoming challenge of the environment.

The function of the circadian system is organized into three major parts: the core machinery of clock that keeps the time; the input pathway through which the zeitgeber synchronize the core clock machinery and the output pathway that organize the physiology and behavior[34,35]. I will introduce the core molecular machinery of the circadian clock, focused on the Drosophila molecular clocks. However, the molecular clocks operate with similar mechanisms across the animal kingdom.

2.2 Mechanisms of *Drosophila* circadian clocks at molecular level

Molecular mechanisms of biological clocks rely on a handful of core circadian genes, whose expression levels oscillate within a 24 hour periodicity[33]. Although many genes shows oscillating expression, only a couple of them are essential for the function of the time-keeping function of circadian clock. Null mutations in these genes lead to complete disruption of the circadian clock. Genetic and biochemical analysis of these core circadian genes and their products (molecular clocks) in various model animals has uncovered an evolutionarily conserved mechanism of biological timekeeping—multiple coupled transcriptional feedback loops modulated by posttranscriptional modifications to introduce patterned, temporal delay.

In *Drosophila*, the positive arm of the transcriptional feedback loop is a protein heterodimer which functions as a transcriptional activator. It is composed of CLOCK and CYCLE, whose expression levels oscillate[36]. They bind to E-box sequences of target promoters to activate gene transcription. Among all CLOCK/CYCLE targets are core circadian genes such as period and timeless, whose mRNA levels peak during late day. PER and TIM proteins accumulate and dimerize in the cytoplasm early in the night and translocate to the nucleus in the mid-night[37]. TIM/PER proteins can bind CLOCK/CYCLE and inhibit their function [36].

Post-translational modification of PER and TIM introduce a temporal delay between CLOCK/CYCLE transcriptional activation activity and its subsequent repression[33]. This temporal delay is essential for regulating the speed of the biological clock. Multiple phosphorylation sites within PER were discovered in *Drosophila*. The phosphorylation status of these sites is mediated by different protein

kinase/phosphatases, including GSK3b, CK2 PPA2 and PP1 repectively[38,39]. Mutations of these kinase/phosphatases affects both the oscillation periodicity of the molecular clock and the periodicity of behavioral rhythmicity. One mechanism of how phosphorylation affects the periodicity of the molecular clock is based on protein degradation. Phosphorylated PER is subject to ubiquitination by E3 ubiquitin ligase SLIMB. That directly affects the half-life of PER protein and the oscillation of other core circadian genes[40].

2.3 Mechanisms of *Drosophila* circadian neuronal circuitry

Although the time-keeping mechanisms employed by core molecular clocks are largely cell autonomous, circadian rhythm depends on an interconnected neuronal network in the central nervous system[33,34,41]. Neurons that belong to this neuronal network are called central pacemaker neurons. In mammals as well as flies, peripheral organs/tissues also have their own clock. Yet, the central pacemaker neurons are capable of influencing the peripheral clocks. Robust oscillation of circadian genes is observed in these pacemaker neurons. Furthermore, functional disruption of circadian genes in central pacemaker neurons leads to physiological and behavioral arrhythmicity. Therefore, a comprehensive understanding of the circadian neuronal network fills the gap between oscillation of circadian clock genes/proteins and rhythmic physiology and behavior.

In adult *Drosophila*, central pacemaker neurons encompass ~ 150 neurons out of around 250,000 neurons in the brain[34]. A major theme of how these 150 neurons

organize circadian behavior is that distinct subsets of these 150 neurons govern different aspects of circadian behavior. They regulate locomotive activity throughout the day and are uniquely affected by different environmental cues. These 150 neurons are divided into four groups: ventral lateral neurons (s-LNvs and l-LNvs), dorsal lateral neurons (LNds), dorsal neurons (DN1-DN3) and lateral posterior neurons.

The LNvs are the most well-characterized central pacemaker neurons in the adult *Drosophila* brains. They are composed of 4 s-LNvs and 4~5 l-LNvs, both of which express the neuropeptide PIGMENT-DISPERSING FACTOR (PDF)[42]. They have different projection patterns in the brain. The s-LNvs project dorsally towards regions where DN1 neurons are located, while l-LNvs have extensive projections in the optical lobes where visual input is processed before it relays into the central brain. A few downstream neurons of s-LNvs were uncovered, including the DN1 group of pacemaker neurons. Feedback communication from other pacemaker neurons that encroach on s-LNvs have also been demonstrated[43]. Ablation of PDF+LNvs or mutations in the *pdf* gene leads to several defects in circadian locomotion behavior[42]. Under L/D conditions, the morning anticipation peak is reduced and the phase of evening peak is advanced. The same phenotype was observed in PDF receptor (PDFR) mutants. PDFR is expressed in a majority of the pacemaker neurons, allowing them to be regulated by PDF released from LNvs. When pdf and pdfr mutant animals were exposed to constant darkness, the rhythmic behavior dampens quickly[44-46]. This highlights the essential role of PDF signaling in orga nizing the whole central pacemaker network for accurate timekeeping.

2.4 Circadian entrainment and light

Light is the most predominant Zeitgeber for circadian entrainment. *Drosophila* establish diurnal locomotive patterns under a 12-hour light/dark cycle with two peaks during the dawn and dusk termed morning and evening peaks;activity increases penultimate to the transitions between light and dark conditions. Locomotive activities are controlled by internal clocks rather than simply the change of light/dark conditions because animals can anticipate the change of the light/dark condition. These anticipation activities are lost in flies with mutations in genes coding for molecular clocks such as Per and Tim. Moreover, expression of molecular clocks in the central pacemaker neurons begin oscillating once the flies are entrained under a 12-hour light/dark cycle.

Light can also affect the circadian clock once it has been established. *Drosophila* can quickly adjust their locomotive activity pattern to a shifted light/dark cycle[47]. Once entrained by 12-hour light/dark cycle, flies can maintain rhythmic behavior under constant darkness due to the coupled oscillation of internal clocks in central pacemaker neurons. However, if flies are released to constant light conditions after photoentrainment, the rhythmic locomotion is dampened[48].

One of the light sensors for circadian entrainment is cryptochrome[49,50]. Cryptochrome is a member of a large protein family that includes blue light photoreceptors in plants, photolyases involved in DNA repair after photo-damaging and class II CPD (cyclobutane pyrimidine dimers) photolyase in bacteria. Cryptochromes use different photochemical mechanisms from rhodopsin for light sensation. They use Flavin based chromophores and are located in the cytosol instead of the plasma membrane.

Light activation of the Flavin component leads to a conformational change of cryptochome which leads to the exposure of binding domain that recruits other proteins, engendering a protein complex[51]. Cryptochromes in mammals are part of the molecular clock in the central pacemaker neurons and function as a transcriptional factor. However, they have lost their photosensitivity during evolution.

Drosophila cryptochrome is activated by blue light through Flavin as the chromophore. Once activated, cryptochrome interacts with the Per/Tim dimer and leads to the degradation of Timless/Per. Both the mRNA and protein of crytochrome is cycling under the regulation of core clock proteins[33]. The mechanism of cryptochrome light-dependent degradation of Timeless is through the recruitment of an E3 ligase Jetlag[52]. Cryptochrome also mediates light evoked firing of central pacemaker neurons[53]. Activation of pacemaker neurons can also lead to degradation of Timless in a Jetlag independent mechanism that is not fully understood[54]. Cryptochrome mutant flies show defects in multiple types of light mediated circadian responses. However, flies can be entrained by light/dark cycles without Cryptochrome.

Rhodopsin mediated phototransduction also contributes to circadian light entrainment. Yet, the detailed mechanism remains unknown. Mutations that affect compound eye development or phototransduction in the compound eye do not lead to obvious defects in either circadian photoentrainment or other types of circadian photoresponse. Whether or not photoreceptor cells in the compound eye relay optical information to the central pacemaker neurons remains unknown. The adult eyelet, reminiscent of the larval eye bowie organ, indeed project their axons proximal to PDF+

LNvs. It is possible that eyelets communicate with LNvs for circadian photoentrainment[55,56].

3. Regulation of sleep-wake cycle

3.1 Drosophila as a model for sleep-wake cycle

Sleep is a ubiquitous and essential neurological and behavioral phenomena in animal kingdom, yet the mechanism of sleep regulation and sleep function is under-investigated. Sleep is a fundamental physiological process conserved across a diverse range of metazoan animals. Animals spend a large proportion of their life sleeping, which is essential for survival[57]. Deficits in sleep are linked to neurological diseases such as Alzheimer's, Parkinson's, depression, and schizophrenia[58]. Sleep deficits also leads to metabolic disorders[59] and immunologial dysfunction[60].

3.2 Circadian and homeostatic regulation of sleep-wake cycle

Sleep regulatory mechanisms have been described in model organisms, such as Drosophila[57,61] and mice[62] that appear to be conserved in humans[63]. These include dual regulation by the circadian clock, and by homeostatic-drive, which is essential for maintaining appropriate sleep levels. Animal's sleep/wake cycle are regulated by internal biological clock. Animals do not sleep whenever needed. They compartmentalize their sleep behavior in certain time of the day. Defects in clock proteins in human lead to abnormal sleep patterns.

Increased sleep pressure due to deprivation leads to compensatory sleep. In *Drosophila*, a group of neurons project to the dorsal fan-shaped body (dFSB neurons) of the central complex and are proposed to be the effector component of the sleep homeostat[64,65].

3.3 Neuromodulators for sleep regulation in Drosophila

While essential for the survival of the organism, sleep comes with a large trade-off. Other critical behaviors, such as feeding and mating, only take place when animals are awake[66]. Therefore, arousal-promoting neurons stimulate wakefulness. In *Drosophila*, various arousal signals have been identified[67-69] and their functions in promoting wakefulness are conserved in mammals[57]. These include biogenic amines (dopamine and octopamine) and neuropeptides such as Pigment Dispersing Factor (PDF)[70]. Animals transit between wake and sleep states with rapid changes in a host of physiological processes, including sensory processing, motor output, memory consolidation, and metabolism. However, the coordination of sleep-promoting and wake-promoting neuronal circuits, and the key neuronal modulators are poorly understood.

4. Reference

1 Yau, K. W. & Hardie, R. C. Phototransduction motifs and variations. Cell 139, 246-264 (2009).

2 Montell, C. Drosophila visual transduction. Trends Neurosci. 35, 356-363 (2012).

3 Wang, X., Wang, T., Jiao, Y., von Lintig, J. & Montell, C. Requirement for an enzymatic visual cycle in Drosophila. Curr. Biol. 20, 93-102 (2010).

4 Wang, X., Wang, T., Ni, J., Von Lintig, J. & Montell, C. The Drosophila visual cycle and de novo chromophore synthesis depends on rdhB. J. Neurosci. 32, 3485-3491 (2012).

5 Nathans, J. Rhodopsin: structure, function, and genetics. Biochemistry 31, 4923-4931 (1992).

6 Nathans, J., Piantanida, T. P., Eddy, R. L., Shows, T. B. & Hogness, D. S. Molecular genetics of inherited variation in human color vision. Science 232, 203-210 (1986).

7 Nathans, J. & Hogness, D. S. Isolation and nucleotide sequence of the gene encoding human rhodopsin. Proc. Natl. Acad. Sci. USA 81, 4851-4855 (1984).

8 Govorunova, E. G., Sineshchekov, O. A., Janz, R., Liu, X. & Spudich, J. L. NEUROSCIENCE. Natural light-gated anion channels: A family of microbial rhodopsins for advanced optogenetics. Science 349, 647-650 (2015).

9 Fu, Y. & Yau, K. W. Phototransduction in mouse rods and cones. Pflugers Arch. 454, 805-819 (2007).

10 Bloomquist, B. T. et al. Isolation of a putative phospholipase C gene of Drosophila, norpA, and its role in phototransduction. Cell 54, 723-733 (1988).

11 Montell, C. & Rubin, G. M. Molecular characterization of the Drosophila trp locus: a putative integral membrane protein required for phototransduction. Neuron 2, 1313-1323 (1989).

12 Guerini, D., Montell, C. & Klee, C. B. Molecular cloning and characterization of the genes encoding the two subunits of Drosophila melanogaster calcineurin. Journal of Biological Chemistry 267, 22542-22549 (1992).

13 Zuker, C. S., Cowman, A. F. & Rubin, G. M. Isolation and structure of a rhodopsin gene from D. melanogaster. Cell 40, 851-858 (1985).

14 Cowman, A. F., Zuker, C. S. & Rubin, G. M. An opsin gene expressed in only one photoreceptor cell type of the Drosophila eye. Cell 44, 705-710 (1986).

15 Zuker, C. S., Montell, C., Jones, K., Laverty, T. & Rubin, G. M. A rhodopsin gene expressed in photoreceptor cell R7 of the Drosophila eye: homologies with other signal-transducing molecules. J. Neurosci. 7, 1550-1557 (1987).

16 Montell, C., Jones, K., Zuker, C. & Rubin, G. A second opsin gene expressed in the ultraviolet-sensitive R7 photoreceptor cells of Drosophila melanogaster. J. Neurosci. 7, 1558-1566 (1987).

17 Jukam, D., Lidder, P. & Desplan, C. in Visual Transduction and Non-Visual Light Perception (eds J. Tombran-Tink & C. J. Barnstable) Ch. 11, 252-266 (Humana Press, 2008).

18 Scott, K., Becker, A., Sun, Y., Hardy, R. & Zuker, C. Gqα protein function in vivo: genetic dissection of its role in photoreceptor cell physiology. Neuron 15, 919-927 (1995).

19 Niemeyer, B. A., Suzuki, E., Scott, K., Jalink, K. & Zuker, C. S. The Drosophila light-activated conductance is composed of the two channels TRP and TRPL. Cell 85, 651-659 (1996).

20 Venkatachalam, K. & Montell, C. TRP channels. Annu. Rev. Biochem. 76, 387-417 (2007).

21 Hardie, R. C. Photosensitive TRPs. Handb. Exp. Pharmacol. 223, 795-826 (2014).

22 Chen, Z., Chen, H. C. & Montell, C. TRP and rhodopsin transport depends on dual XPORT ER chaperones encoded by an operon. Cell Rep. 13, 573–584 (2015).

23 Hattar, S., Liao, H. W., Takao, M., Berson, D. M. & Yau, K. W. Melanopsin-containing retinal ganglion cells: architecture, projections, and intrinsic photosensitivity. Science 295, 1065-1070 (2002).

24 Do, M. T. & Yau, K. W. Intrinsically photosensitive retinal ganglion cells. Physiol. Rev. 90, 1547-1581 (2010).

25 Xue, T. et al. Melanopsin signalling in mammalian iris and retina. Nature 479, 67-73 (2011).

26 Hattar, S. et al. Melanopsin and rod-cone photoreceptive systems account for all major accessory visual functions in mice. Nature 424, 76-81 (2003).

27 Güler, A. D. et al. Melanopsin cells are the principal conduits for rod-cone input to non-image-forming vision. Nature 453, 102-105 (2008).

28 Walker, M. T. et al. RdgB2 required for dim light input into intrinsically photosensitive retinal ganglion cells. Mol. Biol. Cell 26, 3671-3678 (2015).

29 Schmidt, T. M., Chen, S. K. & Hattar, S. Intrinsically photosensitive retinal ganglion cells: many subtypes, diverse functions. Trends Neurosci. 34, 572-580 (2011).

30 Bellono, N. W., Kammel, L. G., Zimmerman, A. L. & Oancea, E. UV light phototransduction activates transient receptor potential A1 ion channels in human melanocytes. Proc. Natl. Acad. Sci. USA 110, 2383-2388 (2013).

31 Wicks, N. L., Chan, J. W., Najera, J. A., Ciriello, J. M. & Oancea, E. UVA phototransduction drives early melanin synthesis in human melanocytes. Curr Biol 21, 1906-1911 (2011).

32 Mohawk, J. A., Green, C. B. & Takahashi, J. S. Central and peripheral circadian clocks in mammals. Annu. Rev. Neurosci. 35, 445-462 (2012).

33 Allada, R. & Chung, B. Y. Circadian organization of behavior and physiology in Drosophila. Annu. Rev. Physiol. 72, 605-624 (2010).

34 Nitabach, M. N. & Taghert, P. H. Organization of the Drosophila circadian control circuit. Curr. Biol. 18, R84-93 (2008).

35 Helfrich-Förster, C., Nitabach, M. N. & Holmes, T. C. Insect circadian clock outputs. Essays Biochem. 49, 87-101 (2011).

36 Yu, W., Zheng, H., Houl, J. H., Dauwalder, B. & Hardin, P. E. PER-dependent rhythms in CLK phosphorylation and E-box binding regulate circadian transcription. Genes Dev 20, 723-733 (2006).

37 Meyer, P., Saez, L. & Young, M. W. PER-TIM interactions in living Drosophila cells: an interval timer for the circadian clock. Science 311, 226-229 (2006).

38 Kivimae, S., Saez, L. & Young, M. W. Activating PER repressor through a DBT-directed phosphorylation switch. PLoS Biol 6, e183 (2008).

39 Meissner, R. A., Kilman, V. L., Lin, J. M. & Allada, R. TIMELESS is an important mediator of CK2 effects on circadian clock function in vivo. J Neurosci 28, 9732-9740 (2008).

40 Chiu, J. C., Vanselow, J. T., Kramer, A. & Edery, I. The phospho-occupancy of an atypical SLIMB-binding site on PERIOD that is phosphorylated by DOUBLETIME controls the pace of the clock. Genes Dev 22, 1758-1772 (2008).

41 Nitabach, M. N. et al. Electrical hyperexcitation of lateral ventral pacemaker neurons desynchronizes downstream circadian oscillators in the fly circadian circuit and induces multiple behavioral periods. J. Neurosci. 26, 479-489 (2006).

42 Renn, S. C., Park, J. H., Rosbash, M., Hall, J. C. & Taghert, P. H. A pdf neuropeptide gene mutation and ablation of PDF neurons each cause severe abnormalities of behavioral circadian rhythms in Drosophila. Cell 99, 791-802 (1999).

43 Guo, F. et al. Circadian neuron feedback controls the Drosophila sleep--activity profile. Nature 536, 292-297 (2016).

44 Hyun, S. et al. Drosophila GPCR Han is a receptor for the circadian clock neuropeptide PDF. Neuron 48, 267-278 (2005).

45 Lear, B. C. et al. A G protein-coupled receptor, groom-of-PDF, is required for PDF neuron action in circadian behavior. Neuron 48, 221-227 (2005).

46 Mertens, I. et al. PDF receptor signaling in Drosophila contributes to both circadian and geotactic behaviors. Neuron 48, 213-219 (2005).

47 Vinayak, P. et al. Exquisite light sensitivity of Drosophila melanogaster cryptochrome. PLoS. Genet. 9, e1003615 (2013).

48 Emery, P. et al. Drosophila CRY is a deep brain circadian photoreceptor. Neuron 26, 493-504 (2000).

49 Emery, P., Stanewsky, R., Hall, J. C. & Rosbash, M. A unique circadian-rhythm photoreceptor. Nature 404, 456-457 (2000).

50 Emery, P., So, W. V., Kaneko, M., Hall, J. C. & Rosbash, M. CRY, a Drosophila clock and light-regulated cryptochrome, is a major contributor to circadian rhythm resetting and photosensitivity. Cell 95, 669-679 (1998).

51 Okano, S. et al. A putative blue-light receptor from Drosophila melanogaster. Photochem. Photobiol. 69, 108-113 (1999).

52 Koh, K., Zheng, X. & Sehgal, A. JETLAG resets the Drosophila circadian clock by promoting light-induced degradation of TIMELESS. Science 312, 1809-1812 (2006).

53 Fogle, K. J., Parson, K. G., Dahm, N. A. & Holmes, T. C. CRYPTOCHROME is a blue-light sensor that regulates neuronal firing rate. Science 331, 1409-1413 (2011).

54 Guo, F., Cerullo, I., Chen, X. & Rosbash, M. PDF neuron firing phase-shifts key circadian activity neurons in Drosophila. Elife 3, (2014).

55 Malpel, S., Klarsfeld, A. & Rouyer, F. Larval optic nerve and adult extra-retinal photoreceptors sequentially associate with clock neurons during Drosophila brain development. Development 129, 1443-1453 (2002).

56 Sprecher, S. G. & Desplan, C. Switch of rhodopsin expression in terminally differentiated Drosophila sensory neurons. Nature 454, 533-537 (2008).

57 Sehgal, A. & Mignot, E. Genetics of sleep and sleep disorders. Cell 146, 194-207 (2011).

58 Iranzo, A. Sleep in Neurodegenerative Diseases. Sleep Med Clin 11, 1-18 (2016).

59 Tsuneki, H., Sasaoka, T. & Sakurai, T. Sleep Control, GPCRs, and Glucose Metabolism. Trends Endocrinol Metab 27, 633-642 (2016).

60 Westermann, J., Lange, T., Textor, J. & Born, J. System consolidation during sleep - a common principle underlying psychological and immunological memory formation. Trends Neurosci 38, 585-597 (2015).

61 Griffith, L. C. Neuromodulatory control of sleep in Drosophila melanogaster: integration of competing and complementary behaviors. Curr Opin Neurobiol 23, 819-823 (2013).

62 Weber, F. & Dan, Y. Circuit-based interrogation of sleep control. Nature 538, 51-59 (2016).

63 Borbely, A. A. A two process model of sleep regulation. Hum Neurobiol 1, 195-204 (1982).

64 Liu, S., Liu, Q., Tabuchi, M. & Wu, M. N. Sleep Drive Is Encoded by Neural Plastic Changes in a Dedicated Circuit. Cell 165, 1347-1360 (2016).

65 Donlea, J. M., Pimentel, D. & Miesenbock, G. Neuronal machinery of sleep homeostasis in Drosophila. Neuron 81, 860-872 (2014).

66 Crocker, A. & Sehgal, A. Octopamine regulates sleep in drosophila through protein kinase A-dependent mechanisms. J Neurosci 28, 9377-9385 (2008).

67 Crocker, A., Shahidullah, M., Levitan, I. B. & Sehgal, A. Identification of a neural circuit that underlies the effects of octopamine on sleep:wake behavior. Neuron 65, 670-681 (2010).

68 Ueno, T. et al. Identification of a dopamine pathway that regulates sleep and arousal in Drosophila. Nat Neurosci 15, 1516-1523 (2012).

69 Liu, Q., Liu, S., Kodama, L., Driscoll, M. R. & Wu, M. N. Two dopaminergic neurons signal to the dorsal fan-shaped body to promote wakefulness in Drosophila. Curr Biol 22, 2114-2123 (2012).

70 Parisky, K. M. et al. PDF cells are a GABA-responsive wake-promoting component of the Drosophila sleep circuit. Neuron 60, 672-682 (2008).

Chapter 2: A rhodopsin in the brain functions in circadian photoentrainment in Drosophila

(This work in in press on Nature as A rhodopsin in the brain functions in circadian photoentrainment in Drosophila. Jinfei D. Ni, Lisa S. Baik, Todd C. Holmes and Craig Montell*)

Introduction

Animals partition their daily activity rhythms through their internal circadian clocks, which are synchronized robustly by oscillating day-night cycles of light[1,2]. The fruit fly, *Drosophila melanogaster*, senses day/night cycles in part through rhodopsin-dependent light reception in the compound eye, and photoreceptor cells in the Hofbauer-Buchner (H-B) eyelet positioned between the retina and optic lobes[3]. However, a more significant pathway for light entrainment is mediated in central pacemaker neurons. The *Drosophila* circadian clock is extremely light sensitive. However, the only known light sensor in pacemaker neurons is the flavoprotein, cryptochrome (Cry)[4,5], which responds only to high levels of light *in vitro*[6]. These observations indicate the existence of an additional light-sensing pathway in pacemaker neurons[7]. Here, we identified a previously uncharacterized rhodopsin, Rh7, which functions in circadian light entrainment through circadian pacemaker neurons in the central brain. The subset of pacemaker neurons expressed the neuropeptide, pigment-dispersing factor (PDF), and the clock proteins Cry and Period (Per). We performed *in vivo* patch-clamp recordings and found that these

neurons responded to violet light, which was dependent on Rh7. While loss of either *cry* or *rh7* caused minor affects on photoentrainment, the defects in the double mutant were profound. The circadian photoresponse to constant light was impaired in the *rh7* mutant, especially under dim light conditions. The demonstration that Rh7 functions in circadian pacemaker neurons represents the first role for a rhodopsin in the central brain.

Results

Light entrainment of circadian clock in Drosophila

Circadian rhythms regulate a variety of Drosophila behaviors, including sleep, locomotion, feeding patterns, eclosion and reproduction[8,9]. The central pacemaker neurons in the brain that are critical for entraining these behaviors are synchronized to oscillating environmental cues, referred to as Zeitgebers[8,9]. Cry is a light detector in the brain that contributes to phototrainment[4,5]. However, the *cry* mutant still entrains to light/dark (L/D) cycles[4,5]. Therefore, we wondered whether there is another light sensor in the central pacemaker neurons that participates in setting circadian rhythms.

We screened for an additional light sensor that functions in circadian photoentrainment using the Drosophila Activity Monitoring (DAM) system[10,11]. We entrained the flies under light/dark (L/D) cycles for 4 days, switched them to dark-dark (D/D) conditions, and plotted their daily activities. Under these experimental conditions, control animals (w^{1118}) display diurnal activity patterns with two peaks during the dawn and dusk, termed morning and evening peaks (Fig. 1a; note these are double plots). Activity increased before the transitions of the light and dark condition (Fig. 1a). This capacity to anticipate changes in light conditions is one hallmark of the circadian clock[2,9].

Another is the ability to maintain the activity patterns established under L/D cycles, after being transferred to constant darkness (dark/dark; D/D)[11] (Fig. 1a and Extended Data Fig. 1a, h).

Mutation of the gene encoding the light sensor *cry* causes only subtle effects on circadian behavior compared to control flies, when exposed to L/D and D/D cycles (Extended Data Fig. 1a, b, h)[5]. In addition, flies show rhythmic behavior after photoentrainment if they are missing the phospholipase C (PLC) NORPA[4,7] which is required for phototransduction in the compound eye[12], or if they are doubly mutant for *norpA* and *cry* (Extended Data Fig. 1c, d, h)[4,7]. H-B eyelet photoreceptors at the base of the eye are derived from larval Rh5-and Rh6-expressing photoreceptor cells[13] and depend on a phototransduction cascade that couples to Rh6 and the TRPL channel[14-16], but is suggested to be NORPA independent[7]. Flies triply mutant for *rh5, rh6* and *cry* are entrained by L/D cycles (Extended Data Fig. 1e, h)[7]. In addition, flies that are triply mutant for *norpA*, *cry* and *trp*, or for *norpA*, *trpl* and *cry* also established rhythmic behavior (Extended Data Fig. 1f—h). Thus, as previously proposed, there is likely to be an additional light input pathway that impacts on the circadian clock preceding exposure to D/D[7].

Rh7 function as extra-retina photopigment in Drosophila

The Drosophila genome encodes a seventh member of the rhodopsin family, Rh7 (Extended Data Fig. 2a); however, its role is uncharacterized. Rh7 shares 27-30% overall amino acid identities with other rhodopsins in *Drosophila melanogaster*, and is

conserved in other Drosophila species (79-99% identities) as well as in more distantly related Dipteran such as the mosquitoes *Aedes aegypti* and *Anopheles gambiae* (49% and 52% identity, respectively)[17]. Rh7 might function outside of the eye, since all eight of the photoreceptor cells in the fly visual system express one of the six characterized rhodopsins (Extended Data Fig. 2b–c)[18]. Consistent with extra-ocular expression, a mutation (gl^{60j})[19] that eliminates photoreceptor cells in the compound eyes, the H-B eyelet and simple eyes (ocelli) did not reduce *rh7* RNA levels in whole heads (Fig. 1b). In contrast, expression levels of the six other opsins (*rh1-rh6*) were reduced dramatically (Fig. 1b). We also performed RNAseq to compare the number of opsin transcripts in heads from controls and from flies that express a transgene (*GMR-hid*)[20] that eliminates photoreceptor cells in the eyes and H-B eyelet. We found that the numbers of *rh1-rh6* mRNA transcripts were dramatically reduced, while *rh7* transcripts were unchanged (Fig. 1c). Furthermore, we did not detect the Rh7 protein with an Rh7 antibody (see below) in the compound eye (Extended Data Fig. 2b—e). We generated an *rh7* null allele, $rh7^1$, by homologous recombination (Extended Data Fig. 2f—g) and tested their light responses by performing electroretinogram (ERG) recordings. The control and $rh7^1$ ERG responses were similar over a range of light intensities (Extended Data Fig. 2h—j).

To address whether Rh7 is capable of functioning as a light receptor, we expressed Rh7 in R1-R6 photoreceptor cells and tested whether it could substitute for the endogenous rhodopsin, Rh1, which is expressed in six out of the eight photoreceptor cells (R1-6)[21,22]. Indeed, we rescued a wild-type like ERG amplitude and on-off transients, both of which are defective in the *rh1* mutant ($ninaE^{I17}$; Extended Data Fig. 2k—m).

Furthermore, we eliminated the light responses from the remaining two photoreceptor cells (R7 and R8), which express other rhodopsins (Extended Data Fig. 2c), so that we could assess the light response due to Rh7 only. Phototransduction is abolished in all photoreceptor cells in *norpA*^{P24} flies (Fig. 1d, e). We restored a photoresponse exclusively in R1-6 cells of *norpA*^{P24} by expressing a wild-type *norpA* transgene under control of the *rh1* (*ninaE*) promoter (*rh1>norpA*; Fig. 1f). When we genetically eliminated *rh1* (*ninaE*^{I17}) from the *norpA*^{P24};*rh1>norpA* flies, the animals were unresponsive to light (Fig. 1g). Of significance here, we recovered an ERG response in these latter flies by ectopically expressing *rh7* in the R1-6 cells (*rh1>rh7*; Fig.1h). Thus, Rh7 can substitute for Rh1, indicating that Rh7 is a functional light sensor, which is capable of coupling to a Gq/PLC dependent signaling pathway.

To determine the spectral sensitivity of Rh7, we expressed the protein in HEK293T cells. Despite the challenges in functionally expressing most insect rhodopsins *in vitro*, Rh7 largely localized to the cell cortex (Fig. 1i). We found that membranes prepared from Rh7-expressing cells responded to light with a peak at 397 nm (Fig. 1j).

Rh7 function in Drosophila circadian photoentrainment

We raised Rh7 antibodies and found that it stained two groups of cells in the brain (Fig. 2a and Extended Data Fig. 3a, c). The spatial distribution of these cells was indicative of a subset of central pacemakers neurons. The ~150 pacemaker neurons are defined based on expression of Period (Per), one of the core components of the circadian clock[23-25]. These neurons are broadly classified as dorsal and lateral neurons (DNs and LNs), respectively (Extended Data Fig. 3a)[1]. The 15 or 16 LNs include 5-6

dorsal lateral neurons (LNds), 4 to 5 large ventrolateral neurons (l-LNvs), and 4 to 5 small ventrolateral neurons (s-LNvs), which are components of the circadian clock neuronal network[26]. Rh7 and Per were co-expressed in the LNvs (Fig. 2a—c), which also express the neuropeptide, Pigment Disperse Factor (PDF)[27] (Fig. 2d—f). In addition, we detected Rh7-positive neurons in the vicinity of the DN1s (Extended Data Fig. 3a, c), a cluster of clock neurons, roughly half of which express *cry* (Extended Data Fig. 3d, e)[28]. However, the dorsal Rh7-expressing neurons did not co-stain with the *cry* reporter (*cry-Gal4.E13* [4,29]) (Extended Data Fig. 3e). We did not detect Rh7 staining in the brain of the $rh7^{1}$ mutant (Fig. 2g and Extended Data Fig. 3b).

Cry mediates rapid increases in blue light (450 nm peak) evoked action potential firing in Drosophila l-LNvs[30,31], which regulates acute behavioral responses to blue light[32]. Because *rh7* was expressed in the l-LNvs, we compared the electrophysiological responsiveness of these cells to white (400—1000 nm) and violet (405 nm) light in control and $rh7^{1}$ flies. We found that the l-LNv response to white light was attenuated significantly in both cry^{01} and $rh7^{1}$ flies (Fig. 2j). Consistent with the peak spectral sensitivities of Rh7 (Fig. 1j) and Cry[30,33], the l-LNv response to violet light was greatly diminished in both cry^{01} and $rh7^{1}$ flies (Fig. 2k, m, n, o). The control, cry^{01} and $rh7^{1}$ had minimal or no response to orange light (550-1000nm; Fig. 2l).

One way to address the importance of a circadian light receptor to entrainment is to investigate its contribution to circadian phase changes in response to a nighttime light pulse[34]. A light pulse at night shifts the phase of the clock. The direction of the phase shift depends on the time of night that the light stimulation is presented[34-36]. ZT0 and

ZT12 indicate the times that lights are turned on and off, respectively. In control flies, a light pulse early in the night (ZT14-18) leads to a phase delay, while a light pulse late at night (ZT20-22) causes a phase advance (Fig. 3a)[34]. Consistent with previous reports[5,35], cry^{01} flies display severe defects in phase-shifting regardless of when the animals were exposed to the light stimulus (Fig. 3a).

To address a requirement for Rh7 for responding to nighttime light pulses, we exposed $rh7^{1}$ flies to light pulses at various times. We found that the mutant flies showed a normal phase delay response if the stimulus was presented early in the night (ZT14; Fig. 3a; Extended Data Fig. 4). However if the light pulse occurred later, the degree of phase shift was significantly reduced (ZT16-ZT22; Fig. 3a; Extended Data Fig. 4). We performed RNAi-mediated knockdown of *rh7* (*UAS-rh7*^{RNAi}) using a *pdf-Gal4* (Extended Data Fig. 3f—i), and then exposed the flies to light at ZT22. We found that these flies exhibited the same phase advance defect as the $rh7^{1}$ mutant (Fig. 3b), supporting the model that Rh7 is required in PDF-positive neurons for normal photoentrainment.

Phase advances in response to light pulses late at night (ZT22) are correlated with light-induced degradation of Timeless (Tim), one of the core clock proteins that are rapidly degraded upon light exposure[37]. Degradation of Tim depends on binding to Cry[37], or can occur as a consequence of neuronal activation[38]. Since light-induced neuronal firing is reduced in the $rh7^{1}$ brain (Fig. 2j, k, m, o), we reasoned that light-induced degradation of Tim might be impaired. To test this hypothesis, we applied a 5-minute white light pulse at ZT22 and kept the flies in the dark for 55 min. We performed anti-Tim staining on dissected brains, and imaged the signals in PDF-positive neurons (l-LNvs

and s-LNvs; Fig. 3c—f). In control flies, light caused a 4.8-fold decline in Tim protein (Fig. 3c, f). In contrast, in *rh7*^{1} LNvs, the light pulse caused only a slight reduction in anti-Tim staining, which was not statistically significant (Fig. 3d, f). We rescued the defect in *rh7*^{1} with a genomic transgene (Fig. 3e, f).

Another test of a contribution of a gene product to photoentrainment is to assess the number of days required to adjust to a delay in the light-to-dark transition. If control flies are entrained under a L/D cycle, and then the transition from light to darkness is delayed for 8 hours, the animals re-entrain quickly to the new L/D cycle[3] (Fig. 3g, h). The evening peak shifts 7.6 ±0.1 hours on the first day and 7.9 ±0.1 hours on the second day (Fig. 3g). Consistent with a previous study[3], *cry*^{01} flies shifted only 4.6 ±0.2 hours on the first day and 6.5 ±0.1 hours on the second day and required 3 days to establish a stable peak activity (Fig. 3g, i). We found that *rh7*^{1} flies displayed significant delays in the phase shift on both the first and second day (day 1, 6.5 ±0.2 hrs; day 2, 7.1 ±0.1 hrs; Fig. 3g, j). We rescued the phase-shift defect with an *rh7* genomic transgene (Fig. 3g, k). The impairment in the phase-shift exhibited by the *rh7*^{1}*,cry*^{01} double mutant (day 1, 3.1 ±0.2 hrs; day 2, 5.3 ±0.2 hrs) was more severe than *cry*^{01} and *rh7*^{1} single mutant (Fig. 3g, l), consistent with a contribution of *rh7* to photoentrainment.

Exposure to constant light (L/L) leads to arrhythmic circadian behavior in wild-type flies (Fig. 4a, d)[39]. This response is dependent on Cry, as *cry* mutant flies remain rhythmic in constant light[39] (93.1%; Fig. 4d and Extended Data Fig. 5a). Under L/L conditions, 19.0% of *rh7*^{1} flies are also rhythmic, and this phenotype is rescued by a wild-type *rh7* transgene (Fig. 4b—d and Extended Data Fig. 5b).

Because rhodopsin-dependent signaling cascades promote signal amplification and sensitivity to low levels of light, we tested the effects on rhythmicity, after photoentraining the *rh7*^{1} mutant, and then exposing the animals to constant dim light (10 lux). Few control flies maintained rhythmicity even under dim light, while all *cry*^{01} flies were rhythmic (Fig. 4e, h and Extended Data Fig. 5c). However, the majority of *rh7*^{1} flies maintained rhythmicity in the presence of constant dim light exposure (66.7%; Fig. 4f—h). We restored wild-type responses to constant light by introducing an *rh7*$^{+}$ genomic transgene in *rh7*^{1} background (Extended Data Fig. 5d). These data suggest that Rh7 is required for sensitizing the Cry-dependent circadian photoresponse under dim light conditions.

PDF-expressing LNvs function in light-dependent arousal[40,41]. To test if Rh7 plays a role in arousal, we stimulated the flies during their subjective night (ZT22) with a 5-minute white light pulse. “Light-coincident arousal” is the increase in bin-crosses during the 5-minute white light stimulation compared to the 5 minutes before the light was turned on. “Arousal delay” is the time between lights on and when the maximum activity occurred. The *rh7*^{1} flies displayed a decrease in light-coincident arousal (Fig. 4i and Extended Data Fig. 5e) and a much longer arousal delay than the control flies (Extended Data Fig. 5f), which were at least as great as the arousal deficits exhibited by *cry* null flies[30,32] (Fig. 4i and Extended Data Fig. 5e, f). The responses to red light were not impaired significantly in either *rh7*^{1} or *cry*^{01} or *rh7*^{1},*cry*^{01} double mutant flies (Extended Data Fig. 5g). The *rh7*^{1},*cry*^{01} double mutant exhibited a violet light arousal deficit (405 nm; Extended Data Fig. 5h), consistent with the blue and violet absorption spectra of Cry[30,33]

and Rh7. However, we did not observe arousal defects in *rh7*^{1} or *cry*^{01} single mutants (Extended Data Fig. 5h), indicating that these two light sensors compensate for each other during the arousal response.

Synergic interaction between Rh7 and other light sensitive pathway in Circadian rhythm

To test for a potential role of Rh7 for maintaining rhythmic behavior during constant darkness (D/D) following entrainment using a L/D regime, we exposed the *rh7*^{1} flies to cycles of white light. The mutant flies showed rhythmic diurnal and circadian behavior similar to the wild-type control (Fig. 4j, k, p). As previously shown[3], *cry*^{b} mutant flies also photoentrained and exhibited rhythmic diurnal and circadian behavior (Fig. 4l, p). However, *rh7*^{1},*cry*^{b} double mutants had profound deficits in rhythmic diurnal and circadian behavior. 37.2% of the *rh7*^{1},*cry*^{b} animals were arrhythmic (Fig. 4m, p). This is possibly due to insufficient synchronization of the molecular clock between different groups of central pacemaker neurons, in the absence of both light sensors intrinsic to these cells. The remaining rhythmic flies displayed periodicity during the D/D cycles that was much longer than control flies (control, 23.8 ±0.08 hrs; *rh7*^{1},*cry*^{b}, 27.3 ±0.07 hrs, $p<0.01$; Fig. 4j, n). The *rh7*^{1},*cry*^{01} double mutants displayed similar impairments (Extended Data Fig. 6a—c). Thus, at least one of the two light receptors in central pacemaker neurons is required for rhythmic behavior. We rescued these defects with a wild-type *rh7* genomic transgene (Fig. 4o, p).

While *gl*^{60j}, *rh7*^{1} and *cry* single mutants display photoentrainment impairments[3], they are capable of circadian rhythmicity. Thus, any two of these three photoreceptors (Cry,

Rh7 and *gl*-dependent) are sufficient for rhythmic circadian behavior. However, Rh7 is insufficient on its own since gl^{60j},cry^{b} *flies* are circadian blind[3]. To test whether *cry* alone is sufficient for rhythmic behavior, we subjected the $rh7^{1}$,gl^{60j} double mutant to a L/D regime followed by constant darkness, and found that 25% were arrhythmic (Extended Data Fig. 6d—h). Thus, while Cry alone cannot preserve fully wild-type circadian behavior, it alone enables flies to maintain greater rhythmicity than either Rh7 on its own, or the just the *gl* photoreceptor cells. In addition, we subjected the $rh7^{1}$,gl^{60j} flies to a 5-minute light pulse at ZT22 to test their circadian phase-response. While the $rh7^{1}$ and gl^{60j} single mutants showed a decreased phase-advance relative to the control, the $rh7^{1}$,gl^{60j} double mutant displayed a greater impairment (Extended Data Fig. 6i). Since the cry^{01} mutant also showed defects in phase-response in response to a 5-minute light pulse (Fig. 3a), multiple light input pathways contribute to circadian light sensation.

To test whether *rh7* functioned in LNvs neurons, we performed phenotypic rescue experiments. We found that expression of *rh7* (*UAS-rh7*) using either the *tim-GAL4* or an LNv-specific driver, *pdf-GAL4*, rescued the increase in arrhythmicity exhibited by $rh7^{1}$,cry^{b} flies (Extended Data Fig. 7). Introduction of other rhodopsins (*rh3*, *rh4* and *rh5*) in *pdf*-positive cry^{b},$rh7^{1}$ neurons flies, also restored normal rhythmicity and (Extended Data Fig. 8), further supporting a rhodopsin-based mechanism for circadian function in LNvs.

In s-LNvs and l-LNvs from control animals, Per protein peaks during dawn (ZT22 to ZT2) and enters a trough during the rest of the day until the middle of the night (Extended Data Fig. 9a; Extended Data Fig. 10, a—b)[42]. In the $rh7^{1}$ mutant, Per also

displayed oscillations in LNv neurons,(Extended Data Fig. 9b; Extended Data Fig. 10, c—d), consistent with the observation that *rh7*^{1} flies establish rhythmic behavior under L/D cycles. However, Per peaked earlier in *rh7*^{1} (ZT18—ZT22) than controls (ZT2). Per oscillations in LNvs are altered in *cry*^{b} flies[5]. There is a delayed trough and peak in s-LNVs, and a large reduction in oscillation amplitude in l-LNVs (Extended Data Fig. 9c; Extended Data Fig. 10, e—f). In *rh7*^{1},*cry*^{b} animals, Per levels remained high throughout the day in s-LNvs (ZT2 to ZT14; Extended Data Fig. 9d; Extended Data Fig. 10g). In l-LNvs of *rh7*^{1},*cry*^{b} animals, Per peaked shortly after dusk (ZT14; Extended Data Fig. 10h). PDF did not oscillate in the LNv cell bodies during the circadian cycle[43], and no differences in PDF levels in the LNv cell bodies were seen between the wild-type control and *rh7*^{1} (Extended Data Fig. 9)[44].

The rhodopsins in the compound eye signal through the PLC encoded by *norpA*[12,18]. However, *norpA* and *cry* double mutant flies exhibit normal rhythmicity during the constant darkness following a L/D regime[7] (Extended Data Fig. 1d, h), indicating that Rh7 signaling in LNvs is not coupled to NORPA. To address if the second fly PLCβ (PLC21C)[45] functioned in PDF neurons, we used two *UAS-plc21C-RNAi* lines (Extended Data Fig. 11a) to perform RNAi knock down. We combined the RNAi lines with the *pdf-Gal4*, and then exposed the flies to a white-light pulse for 5 minutes at ZT22. We found that knockdown of *plc21C* caused reductions in phase-advance at ZT22 (Extended Data Fig. 11b), similar to *rh7*^{1} mutant flies (Fig. 3a).

In summary, our work establishes a functional role for a rhodopsin in the central brain. Rh7 is strategically expressed in the PDF-positive cells, which appear to be master light

input clock neurons that also receive input from the optical lobes[40]. The fact that PDF-positive neurons express two spectrally distinct light sensors (Rh7 and Cry) highlights their key role in circadian photoentrainment. In the mammalian retina, ~1% of the retinal ganglion cells are intrinsically photosenstive (ipRGCs), and function in circadian entrainment[46,47]. These ipRGCs are not only directly light sensitive due to expression of melanopsin, which is similar to Drosophila rhodopsins, but also receive light-induced information from rod and cone photoreceptor cells[48]. The striking similarities between Drosophila PDF-positive neurons and ipRGCs indicate a common strategy for circadian photoentrainment. Opsins are also expressed in the mammalian brain, although their functions are unknown[49-51]. Because light has been proposed to penetrate the mammalian skull[52-55], our findings raise questions as whether neurons in the mammalian brain also sense light and contribute to photoentrainment of circadian rhythms.

References

1 Nitabach, M. N. & Taghert, P. H. Organization of the *Drosophila* circadian control circuit. *Curr. Biol.* **18**, R84-93 (2008).

2 Mohawk, J. A., Green, C. B. & Takahashi, J. S. Central and peripheral circadian clocks in mammals. *Annu. Rev. Neurosci.* **35**, 445-462 (2012).

3 Helfrich-Förster, C., Winter, C., Hofbauer, A., Hall, J. C. & Stanewsky, R. The circadian clock of fruit flies is blind after elimination of all known photoreceptors. *Neuron* **30**, 249-261 (2001).

4 Emery, P. *et al. Drosophila* CRY is a deep brain circadian photoreceptor. *Neuron* **26**, 493-504 (2000).

5 Stanewsky, R. *et al.* The *cry*^{b} mutation identifies cryptochrome as a circadian photoreceptor in *Drosophila*. *Cell* **95**, 681-692 (1998).

6 Ozturk, N., Selby, C. P., Annayev, Y., Zhong, D. & Sancar, A. Reaction mechanism of *Drosophila* cryptochrome. *Proc. Natl. Acad. Sci. USA* **108**, 516-521 (2011).

7 Szular, J. *et al. Rhodopsin 5*- and *Rhodopsin 6*-mediated clock synchronization in *Drosophila melanogaster* is independent of retinal phospholipase C-**ß** signaling. *J. Biol. Rhythms.* **27**, 25-36 (2012).

8 Helfrich-Förster, C., Nitabach, M. N. & Holmes, T. C. Insect circadian clock outputs. *Essays Biochem.* **49**, 87-101 (2011).

9 Allada, R. & Chung, B. Y. Circadian organization of behavior and physiology in *Drosophila*. *Annu. Rev. Physiol.* **72**, 605-624 (2010).

10 Lee, Y. & Montell, C. *Drosophila* TRPA1 functions in temperature control of circadian rhythm in pacemaker neurons. *J. Neurosci.* **33**, 6716-6725 (2013).

11 Chiu, J. C., Low, K. H., Pike, D. H., Yildirim, E. & Edery, I. Assaying locomotor activity to study circadian rhythms and sleep parameters in *Drosophila*. *J. Vis. Exp.*, (2010).

12 Bloomquist, B. T. *et al.* Isolation of a putative phospholipase C gene of Drosophila, *norpA*, and its role in phototransduction. *Cell* **54**, 723-733 (1988).

13 Sprecher, S. G. & Desplan, C. Switch of *rhodopsin* expression in terminally differentiated *Drosophila* sensory neurons. *Nature* **454**, 533-537 (2008).

14 Helfrich-Förster, C. *et al.* The extraretinal eyelet of *Drosophila*: development, ultrastructure, and putative circadian function. *J. Neurosci.* **22**, 9255-9266 (2002).

15 Malpel, S., Klarsfeld, A. & Rouyer, F. Larval optic nerve and adult extra-retinal photoreceptors sequentially associate with clock neurons during *Drosophila* brain development. *Development* **129**, 1443-1453 (2002).

16 Yasuyama, K. & Meinertzhagen, I. A. Extraretinal photoreceptors at the compound eye's posterior margin in *Drosophila melanogaster*. *J. Comp. Neurol.* **412**, 193-202 (1999).

17 Senthilan, P. R. & Helfrich-Förster, C. Rhodopsin 7-The unusual Rhodopsin in Drosophila. *PeerJ* **4**, e2427 (2016).

18 Montell, C. *Drosophila* visual transduction. *Trends. Neurosci.* **35**, 356-363 (2012).

19 Moses, K., Ellis, M. C. & Rubin, G. M. The *glass* gene encodes a zinc-finger protein required by *Drosophila* photoreceptor cells. *Nature* **340**, 531-536 (1989).

20 Grether, M. E., Abrams, J. M., Agapite, J., White, K. & Steller, H. The *head involution defective* gene of *Drosophila melanogaster* functions in programmed cell death. *Genes Dev.* **9**, 1694-1708 (1995).

21 O'Tousa, J. E. *et al.* The Drosophila *ninaE* gene encodes an opsin. *Cell* **40**, 839-850 (1985).

22 Zuker, C. S., Cowman, A. F. & Rubin, G. M. Isolation and structure of a rhodopsin gene from D. melanogaster. *Cell* **40**, 851-858 (1985).

23 Zerr, D. M., Hall, J. C., Rosbash, M. & Siwicki, K. K. Circadian fluctuations of *period* protein immunoreactivity in the CNS and the visual system of *Drosophila*. *J. Neurosci.* **10**, 2749-2762 (1990).

24 Kaneko, M. & Hall, J. C. Neuroanatomy of cells expressing clock genes in

Drosophila: transgenic manipulation of the *period* and *timeless* genes to mark the perikarya of circadian pacemaker neurons and their projections. *J. Comp. Neurol.* **422**, 66-94 (2000).

25 Konopka, R. J. & Benzer, S. Clock mutants of *Drosophila melanogaster*. *Proc. Natl. Acad. Sci. USA* **68**, 2112-2116 (1971).

26 Helfrich-Förster, C. Robust circadian rhythmicity of *Drosophila melanogaster* requires the presence of lateral neurons: a brain-behavioral study of *disconnected* mutants. *J. Comp. Physiol. A* **182**, 435-453 (1998).

27 Renn, S. C., Park, J. H., Rosbash, M., Hall, J. C. & Taghert, P. H. A *pdf* neuropeptide gene mutation and ablation of PDF neurons each cause severe abnormalities of behavioral circadian rhythms in *Drosophila*. *Cell* **99**, 791-802 (1999).

28 Yoshii, T., Todo, T., Wulbeck, C., Stanewsky, R. & Helfrich-Förster, C. Cryptochrome is present in the compound eyes and a subset of *Drosophila*'s clock neurons. *J. Comp. Neurol.* **508**, 952-966 (2008).

29 Helfrich-Förster, C. *et al.* Development and morphology of the clock-gene-expressing lateral neurons of *Drosophila melanogaster*. *J. Comp. Neurol.* **500**, 47-70 (2007).

30 Fogle, K. J., Parson, K. G., Dahm, N. A. & Holmes, T. C. CRYPTOCHROME is a blue-light sensor that regulates neuronal firing rate. *Science* **331**, 1409-1413 (2011).

31 Sheeba, V., Gu, H., Sharma, V. K., O'Dowd, D. K. & Holmes, T. C. Circadian- and light-dependent regulation of resting membrane potential and spontaneous action

potential firing of *Drosophila* circadian pacemaker neurons. *J. Neurophysiol.* **99**, 976-988 (2008).

32 Fogle, K. J. *et al.* CRYPTOCHROME-mediated phototransduction by modulation of the potassium ion channel ß-subunit redox sensor. *Proc. Natl. Acad. Sci. USA* **112**, 2245-2250 (2015).

33 Okano, S. *et al.* A putative blue-light receptor from *Drosophila melanogaster*. *Photochem. Photobiol.* **69**, 108-113 (1999).

34 Dushay, M. S. *et al.* Phenotypic and genetic analysis of *Clock*, a new circadian rhythm mutant in *Drosophila melanogaster*. *Genetics* **125**, 557-578 (1990).

35 Kistenpfennig, C., Hirsh, J., Yoshii, T. & Helfrich-Förster, C. Phase-shifting the fruit fly clock without cryptochrome. *J. Biol. Rhythms.* **27**, 117-125 (2012).

36 Vinayak, P. *et al.* Exquisite light sensitivity of *Drosophila melanogaster* cryptochrome. *PLoS. Genet.* **9**, e1003615 (2013).

37 Koh, K., Zheng, X. & Sehgal, A. JETLAG resets the *Drosophila* circadian clock by promoting light-induced degradation of TIMELESS. *Science* **312**, 1809-1812 (2006).

38 Guo, F., Cerullo, I., Chen, X. & Rosbash, M. PDF neuron firing phase-shifts key circadian activity neurons in *Drosophila*. *Elife* **3**, (2014).

39 Emery, P., Stanewsky, R., Hall, J. C. & Rosbash, M. A unique circadian-rhythm photoreceptor. *Nature* **404**, 456-457 (2000).

40 Sheeba, V. *et al.* Large ventral lateral neurons modulate arousal and sleep in *Drosophila*. *Curr. Biol.* **18**, 1537-1545 (2008).

41 Shang, Y., Griffith, L. C. & Rosbash, M. Light-arousal and circadian photoreception

circuits intersect at the large PDF cells of the *Drosophila* brain. *Proc. Natl. Acad. Sci. USA* **105**, 19587-19594 (2008).

42 Siwicki, K. K., Eastman, C., Petersen, G., Rosbash, M. & Hall, J. C. Antibodies to the *period* gene product of Drosophila reveal diverse tissue distribution and rhythmic changes in the visual system. *Neuron* **1**, 141-150 (1988).

43 Nitabach, M. N. *et al.* Electrical hyperexcitation of lateral ventral pacemaker neurons desynchronizes downstream circadian oscillators in the fly circadian circuit and induces multiple behavioral periods. *J. Neurosci.* **26**, 479-489 (2006).

44 Park, J. H. *et al.* Differential regulation of circadian pacemaker output by separate clock genes in *Drosophila*. *Proc. Natl. Acad. Sci. USA* **97**, 3608-3613 (2000).

45 Shortridge, R. D. *et al.* A *Drosophila* phospholipase C gene that is expressed in the central nervous system. *J. Biol. Chem.* **266**, 12474-12480 (1991).

46 Hattar, S., Liao, H. W., Takao, M., Berson, D. M. & Yau, K. W. Melanopsin-containing retinal ganglion cells: architecture, projections, and intrinsic photosensitivity. *Science* **295**, 1065-1070 (2002).

47 Berson, D. M., Dunn, F. A. & Takao, M. Phototransduction by retinal ganglion cells that set the circadian clock. *Science* **295**, 1070-1073 (2002).

48 Güler, A. D. *et al.* Melanopsin cells are the principal conduits for rod-cone input to non-image-forming vision. *Nature* **453**, 102-105 (2008).

49 Blackshaw, S. & Snyder, S. H. Encephalopsin: a novel mammalian extraretinal opsin discretely localized in the brain. *J. Neurosci.* **19**, 3681-3690 (1999).

50 Nissilä, J. *et al.* Encephalopsin (OPN3) protein abundance in the adult mouse brain.

J. Comp. Physiol. A Neuroethol. Sens. Neural Behav. Physiol. **198**, 833-839 (2012).

51 Nissilä, J. S. *et al.* The distribution of melanopsin (OPN4) protein in the human brain. *Chronobiol. Int.*, 1-8 (2016).

52 Flyktman, A., Manttari, S., Nissila, J., Timonen, M. & Saarela, S. Transcranial light affects plasma monoamine levels and expression of brain encephalopsin in the mouse. *J Exp Biol* **218**, 1521-1526 (2015).

53 Sun, L. *et al.* Human brain reacts to transcranial extraocular light. *PLoS One* **11**, e0149525 (2016).

54 Vandewalle, G., Maquet, P. & Dijk, D. J. Light as a modulator of cognitive brain function. *Trends Cogn Sci* **13**, 429-438 (2009).

55 Wade, P. D., Taylor, J. & Siekevitz, P. Mammalian cerebral cortical tissue responds to low-intensity visible light. *Proc Natl Acad Sci U S A* **85**, 9322-9326 (1988).

Methods

No statistical methods were used to predetermine sample sizes. All behavior data were collected in a random manner. No blinding method was used in assessing experimental outcomes.

Fly stocks

The following flies were obtained from Bloomington Stock Center: isogenized w^{1118} (BL5905), $norpA^{P24}$ (BL9048), *ninaE-norpA* (BL52276), *ninaE-Gal4* (BL8691), trp^{MB} (BL23636), $trpl^{MB}$ (BL29314), *UAS-mcherry-NLS* (BL38425), gl^{60j} (BL 509), *pdf-Gal4* (BL6900), and two *plc21C* RNAi lines (01210, BL 31269 and 01211, BL31270). *GMR-hid*

was obtained from the Drosophila Genetic Resource Center, Kyoto (108419). We used the w^{1118} as the control strain. The *rh7* RNAi line (v1478) was from VDRC Stock Center. The *tim-Gal4* [1] was provided by A. Sehgal (University of Pennsylvania). The *cry-Gal4.E13* [2] was from M. Rosbash (Brandeis University). The cry^{b} [2] and cry^{01} [3] flies were provided by Mark Wu (The Johns Hopkins University School of Medicine) and the $rh5^{02}$ [4], $rh6^{01}$ [5], *UAS-rh3* [5], *UAS-rh4* [5] and *UAS-rh5* [5] lines were provided by C. Desplan (New York University). We also used $ninaE^{I17}$ flies[6].

Cloning of the *rh7* cDNA and generation of transgenic flies

To clone the *rh7* coding region, we prepared mRNA from w^{1118} heads, performed RT-PCR using the following primers, and cloned the cDNA into TOPO vector (pCR2.1-TOPO, Invitrogen): *rh7* forward, GCGGCCGCCACCATGGAGGCCATCATCATGACG; *rh7* reverse, GCGGCCGCTCAGAACTTACTCTGTTCCATGAC. To generate the *UAS-rh7* transgene, we subcloned the *rh7* open reading frame into the NotI site of the pUAST vector.

To generate transgenic flies expressing a Rh7::FLAG fusion protein, we first constructed the pUAST-FLAG vector using the following two oligonucleotides, which we annealed and cloned into the XhoI and XbaI site of the pUAST vector: FLAG5'-XbaI, TCGAGGGGATTACAAGGATGACGACGATAAGTAAT and FLAG3'-XhoI, CTAGATTACTTATCGTCGTCATCCTTGTAATCCCC. We amplified the *rh7* coding region using the same forward primer as above, in conjunction with the following reverse primer to eliminate the stop codon: *rh7* reverse$^{no\text{-}stop}$, GCGGCCGCGAACTTACTCTGTTCCATGAC. Both the *UAS-rh7* and *UAS-rh7-FLAG*

transgenic flies were obtained by germline transformation using w^{1118} embryos (Bestgene Inc.).

To generate flies expressing a $rh7^{+}$ genomic transgene (P[$rh7^{+}$]), a BAC genomic DNA clone (CH322180G19) was obtained from the P[*acman*] collection[7]. The germline transformation took advantage of site-specific integration using the Φ31-attB/attP system (Bestgene Inc).

We produced the plasmid for knocking out *rh7* by ends-out homologous recombination[8] as follows. We PCR amplified two homologous arms (left, 3.2 kb and right, 3.3 kb) using the following primers: left arm forward, AATTGCTGGGATCCCTCAATTGGCCTAATCGGTTTCTG; left arm reverse, AATTGCTGGGTACCGACTGACTTGGCCAAATATTTACG; right arm forward, AATGCTGGCGGCCGCTTAAAATGCTGCCCGAGACT; right arm reverse, AATTGCTGGCGGCCGCTGGCTTATGAAGTTGCAAAAAG. We cloned the two arms into the targeting vector, pw35*loxp-Gal4*. This construct was designed to delete 540 bp 3' to the *rh7* translational start site, and was replaced with a cassette containing the mini-*white* marker and *Gal4* flanked by two *loxP* sites. The upstream *loxP* sequence contained a translational start site that rendered the *Gal4* coding region out of frame. Consequently, the Gal4 is not functional. To obtain the donor lines for generating the *rh7* knockout ($rh7^{1}$ allele), the targeting vector was injected into w^{1118} embryos (Bestgene Inc.). We mobilized the donor insertion by crossing the donor line to *y,w;P*[*70FLP*]*11* P[*70I-SceI*]*2B* noc^{Sco}/CyO flies (from the Bloomington Stock Center, BL6934). The progeny were screened for gene targeting in the *rh7* locus by PCR using two pairs of primers. The first pair (P1 and P2) were the following two primers that annealed to the

first and second coding exons, and produced a DNA product (790 bp) only in wild-type (Extended Data Fig. 32g): P1, CTCTCGCTCTCCGAGATGTT and P2, ACCACCGAAATCAGGCAATA. The following second pair of primers (P3 and P4) annealed to the *mini-white* gene and to a sequence 3' to *rh7*, and therefore only generated a product in the $rh7^{1}$ mutant (4.4 kb; Extended Data Fig. 2g): P3, TGTACATAAAAGCGAACCGAACCT and P4, ACTGTGCGACAGAGTGAGAGAGCAATAGTA.

After generating $rh7^{1}$, we outcrossed the flies to the control stain (w^{1118}) for five generations. To confirm that the key fly lines did not harbor the tim^{ls}, jet^{c} or per^{slih} mutations in the genetic background, we performed DNA sequencing. We extracted genomic DNA from adult flies, and amplified the relevant regions in the *tim*, *jet* and *per* genes by PCR (Phusion High-Fidelity DNA Polymerase, NEB) using the following primers: 1) *per*: forward, GTCCACACACAACACCAAGG; reverse, TTGATGATCATGTCGCTGCT. 2) *tim*: forward, TGGCTGGGGATTGAAAATAA; reverse, TTACAGATACCGCGCAAATG, and 3) *jet*: forward, AGCCGATCATAGTGGAGTGC; reverse, AAGGCACGCACAGGTTTACT. We purified the PCR products and subjected them to DNA sequencing (DNA sequencing facility at University of California, Berkeley).

Quantitative RT-PCR of *plc21c* RNAi knockdown

To knock-down *plc21C* expression, we combined each *UAS-plc21C* RNAi transgene (01210 and 01211) with *UAS-Dicer2*;;*actin-Gal4*. To quantify the efficacy of the RNAi, we extracted total RNA from 10 adult flies (5 males and 5 females), and used 1 μg of total RNA from each sample as a temperate for reverse transcription using SuperScript™ III

Reverse Transcriptase (ThermoFisher, cat. 18080093). Oligo dT primers were used for cDNA synthesis. cDNA preparation was subjected to quantitative PCR (Roche, LightCycler 480 system) according to the LightCycler 480 SYBR Green 1 Master Mix (cat. 04707516001) protocol. The *plc21C* primers used were: forward, GGATCTCTCCAAGTCGTTCG; reverse, TAGCCGCTTCACCAGCTTAT. The *rp49* primers were: forward, GACGCTTCAAGGGACAGTATCTG; reverse, AAACGCGGTTCTGCATGAG. In each reaction, we normalized expression of *plc21C* transcripts to *rp49*.

Antibody generation

To obtain Rh7 antibodies, we generated a GST-Rh7 fusion protein by subcloning the region encoding the N-terminal 80 amino acids into the pGEX6P vector. We expressed the fusion protein in *E. coli* (BL21), purified the recombinant protein using glutathione Sepharose beads (GE Healthcare Life Science) and generated antiserum in a rabbit (Covance). We affinity purified the antibodies by conjugating the antigen to Affi-Gel 10 (Bio-Rad).

Immunohistochemistry

We performed immunohistochemistry using whole mount fly brains as described previously[9]. Briefly, we fixed dissected brains for 15—20 min at 4°C in 4% paraformaldehyde in phosphate buffer (0.1 M Na_3PO_4, pH 7.4) with 0.3% Triton-X100 (Sigma), hereafter referred to as PBT. The brains were blocked with 5% normal goat serum (Sigma) in phosphate buffer for 1 hr at 4°C. We then incubated the tissue with primary antibodies at 4°C for ≥24 hrs. After three washes in PBT, the brains were

incubated overnight at 4°C with the following secondary antibodies from Life Technologies: anti-mouse Alexa Fluor 488 or 568 Dyes, anti-rabbit Alexa Fluor 488 or 568 Dyes or AlexA dyes. The brains were washed three times with PBT and mounted in VECTASHIELD mounting medium (Vector Labs) for imaging. For Rh7 and PDF co-staining (Fig. 2d-i), four brains were examined.

To perform staining with anti-Per and anti-Tim, we handled the flies under a red photographic safety light. We prefixed whole flies at 4°C with 4% paraformaldehyde in PBT for 45 min before dissecting out the brains. We used the following primary antibodies: anti-Rh7 (1:250, rabbit), anti-Per (1:1000, guinea pig), anti-Tim (1:1000, rat)[10], anti-PDF (1:1000, c7 mouse monoclonal antibody from the Developmental Studies Hybridoma Bank), anti-dsRed (1: 500, mouse, Clontech Catalog # 632392). The Per and Tim antibodies were contributed by A. Sehgal. The secondary antibodies (Life Technologies) were anti-rat AlexA Fluor 568 Dye and anti-guinea pig AlexA Fluor 555 Dye. We acquired the images using a Zeiss LSM 700 confocal microscope.

To perform whole-mount staining of the retina, we dissected the retina (within the eye cup) and fixed the tissue at 4°C in 4% paraformaldehyde in PBT for 20 minutes. After washing briefly in PBT, we blocked the retina for 1 hr in PBT plus with 5% normal goat serum. We used the following primary antibodies: anti-Rh7 (1:250, rabbit), anti-Rh3 (1:200, mouse, gift from S. Britt, University of Colorado, Denver) and anti-Rh5 (1:200, mouse, gift from S. Britt, University of Colorado, Denver). The secondary antibodies were: anti-rabbit AlexA Fluor 568 Dye (1:1000) and anti-mouse AlexA Fluor 488 Dye (1:1000).

Circadian behavior

Circadian experiments were performed at 25°C using the Drosophila Activity Monitoring (DAM) System (Trikinetics). Three to seven-day-old male flies were loaded into monitoring tubes, which contained 1% agarose (Invitrogen) and 5% sucrose (Sigma) as the food source. The flies were entrained to 12-hr light/12-hr dark cycles for four days and released to constant darkness or constant light (10 lux for dim light condition and 400 lux for bright light condition) for at least seven days to measure the periodicities.

To assay the effects of time shifts, we first entrained the flies for 4 days under 12-hr light/12-hr dark cycles (~600 lux LED white light). For performing light-induced time-shift experiments, we exposed flies at ZT14, ZT16, ZT18, ZT20 or ZT22 to a single 5-min light pulse (LED white light, ~600 Lux), and then maintained the flies under constant darkness. To conduct the phase delay experiments, we first entrained the flies for 4 days under 12-hr light/12-hr dark cycles (~400 lux LED white light). To obtain a phase delay of 8 hrs, on day 5 we extended the light phase to 20 hrs, and then returned the flies to normal 12-hr dark/12-hr light cycles. The phase shift magnitude was calculated as the phase difference between the evening peak of the day before the phase shift and the indicated day after the phase shift.

To assay light dependent arousal, we entrained the flies for 4 days under 12-hr light/12-hr dark cycles and then exposed the flies to a 5-min white light pulse (~600 lux LED lights) at ZT22. We binned the activity data for each fly every min. The arousal index (Δ bin crosses/5min) was calculated as the activity difference between the 5-min light regime and the 5 min immediately preceding the light stimulation.

Data collection and analyses were performed using Clocklab (Actimetrics). Activity

data for each fly was binned every 30 min for circadian analysis. To obtain the periodicity, data from constant darkness were subjected to χ^2 periodograms and Fast Fourier Transfer analysis using Clocklab software. The rhythm strength of a fly was measured as the power minus the significance (p-s). Flies were considered arrhythmic based on either p-s value < 10 or an FFT value (< 0.03). Actograms of weakly rhythmic flies were visually inspected to confirm rhythmicity.

Cell transfection, membrane extraction and spectral photometry

HEK293T (ATCC) cells were cultured to 70% confluency and transfected with 2 μg of the pCS2MT-*rh7* plasmid per 10 cm dish. We used the FuGENE® HD Transfection Reagent (Cat.E2311) for performing the transfections. Cells were harvested 24—36 hrs after transfection and stored at -80°C. For reconstitution of Rh7 with the chromophore, the HEK293T cells were resuspended in cold PBS (phosphate buffered saline pH 7.4,Quality Biological Inc.) supplemented with a protease inhibitor cocktail (Sigma P8340) and incubated with 40 μM 11-*cis*-retinal in the dark for 4 hrs. We prepared membrane protein extracts by resuspending membrane pellets in 0.1% CHAPs in PBS, rotating for 2 hrs at 4°C, then centrifuged (14,000 × *g*) for 20 min at 4°C. The supernatants were removed and analyzed with a UV3600 UV-Nir-NIR Spectrometer (Shimadzu). To obtain the spectral absorption for Rh7, we used membrane extracts from untransfected cells as the blank.

ERG recordings

ERG recordings were performed by filling two glass electrodes with Drosophila Ringer's solution and placing small droplets of electrode cream on the surface of the compound eye and the thorax to increase conductance. We inserted the recording

electrode into the cream on the surface of the compound eye and the reference electrode into the cream on the thorax. Flies were dark adapted for 1 min before stimulating with a 2-sec pulse using a halogen light (~30 mV/cm^2 unless indicated otherwise). The ERG signals were amplified with a Warner electrometer and recorded with a Powerlab 4/30 analog-to-digital converter (AD Instruments). Data were collected and analyzed with the Lab Chart version 6.1 program (AD Instruments).

Patch-clamp recordings and pharmacology

Patch-clamp measurements were performed on acutely dissected adult fly brains as described previously[11,12]. Briefly, all patch-clamp recordings were performed during the daytime to avoid clock-dependent variance in firing rate. All l-LNvs were recorded within a relatively narrow daytime window, which for each genotype tested were normally distributed for the time of day recorded and did not significantly vary between all three genotypes. l-LNv recordings were made in the whole-cell current clamp mode. After allowing the membrane properties to stabilize after whole cell break-in, we recorded for 30-60 sec in the current clamp configuration (unless otherwise stated) under nearly dark conditions (~0.05 mW/cm^2) before the lights were turned on. Lights-on data were collected for 5—20 sec and followed by 60—120 sec of darkness.

Multiple light sources were used for these studies. We used a standard halogen light source on an Olympus BX51 WI microscope (Olympus USA, Center Valley, PA) for all experiments with white light. Wavelength isolation of ≥550 nm for electrophysiological recordings was achieved by placing appropriate combinations of 25 mm long- and short-pass filters (Edmund Industrial Optics, Barrington, NJ) over the halogen light source directly beneath the recording chamber. We changed the filters during the recordings to

internally match the neuronal responses to different wavelengths of light. Recordings using 405 nm light (0.08mW/cm^2) were obtained using the LEDs obtained from Stanford Photonics (Palo Alto, CA), with the UHP-Mic-LED-405, which provides >2 W collimated purple light (405nm peak, 15 nm spectrum half width). Light was measured for all sources using a Newport 818-UV Sensor and the Optical Power/ Energy Meter (842-PE, Newport Corporation, Irvine, CA) and expressed as mW/cm^2.

The control genotype for the electrophysiological recordings was *w*;*pdf-Gal4-dORK-NC1-GFP*. The *cry*^{01} and *rh7*^{1} recordings were performed using *w*;*pdf-Gal4-dORK-NC1-GFP*;*cry*^{01} and *w*;*pdf-Gal4-dORK-NC1-GFP*;*rh7*^{1}.

Statistical analyses

To analyze two sets of data, we used the unpaired Student's *t*-test. To compare multiple sets of behavioral data, we used a one-away ANOVA test (Kruskal-Wallis test) followed by the Dunn's test. Data are presented as mean ±S.E.M.s. We used the Fisher's exact test for analyzing the percentages of rhythmic flies. For the patch-clamp recordings, the data are presented as mean ±S.E.M.s. Values of "n" refer to number of measured lights on/off cycles. In all cases the "n" values were obtained from ≥5 separate recordings (see details in the figure legends). Statistical tests of ANOVA were performed with SigmaPlot 11 (Systat Software Inc) or Prism 6 (Graphpad Sofeware). The data were first tested for normal distributions. If the data were not normally distributed, we performed Kruskal-Wallis One Way Analysis of Variance on Ranks, followed by the Dunn's test. ANOVA on normally-distributed data was followed by Tukey's test to determine significant differences between genotypes.

References

1 Emery, P., So, W. V., Kaneko, M., Hall, J. C. & Rosbash, M. CRY, a *Drosophila* clock and light-regulated cryptochrome, is a major contributor to circadian rhythm resetting and photosensitivity. *Cell* **95**, 669-679 (1998).

2 Emery, P. *et al. Drosophila* CRY is a deep brain circadian photoreceptor. *Neuron* **26**, 493-504 (2000).

3 Dolezelova, E., Dolezel, D. & Hall, J. C. Rhythm defects caused by newly engineered null mutations in Drosophila's *cryptochrome* gene. *Genetics* **177**, 329-345 (2007).

4 Yamaguchi, S., Wolf, R., Desplan, C. & Heisenberg, M. Motion vision is independent of color in *Drosophila*. *Proc. Natl. Acad. Sci. USA* **105**, 4910-4915 (2008).

5 Vasiliauskas, D. *et al.* Feedback from rhodopsin controls *rhodopsin* exclusion in *Drosophila* photoreceptors. *Nature* **479**, 108-112 (2011).

6 O'Tousa, J. E. *et al.* The Drosophila *ninaE* gene encodes an opsin. *Cell* **40**, 839-850 (1985).

7 Venken, K. J. *et al.* Versatile P[acman] BAC libraries for transgenesis studies in *Drosophila melanogaster*. *Nat. Methods* **6**, 431-434 (2009).

8 Gong, W. J. & Golic, K. G. Ends-out, or replacement, gene targeting in *Drosophila*. *Proc. Natl. Acad. Sci. USA* **100**, 2556-2561 (2003).

9 Lee, Y. & Montell, C. *Drosophila* TRPA1 functions in temperature control of circadian rhythm in pacemaker neurons. *J. Neurosci.* **33**, 6716-6725 (2013).

10 Jang, A. R., Moravcevic, K., Saez, L., Young, M. W. & Sehgal, A. *Drosophila* TIM binds importin α1, and acts as an adapter to transport PER to the nucleus. *PLoS. Genet.* **11**, e1004974 (2015).

11 Fogle, K. J., Parson, K. G., Dahm, N. A. & Holmes, T. C. CRYPTOCHROME is a blue-light sensor that regulates neuronal firing rate. *Science* **331**, 1409-1413 (2011).

12 Sheeba, V., Gu, H., Sharma, V. K., O'Dowd, D. K. & Holmes, T. C. Circadian- and light-dependent regulation of resting membrane potential and spontaneous action potential firing of *Drosophila* circadian pacemaker neurons. *J. Neurophysiol.* **99**, 976-988 (2008).

13 Zuker, C. S., Cowman, A. F. & Rubin, G. M. Isolation and structure of a rhodopsin gene from D. melanogaster. *Cell* **40**, 851-858 (1985).

14 Montell, C., Jones, K., Zuker, C. & Rubin, G. A second opsin gene expressed in the ultraviolet-sensitive R7 photoreceptor cells of *Drosophila melanogaster*. *J. Neurosci.* **7**, 1558-1566 (1987).

15 Zuker, C. S., Montell, C., Jones, K., Laverty, T. & Rubin, G. M. A rhodopsin gene expressed in photoreceptor cell R7 of the Drosophila eye: homologies with other signal-transducing molecules. *J. Neurosci.* **7**, 1550-1557 (1987).

16 Chou, W. H. *et al.* Identification of a novel Drosophila opsin reveals specific patterning of the R7 and R8 photoreceptor cells. *Neuron* **17**, 1101-1115 (1996).

17 Papatsenko, D., Sheng, G. & Desplan, C. A new rhodopsin in R8 photoreceptors of Drosophila: evidence for coordinate expression with Rh3 in R7

cells. *Development* **124**, 1665-1673 (1997).

18 Chou, W. H. *et al.* Patterning of the R7 and R8 photoreceptor cells of *Drosophila*: evidence for induced and default cell-fate specification. *Development* **126**, 607-616 (1999).

Figure 1

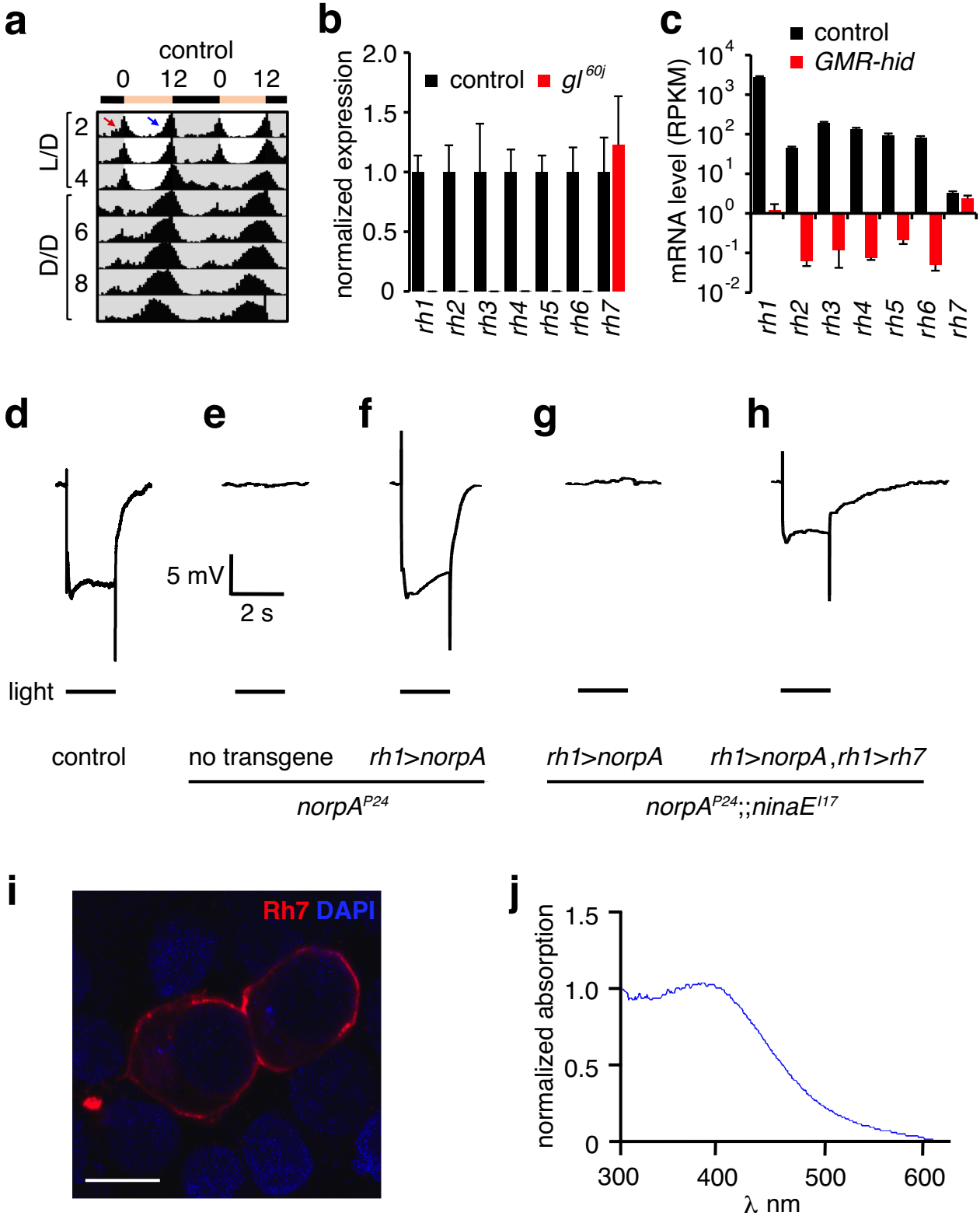
a
control
0 12 0 12
L/D
D/D
2
4
6
8
b
normalized expression
2.0
1.5
1.0
0.5
0
control
gl 60j
rh1 rh2 rh3 rh4 rh5 rh6 rh7
c
control
GMR-hid
mRNA level (RPKM)
10^4
10^3
10^2
10^1
10^0
10^-1
10^-2
rh1 rh2 rh3 rh4 rh5 rh6 rh7
d
e
f
g
h
5 mV
2 s
light
control
no transgene
rh1>norpA
norpA P24
rh1>norpA
rh1>norpA,rh1>rh7
norpA P24;;ninaE I17
i
Rh7 DAPI
j
normalized absorption
1.5
1.0
0.5
0
300
400
500
600
λ nm

Figure 1. *rh7* encodes a functional light receptor. a, Average actogram obtained with control flies (w^{1118}) entrained under 12-hr light/12-hr dark (L/D) cycles for 4 days and released to constant darkness (D/D). The red and blue arrows indicate morning and evening anticipation, respectively. n=62. **b,** Quantitative real-time PCR analysis of rhodopsin genes using RNA prepared from whole heads. The expression levels were normalized using *rp49* expression. The error bars indicate S.E.M.s. n=3 for each genotype. **c**, Quantification of *rhodopsin* transcripts in control and *GMR-hid* flies using RNAseq. The mRNA levels were quantified as Reads Per Kilobase of transcript per Million mapped reads (RPKM). For each genotype, three independent RNA libraries were prepared from ~50 flies heads. The RPKM for each sample was calculated independently and the average RPKM for each *rhodopsin* gene is plotted. The error bars indicate S.E.M.s. **d**—**h**, ERG responses using 2-sec white light pulses and flies of the indicated genotypes. The event markers below the ERGs indicate the initiation and cessation of the light stimuli. The scale bars indicate 5 mV and 2 sec. **d**, Control flies. **e**, $norpA^{P24}$. **f**, Expression of *norpA* under the control of the *rh1* promoter (*rh1>norpA*) in a $norpA^{P24}$ background. **g**, Expression of *rh1>norpA* in a $norpA^{P24}$;;$ninaE^{I17}$ background. **h**, Expression of *rh1>norpA and UAS-rh7* under the control of the *rh1-Gal4* (*rh1>norpA* and *rh1>rh7*, respectively) in a $norpA^{P24}$;;$ninaE^{I17}$ background. **i**, HEK293T cells transfected with an *rh7*-expressing plasmid and stained with anti-Rh7. The cells were co-stained with DAPI to indicate the nuclei. The scale bar indicates 10 μm. **j**, Absorbance spectrum of Rh7 using a membrane fraction from HEK293T cells

expressing Rh7, supplemented with 11-*cis*-retinal. Shown is the spectrum obtained after subtracting the absorbance of non-transfected cells.

Figure 2

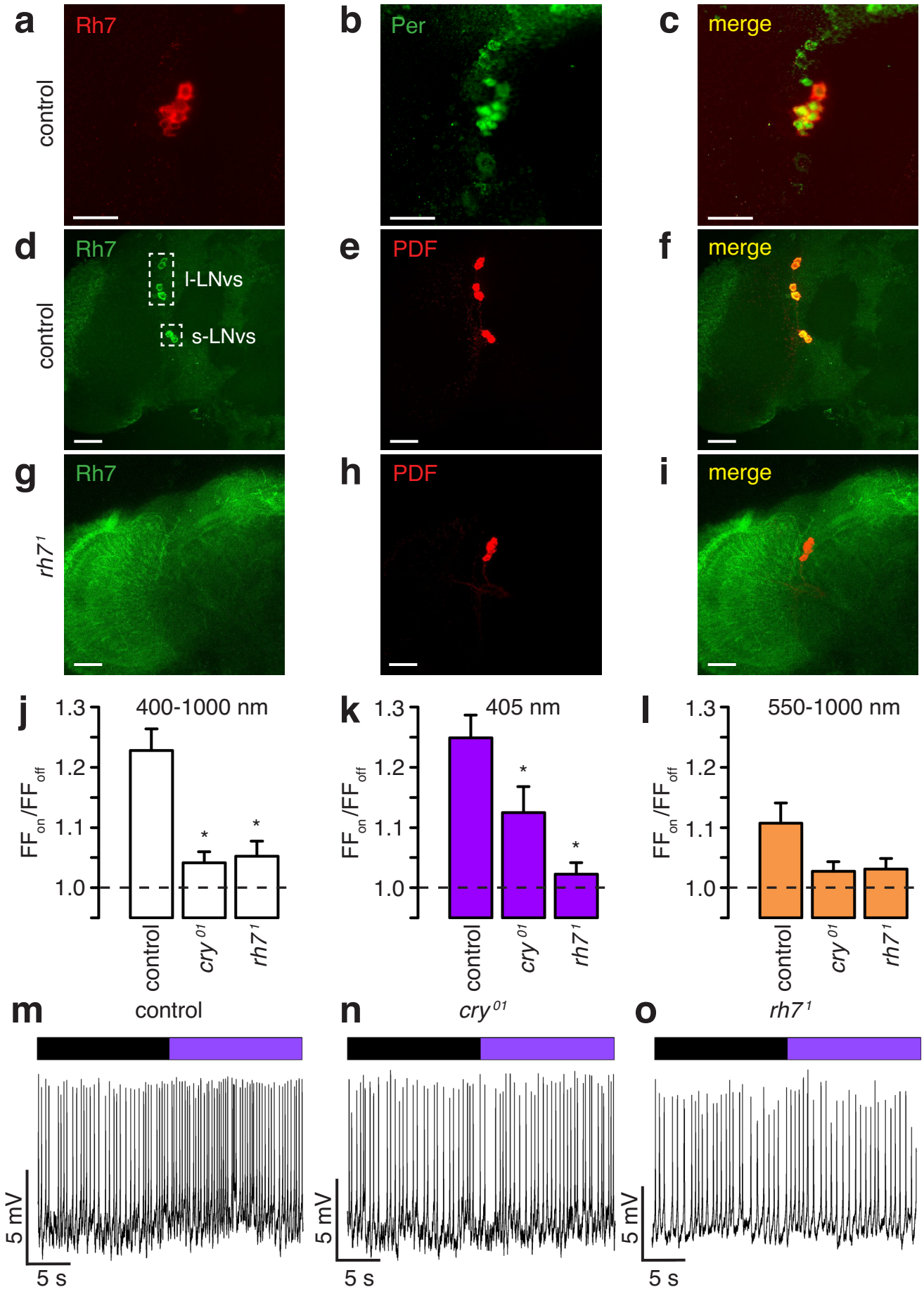
a
Rh7
control
b
Per
c
merge
d
Rh7
l-LNvs
s-LNvs
control
e
PDF
f
merge
g
Rh7
rh7¹
h
PDF
i
merge
j
400-1000 nm
FF_on/FF_off
1.3
1.2
1.1
1.0
control
cry⁰¹
rh7¹
k
405 nm
l
550-1000 nm
m
control
n
cry⁰¹
o
rh7¹
5 mV
5 s

Figure 2. Rh7 expressing circadian pacemaker neurons are activated by violet light. a—f, Control (w^{1118}) brains stained with anti-Rh7 (Rh7), anti-PER (PER) or anti-PDF (PDF) as indicated. The scale bars indicates 20 μm. **a**, Anti-Rh7. **b**, Anti-Per. **c,** Merge of a and b. **d**, Anti-Rh7. **e**, Anti-PDF. **f,** Merge of d and e. **g—i**, $rh7^1$ brain stained with the indicated antibodies. **g**, Anti-Rh7. **h**, Anti-PDF. **i,** Merge of g and h. **j—l**, Average firing frequencies during "lights on" relative to the firing frequencies during "lights off" (FF_{on}/FF_{off}) exhibited by control, cry^{01} and $rh7^1$ flies in response to different wavelengths of light. The dashed line indicates no difference between FF_{on} and FF_{off}. * indicates significant differences from the control ($p<0.05$). **j**, White light (halogen, 400—1000 nm, 4 mW/cm^2). Control (1.23 ±0.04, n =74), cry^{01} (1.04 ±0.02, n =80, $p<0.05$ vs. control) and $rh7^1$ (1.05 ±0.02, n =60, $p<0.05$ vs. control). **k**, 405 nm violet light (Prizmatix 405 LED, 0.8 mW/cm^2). Control (1.25 ±0.04 n=76), cry^{01} (1.13 ±0.04, n=89, $p<0.05$ vs. control) and $rh7^1$ (1.02 ±0.02, n=66, $p<0.05$ vs. control). **l**, Orange light (4 mW/cm^2, 550nm—1000 nm long pass filtered halogen light). Control (1.11 ±0.03, n=58), cry^{01} (1.03 ±0.02, n=65), and $rh7^1$ (1.03 ±0.02, n=46). **m-o**, Representative recordings showing responses of l-LNv neurons to 405 nm light (0.8 mW/cm^2). The scale bars indicate 5 mV and 5 sec. Purple bar= 405 nm; black bar= no light. **m**, Control. **n,** cry^{01}. **o,** $rh7^1$.

Figure 3

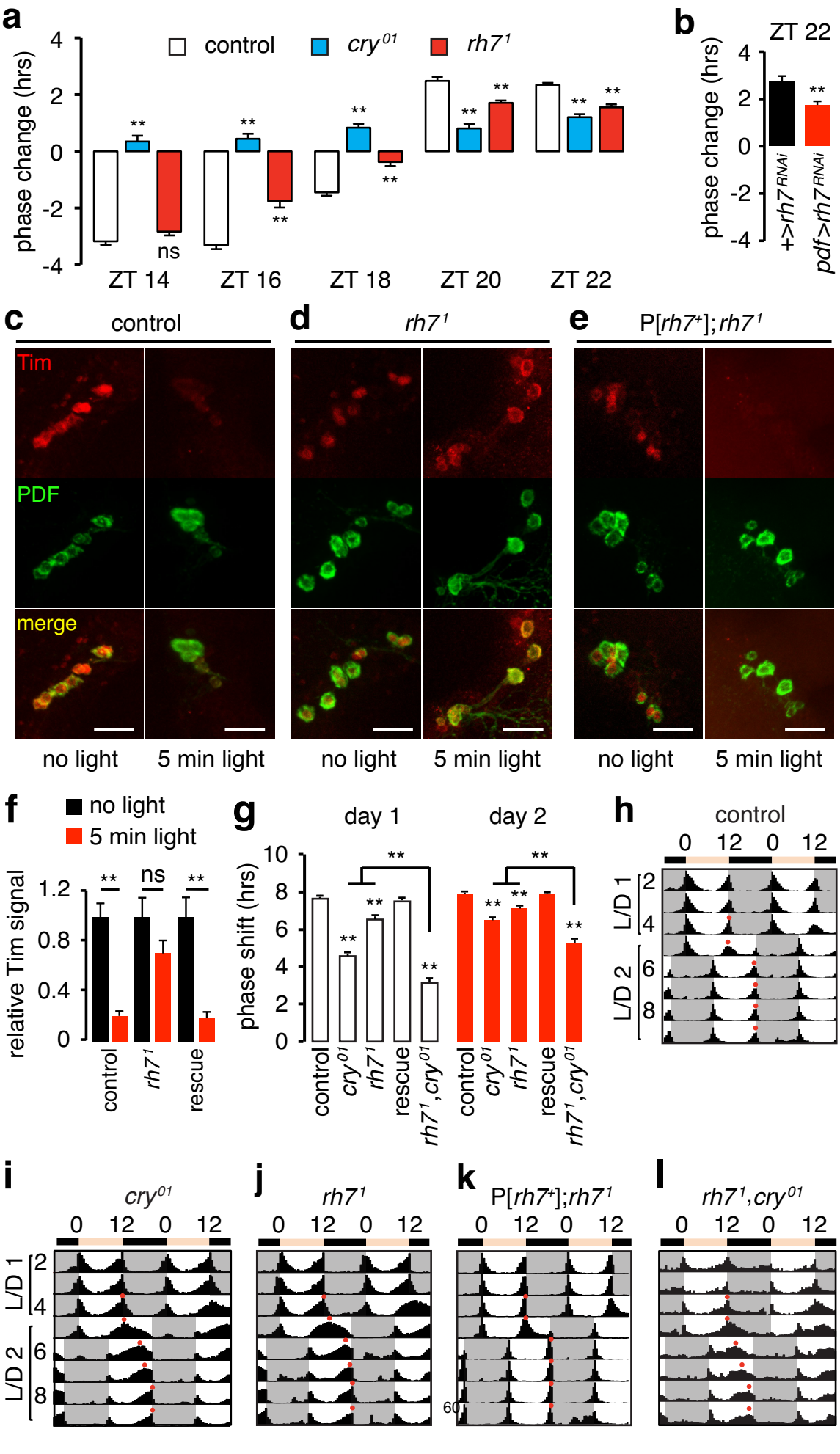
a
control
cry01
rh71
phase change (hrs)
ZT 14
ZT 16
ZT 18
ZT 20
ZT 22
ns
b
ZT 22
+>rh7RNAi
pdf>rh7RNAi
c
control
d
rh71
e
P[rh7+];rh71
Tim
PDF
merge
no light
5 min light
f
relative Tim signal
rescue
g
day 1
day 2
phase shift (hrs)
rh71,cry01
h
control
L/D 1
L/D 2
i
cry01
j
rh71
k
P[rh7+];rh71
l
rh71,cry01

Figure 3. Rh7 functions as a circadian light receptor. a, Phase response of the indicated flies to stimulation with a 5-min white light at the indicated ZT points. The flies were entrained to 12-hr light/12-hr dark cycles (L/D) for 3 days, followed by a fourth day cycle. The flies were then exposed to a 5-min LED light pulse (~600 lux) on the fourth night cycle at different ZTs. A negative phase change indicates a phase delay while a positive phase change indicates a phase advance. Three independent assays were performed for each genotype (n=8—32/experiment). Total flies tested: ZT14, control, n=56; cry^{01}, n=46; $rh7^{1}$, n=55. ZT16, control, n=61; cry^{01}, n=52; $rh7^{1}$, n=57. ZT18, control, n=61; cry^{01}, n=51; $rh7^{1}$, n=77. ZT20, control, n=45; cry^{01}, n=39; $rh7^{1}$, n=48. ZT22, control, n=54; cry^{01}, n=60; $rh7^{1}$, n=48. **b**, Phase response of the indicated genotypes to a 5-min white light stimulation at ZT22. Three independent assays were performed for each genotype (n=8—24/experiment). *+>rh7*^{RNAi} control, n=40; *pdf>rh7*^{RNAi}, n=52. **p<0.01, unpaired Student's *t*-test. **c**—**e**, Brains were stained with anti-PDF and anti-Tim as indicated. The scale bars indicate 40 μm and apply to all panels. The flies were exposed to a 5-min LED light stimulation (~600 lux) at ZT22, fixed at ZT23 and dissected for whole-mount immunostaining. Flies that were not exposed to the nocturnal light treatment were fixed and stained at the same times. **f**, Quantification of light mediated degradation of TIM protein in LNvs. The genotype for the rescue flies is P[$rh7^{+}$];$rh7^{1}$. Animals tested: control, dark n=6, light n=4; $rh7^{1}$, dark n=5, light n=4; rescue, dark n=5, light n=4. n.s. not significant. **p<0.01, unpaired Student's *t*-test. **g**, Quantification of the phase shift (in hours) exhibited by the indicated genotypes on day 1 and day 2 after the 8-hr phase delay. The phase shifts

were calculated as the difference in time between the evening peak on the day before the phase shift and after the phase shift. Three to four independent assays was performed for each genotype (n=10—30/experiment). Total flies tested: control, n=95; cry^{01}, n=96; $rh7^{1}$, n=68; P[$rh7^{+}$];$rh7^{1}$, n=60; $rh7^{1}$,cry^{01}, n=66. The error bars indicate S.E.M.s. One-away ANOVA test (Kruskal-Wallis test) followed by the Dunn's test. $^{**}p<0.01$. **h**—**l**, Actograms displayed by flies of the indicated genotypes. The flies were entrained under 12-hr light/12-hr dark cycles (L/D) using 400 lux white LED lights. On day 5, the day cycle was extended by 8 hours.

Figure 4

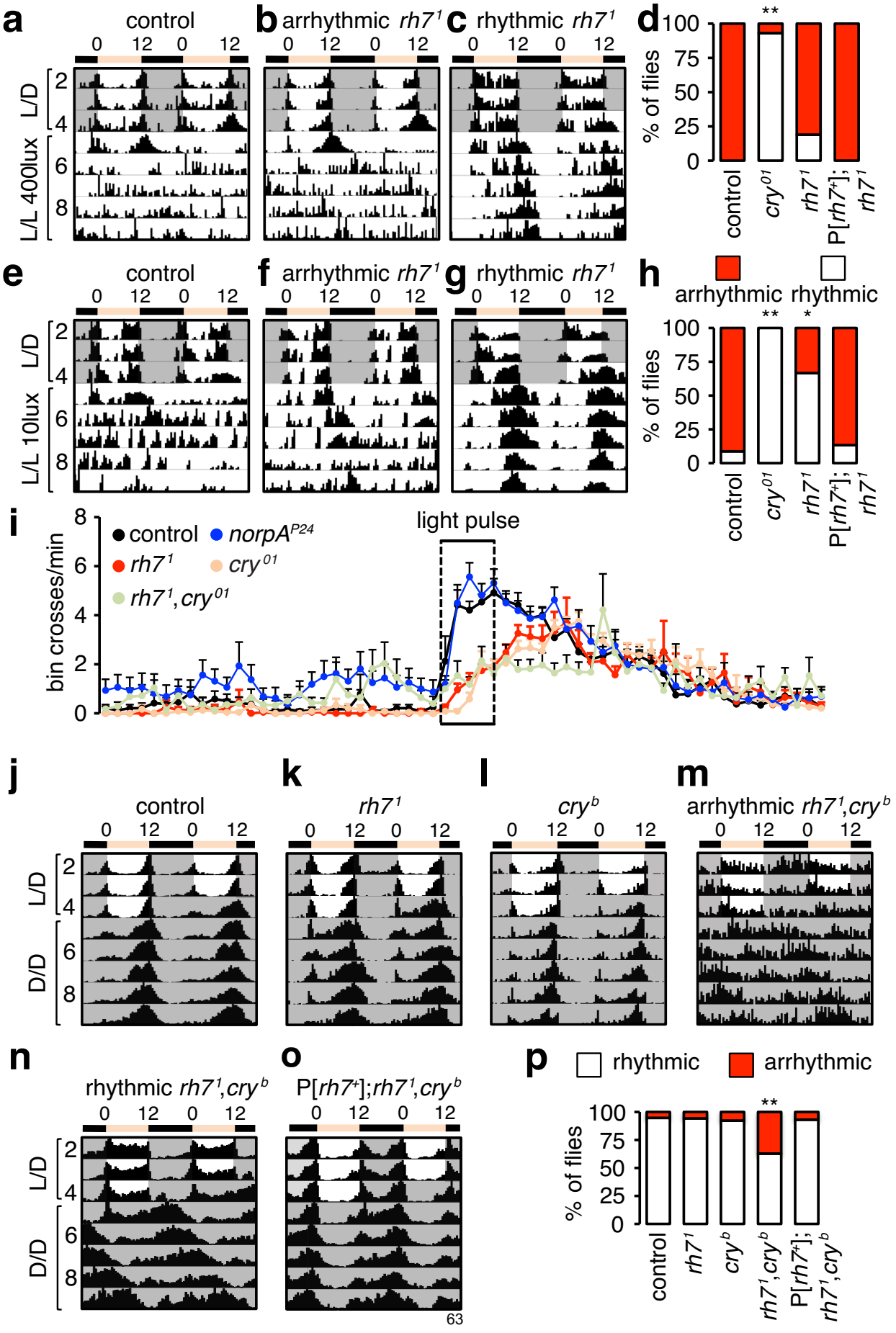
a
control
b arrhythmic rh7¹
c rhythmic rh7¹
0 12 0 12
L/D
L/L 400lux
2
4
6
8
d
% of flies
100
75
50
25
0
**
control
cry⁰¹
rh7¹
P[rh7⁺]; rh7¹
e
control
f arrhythmic rh7¹
g rhythmic rh7¹
L/L 10lux
h
arrhythmic
rhythmic
**
*
i
light pulse
bin crosses/min
8
6
4
2
0
control
norpA^P24
rh7¹
cry⁰¹
rh7¹,cry⁰¹
j
control
k
rh7¹
l
cry^b
m
arrhythmic rh7¹,cry^b
D/D
n
rhythmic rh7¹,cry^b
o
P[rh7⁺];rh7¹,cry^b
p
rhythmic
arrhythmic
control
rh7¹
cry^b
rh7¹,cry^b
P[rh7⁺]; rh7¹,cry^b

Figure 4. Effects of the *rh7* mutation on circadian behavior in response to constant light, constant darkness, and on arousal in response to a light pulse. **a**—**c,** Actograms showing circadian responses to constant bright light. The flies were entrained under 12-hr light/12-hr dark (L/D) cycles and subsequently released to constant light (L/L) of ~400 lux. **a**, Control fly. **b,** $rh7^1$ fly that became arrhythmic under constant light. **c**, $rh7^1$ fly that maintained rhythmicity under constant light. **d**, Percentages of rhythmic and arrhythmic flies. Fisher's exact test. $^{**}p<0.01$. Flies tested: control, n=48; cry^{01}, n=29; $rh7^1$, n=58; P[$rh7^+$];$rh7^1$, n=16. **e**—**g,** Actograms showing circadian response to constant dim light. The flies were entrained under 12-hr light/12-hr dark (L/D) cycles and subsequently released to constant light (L/L) of ~10 Lux. **e**, Control fly. **f,** $rh7^1$ fly that became arrhythmic under constant light. **g**, $rh7^1$ fly that maintained rhythmicity under constant light. **h**, Percentages of rhythmic and arrhythmic flies. Fisher's exact test. $^{*}p<0.05$. $^{**}p<0.01$. Flies tested: control, n=23; cry^{01}, n=30; $rh7^1$, n=27; and P[$rh7^+$];$rh7^1$, n=15. **i**, Light-dependent arousal impaired by the $rh7^1$ mutation. Average activities of the indicated genotypes at ZT22. Activities are plotted as bin crosses per min. The boxed area indicates the 5-min white light pulse. **j**—**p**, Synergistic effect of the cry^b and $rh7^1$ mutations on circadian behavior. Average actograms showing the activities of flies of the indicated genotypes. The flies were entrained to 12-hr light/12 hr dark cycles (L/D) for 4 days and subsequently released to constant darkness (D/D). **j**, actogram of control flies. **k**, actogram of $rh7^1$ flies. **l,** actogram of cry^b flies. **m**, Actogram of arrhythmic $rh7^1$,cry^b flies. **n**, Actogram of rhythmic $rh7^1$,cry^b flies. **o,** Actogram of $rh7^1$,cry^b flies expressing an *rh7* genomic

transgene. **p,** Percentages of rhythmic and arrhythmic flies. **$p<0.01$. Fisher's exact test. Flies tested: control, n=76; $rh7^{1}$ n=29; cry^{b} n=39; $rh7^{1}$,cry^{b}, n=78 and P[$rh7^{+}$]; cry^{b},$rh7^{1}$ n=29.

Extended Data Figure 1

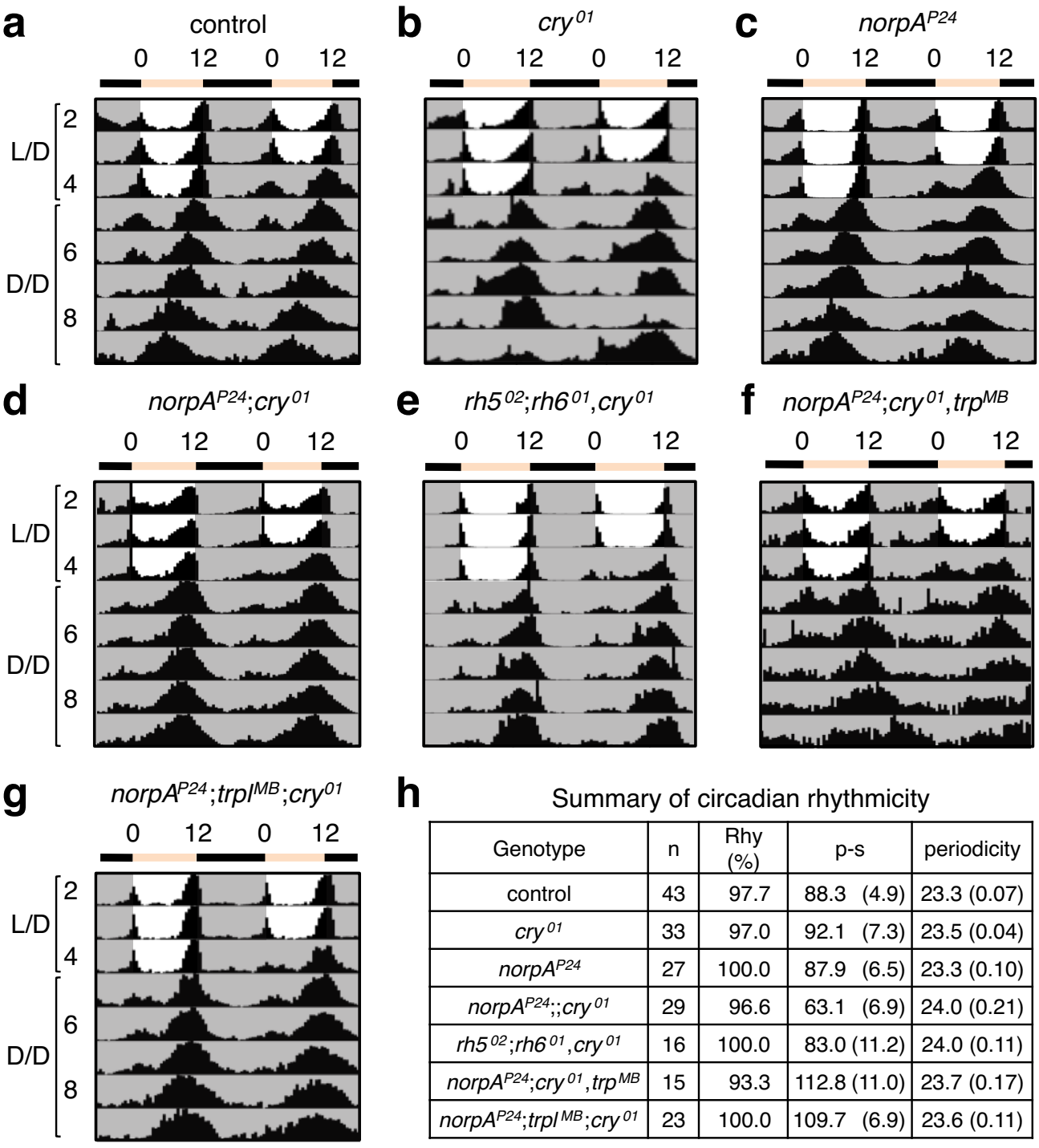

h Summary of circadian rhythmicity

Genotype	n	Rhy (%)	p-s	periodicity
control	43	97.7	88.3 (4.9)	23.3 (0.07)
cry^{01}	33	97.0	92.1 (7.3)	23.5 (0.04)
norpA^{P24}	27	100.0	87.9 (6.5)	23.3 (0.10)
norpA^{P24};;*cry*^{01}	29	96.6	63.1 (6.9)	24.0 (0.21)
rh5^{02};*rh6*^{01},*cry*^{01}	16	100.0	83.0 (11.2)	24.0 (0.11)
norpA^{P24};*cry*^{01},*trp*^{MB}	15	93.3	112.8 (11.0)	23.7 (0.17)
norpA^{P24};*trpl*^{MB};*cry*^{01}	23	100.0	109.7 (6.9)	23.6 (0.11)

Extended Data Figure 1. Circadian photoentrainment in flies lacking crypotochrome and proteins required for phototransduction in the compound eye. a—g, Average actograms exhibited by flies of the indicated genotypes maintained under 12-hr light/12-hr dark (L/D) for four days and then released to constant darkness (D/D). **h**, Summary of circadian rhythmicity of flies in a—g**.** Rhythm strength of a fly was measured as the power minus the significance (p-s).

Extended Data Figure 2

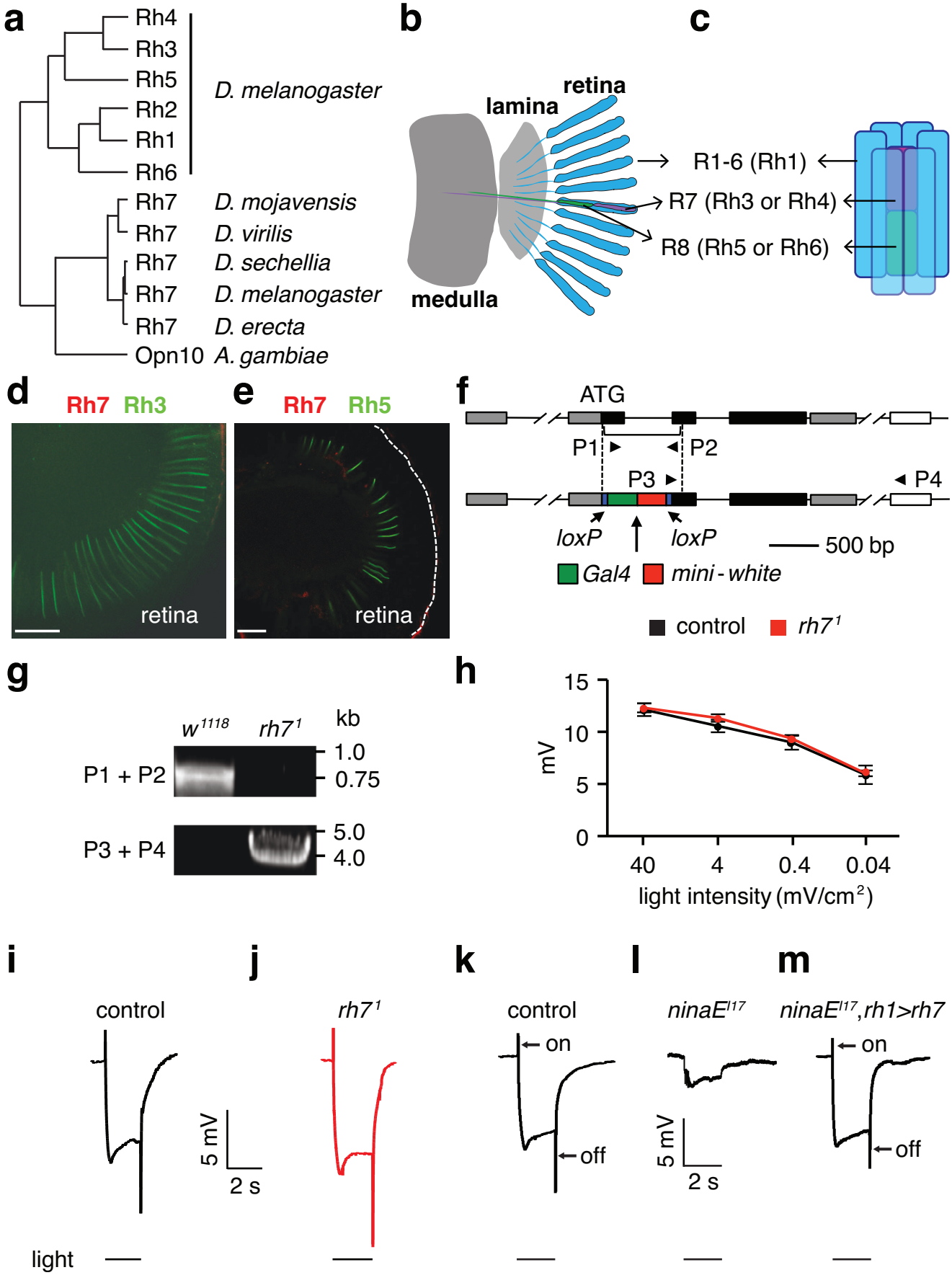

Extended Data Figure 2. Rh7 is an extra-retinal opsin. a, Phylogenetic tree constructed with protein sequences corresponding to the indicated opsins. The full name for *Ae. aegypti* OP10 is GPROP10 (VectorBase). **b**, Cartoon showing a longitudinal view of the main structures in the visual system, including the retina, lamina and medulla. The blue units represent ommatidia, which are comprised of eight photoreceptor cells (R1-8) and support cells. **c,** Cartoon showing the photoreceptor cells in a single ommatidium. The six outer photoreceptor cells (R1-R6) are represented in blue and express Rh1[6,13]. The central R7 photoreceptor cell (purple) expresses either Rh3 or Rh4[14,15], while the R8 photoreceptor cell (green) expresses Rh5 or Rh6[16-18]. **d**, A wild-type retina stained with anti-Rh7 (red) and anti-Rh3 (green). **e,** A wild-type retina stained with anti-Rh7 (red) and anti-Rh5 (green). The scale bars in d and e indicates 30 μm. No Rh7 positive staining was detected in the retina. **f,** Generation of *rh7*^{1} by homologous recombination. Shown are cartoons of the wild-type *rh7* locus (top) and the genomic organization of the *rh7*^{1} allele (bottom). The triangles (P1-P4)

indicate the primers used to verify the *rh7*^{1} mutation. **g**, Confirmation of the *rh7*^{1} mutation by PCR. We prepared genomic DNA from control (*w*^{1118}) and *rh7*^{1} flies and performed PCR using the P1/P2 and P3/P4 primer pairs. The positions of DNA markers (kb) are indicated to the right. **h**, ERG amplitudes of control and *rh7*^{1} flies using 2-sec white light pulses of the indicated intensities. The error bars indicate S.E.M.s. n=4. **i—m**, ERGs from flies of the indicated genotypes. The event markers below the ERGs indicate the initiation and cessation of the light stimuli. The scale bars indicate 5 mV and 2 sec. **i,** Control flies. **j,** *rh7*^{1}. **k—m**, Testing for rescue of the reduced ERG in *ninaE*^{I17} flies with an *rh7*$^{+}$ *transgene*. **k**, Control flies. **l**, *ninaE*^{I17} (*rh1* mutant). **m**, *ninaE*^{I17} fly expressing *UAS-rh7* in R1-R6 cells under control of the *rh1-Gal4* (*ninaE*^{I17},*rh1>rh7*).

Extended Data Figure 3

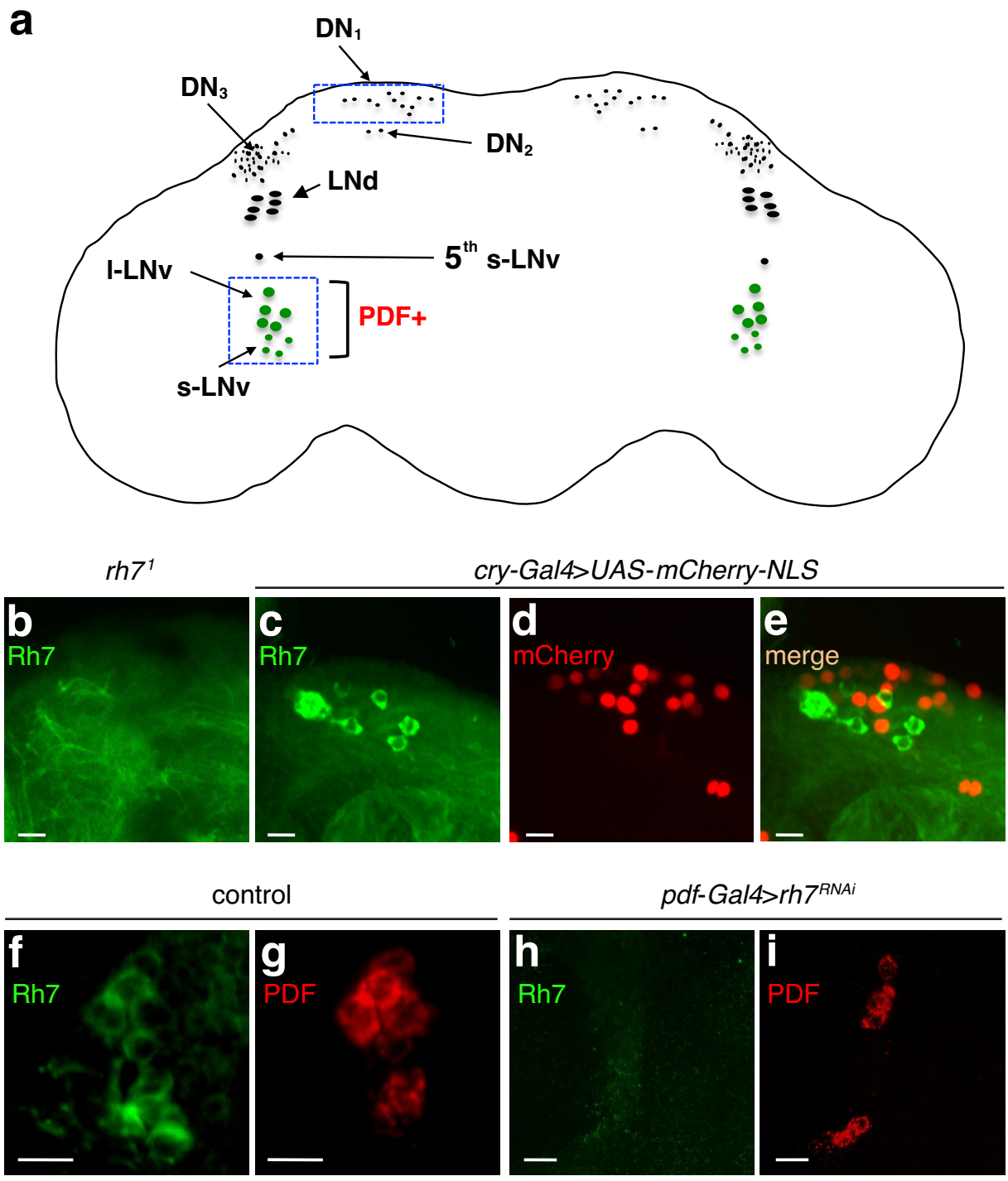

Extended Data Figure 3. Expression of Rh7 in non-clock neurons located in the dorsal part of the brain. a, Cartoon of a fly brain showing different groups of clock neurons. The boxed areas indicate locations of two groups of Rh7-positive cells. **b**, *rh7*^{1} brain stained with anti-Rh7. **c**—**e**, Double labeling of the dorsal region of the brain with a clock neuron reporter (*cry-Gal4E13>UAS-mCherry-NLS*) and anti-Rh7. The scale bars in b—e indicate 20 μm. **c**, Anti-Rh7. **d**, Anti-mCherry. **e**, Merge of **c** and **d**. **f**, Control brain stained with anti-Rh7. **g**, Control brain stained with anti-PDF. **h**, *pdf-Gal4>rh7*^{RNAi} brain stained with anti-Rh7. **i**, *pdf-Gal4>rh7*^{RNAi} brain stained with anti-PDF. The scale bars in f—i indicate 10 μm.

Extended Data Figure 4

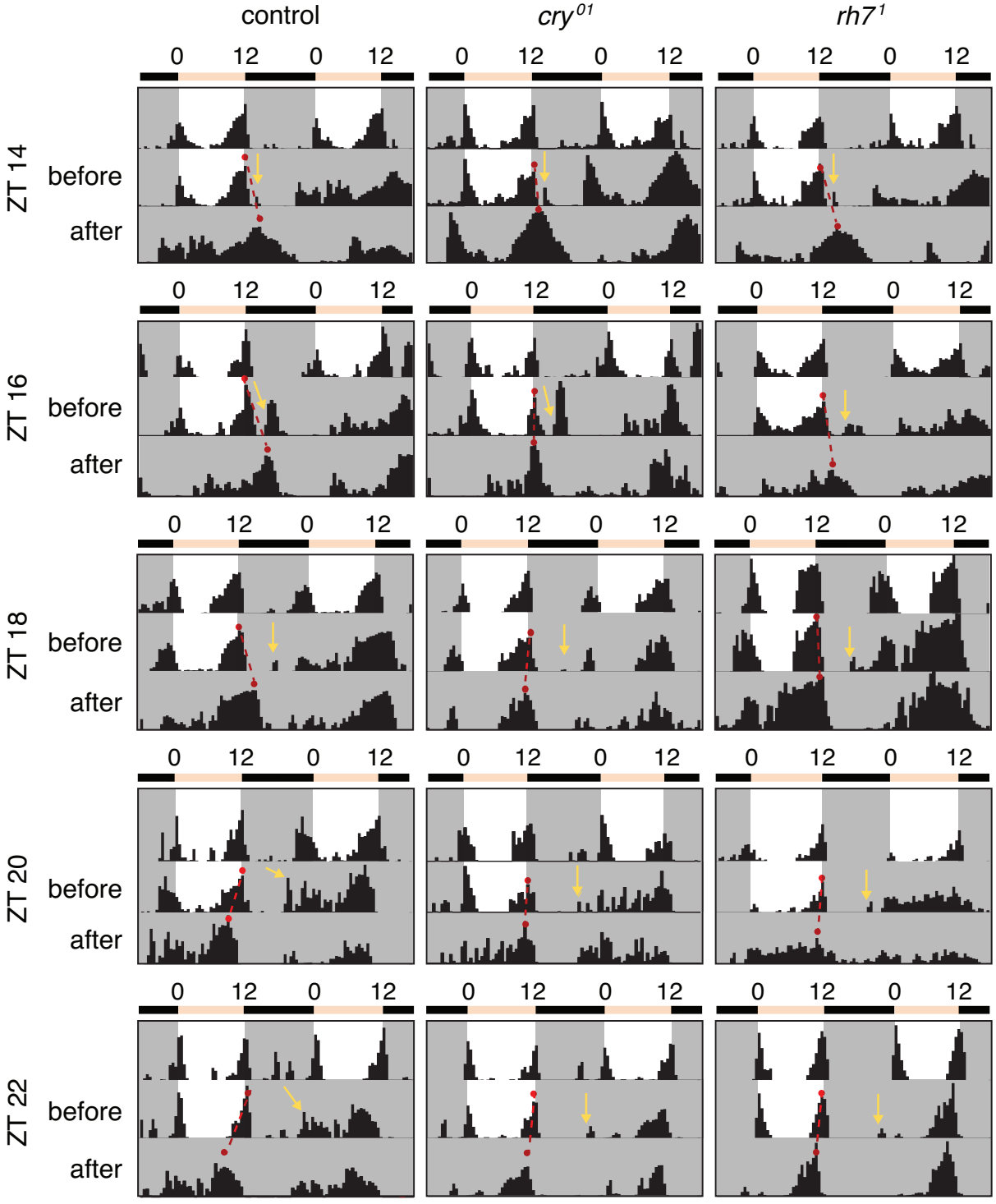

Extended Data Figure 4. Examples of the control and mutant behavior before and after the 5-minute light pulse at the indicated ZT. The red dots connected by the dashed red lines indicate the evening peaks before and after the light pulse. Each yellow arrow indicates the times that the animals were exposed to the 5-minute ~600 lux LED light pulse.

Extended Data Figure 5

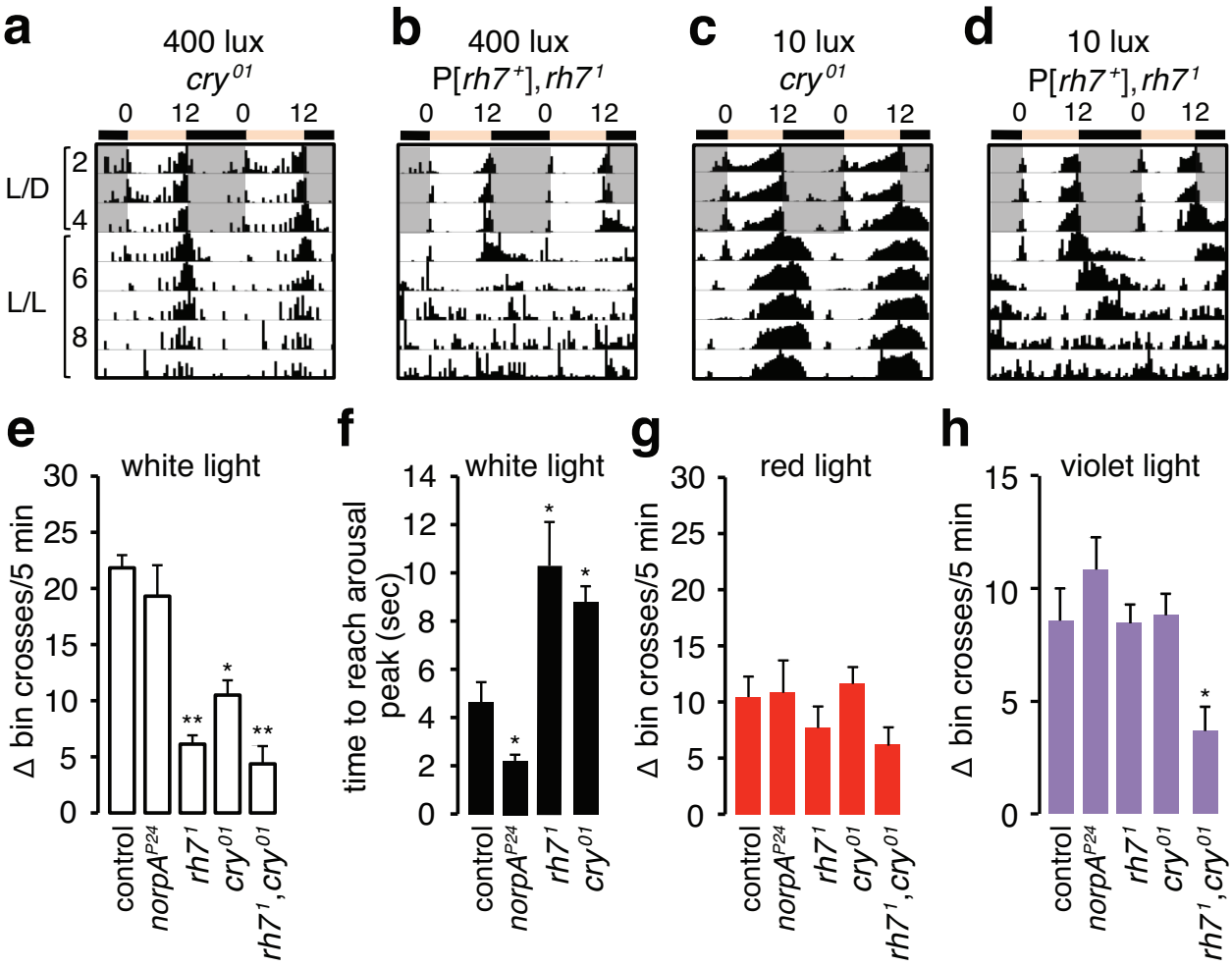

Extended Data Figure 5. Circadian responses to constant light and light-dependent arousal are impaired in *rh7*^{1} flies. a, b, Flies of the indicated genotypes were entrained under 12-hr light/12-hr dark (L/D) cycles and subsequently released to constant ~400 lux light (L/L) . **c**, **d**, Flies of the indicated genotypes were entrained under 12-hr light/12-hr dark (L/D) cycles and subsequently released to constant ~10 lux light (L/L). **e**, Quantification of the effect of a 5-min white light pulse on arousal. Arousal was quantified as increases in total bin crosses during the 5-min light stimulation compared to the total bin crosses during the 5 min before the light stimulation. **f**, Quantification of the time required to reach the maximum activity after white light stimulation. **g, h**, Quantification of the effects on arousal due to a 5-min exposure to red (625 nm) LED lights (**g**) or violet (405 nm) LED lights (**h**). The error bars indicate S.E.M.s. One-away ANOVA test (Kruskal-Wallis test) followed by the Dunn's test. *p<0.05, **p<0.01. Number of flies tested: *norpA*^{P24} , n=16, other genotypes, n=24.

Extended Data Figure 6

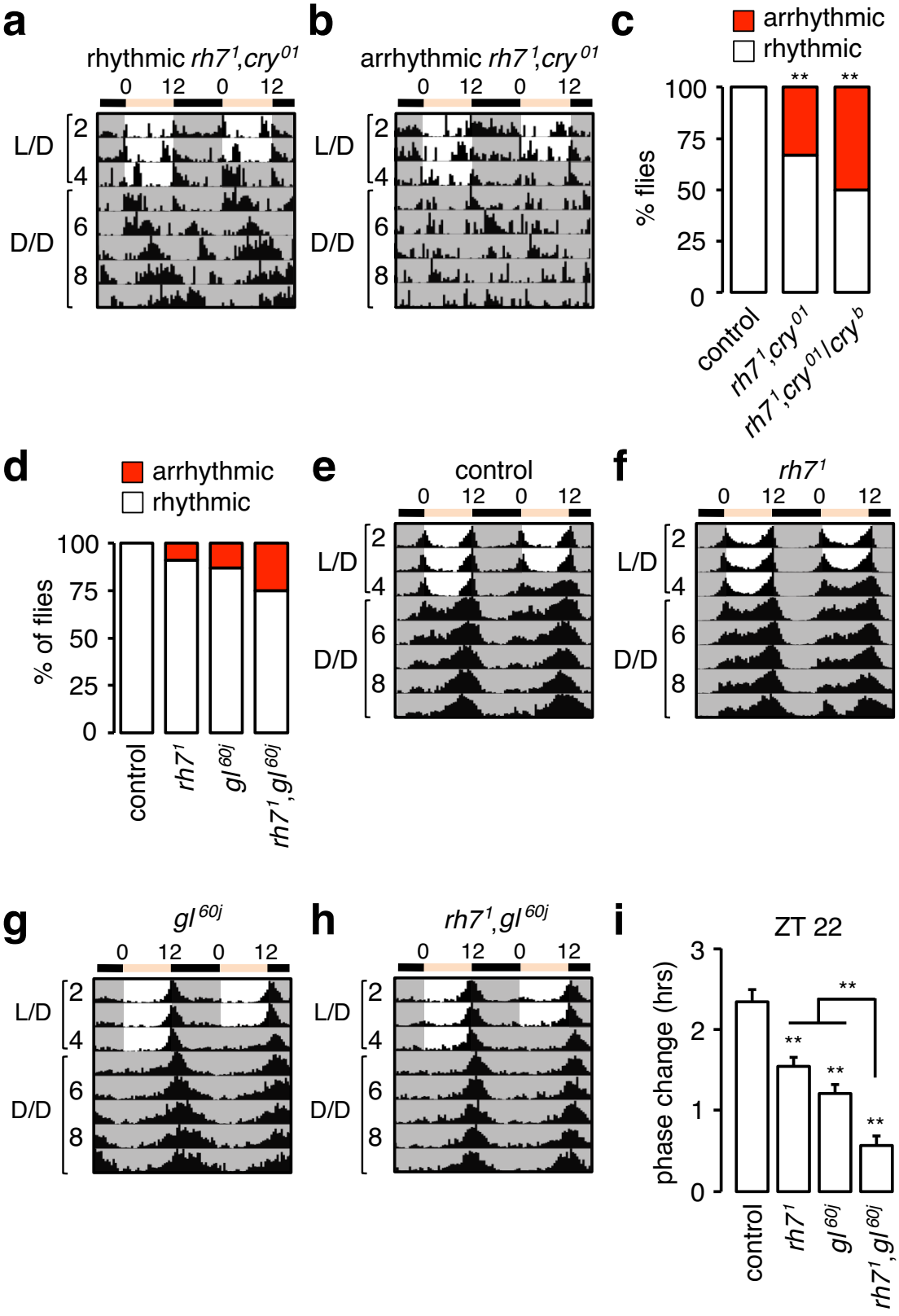

Extended Data Figure 6. Effects of multiple light input pathways on circadian behavior. a, **b**, Actograms showing rhythmic and arrhythmic $rh7^{1}$,cry^{01} double mutants. The flies were entrained under 12-hr light/12-hr dark (L/D) cycles and subsequently released to constant darkness (D/D). **c**, Percentages of rhythmic and arrhythmic flies. Fisher's exact test. $^{**}p<0.01$. Number of flies tested: control, n=16; other genotypes, n=30. **d**—**h** Circadian behavior of gl^{60j} and $rh7^{1}$,gl^{60j} double mutant flies. The flies were entrained to 12-hr light/12 hr dark cycles (L/D) for 4 days and subsequently released to constant darkness (D/D). **d**, Percentages of rhythmic and arrhythmic flies. **e**—**h,** Average actograms showing the activities of flies of the indicated genotypes. Number of flies tested: control, n=46; $rh7^{1}$ n=34; gl^{60j} n=38; $rh7^{1}$,gl^{60j} , n=40. **i**, Phase response of the indicated genotypes to a 5-min white light stimulation at ZT22. The error bars indicate S.E.M.s. One-way ANOVA test (Kruskal-Wallis test) followed by the Dunn's test. $^{**}p<0.01$. Flies tested: control, n=54; $rh7^{1}$ n=49; gl^{60j} n=53; $rh7^{1}$,gl^{60j} , n=57.

Extended Data Figure 7

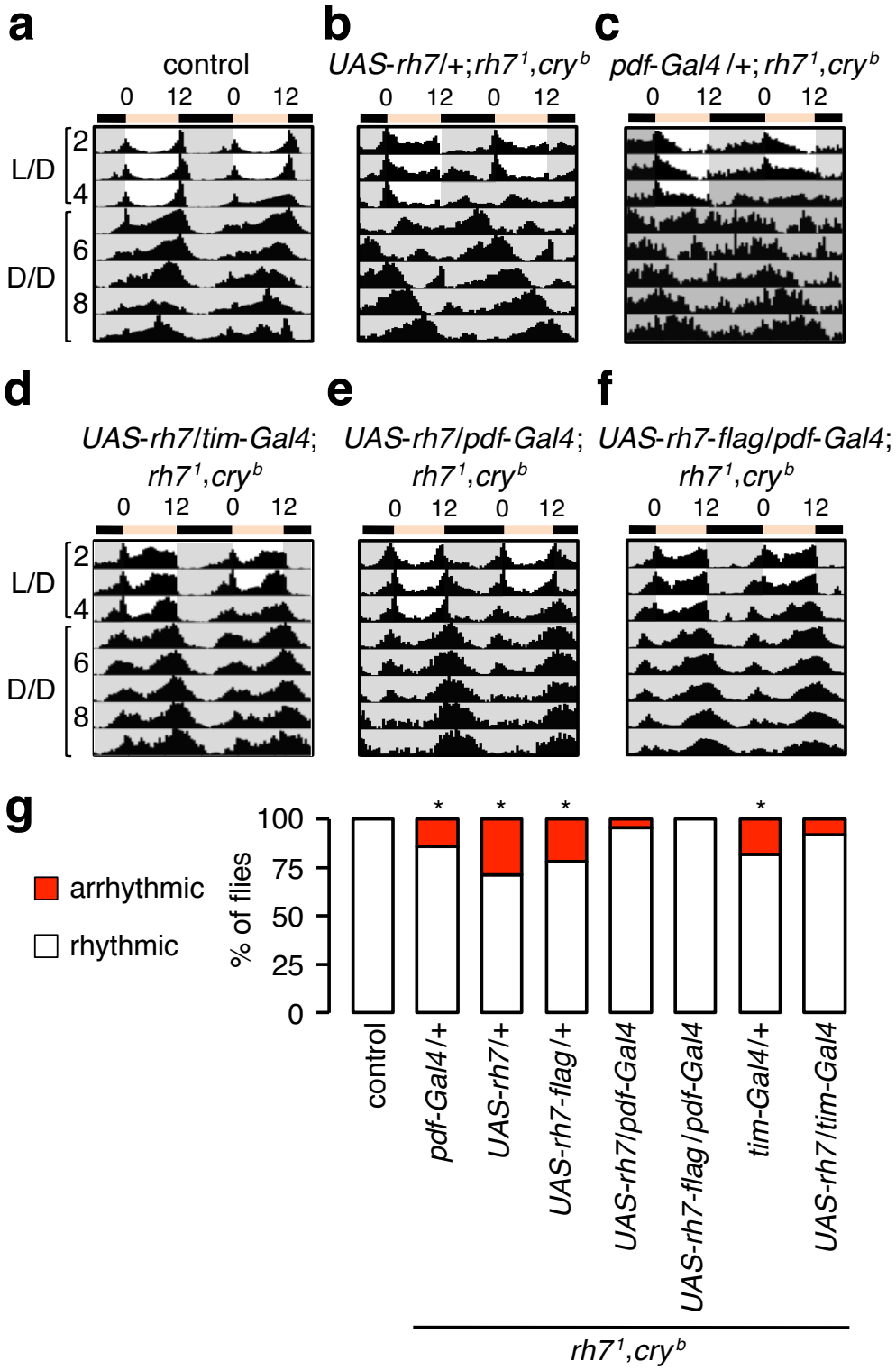

Extended Data Figure 7. Rescue of the *rh7*^{1},*cry*^{b} photoentrainment defect by expression of *rh7* in pacemaker neurons. a—**c**, Actograms of control flies and *rh7*^{1},*cry*^{b} flies harboring only the *UAS-rh7* or *pdf-Gal4* transgenes. Number of flies tested: control, n=16; *UAS-rh7*/+; *rh7*^{1},*cry*^{b}, n=52; *pdf-Gal4*/+; *rh7*^{1},*cry*^{b}, n=21. **d**—**f**, Actograms of *rh7*^{1},*cry*^{b} flies expressing *UAS-rh7* in pacemaker neurons under the control of the *tim-Gal4* or *pdf-Gal4* as indicated. Number of flies tested: *UAS-rh7*/*tim-Gal4*; *rh7*^{1},*cry*^{b}, n=37; *UAS-rh7*/*pdf-Gal4*; *rh7*^{1},*cry*^{b}, n=23; *UAS-rh7-flag*/*pdf-Gal4*; *rh7*^{1},*cry*^{b}, n=21. **g**, Percentages of rhythmic and arrhythmic flies of the indicated genotypes. Fisher's exact test. *p<0.05.

Extended Data Figure 8

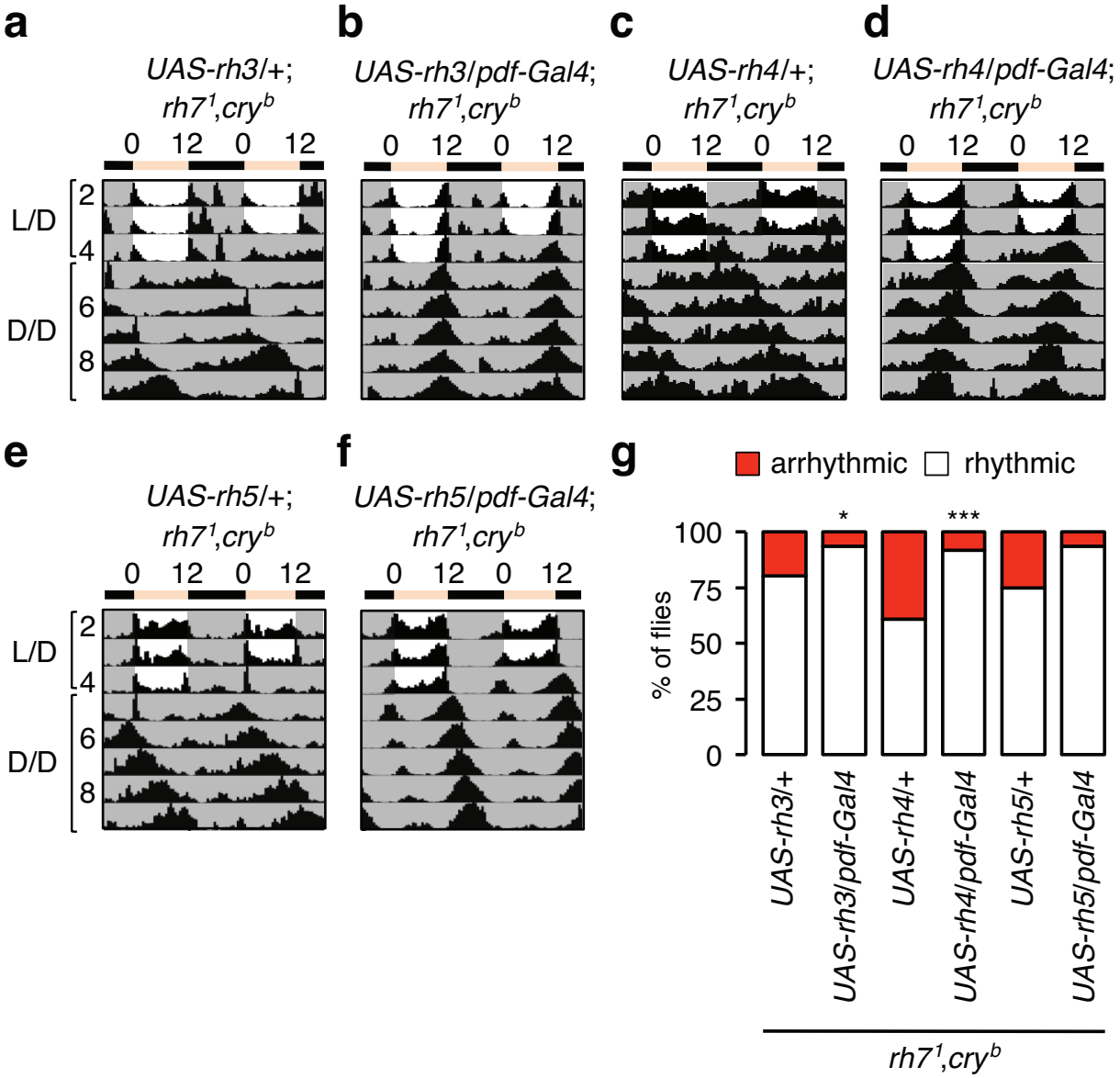

Extended Data Figure 8. Rescue of *rh7*^{1},*cry*^{b} photoentrainment defect by expression of other rhodopsins. a—**f**, Controls showing actograms of *rh7*^{1},*cry*^{b} flies harboring *UAS-rhodopsin* transgenes only, and of *rh7*^{1},*cry*^{b} flies expressing the indicated rhodopsin genes in pacemaker neurons under control of the *pdf-Gal4*. Number of flies tested: *UAS-rh3*/+; *rh7*^{1},*cry*^{b}, n=56; *UAS-rh4*/+; *rh7*^{1},*cry*^{b}, n=46; *UAS-rh5*/+; *rh7*^{1},*cry*^{b}, n=24; *UAS-rh3*/*pdf-Gal4*; *rh7*^{1},*cry*^{b}, n=64; *UAS-rh4*/*pdf-Gal4*; *rh7*^{1},*cry*^{b}, n=25; *UAS-rh5*/*pdf-Gal4*; *rh7*^{1},*cry*^{b}, n=16. **g**, Percentages of rhythmic and arrhythmic flies of the indicated genotypes. Fisher's exact test. *p<0.05. ***p<0.001.

Extended Data Figure 9

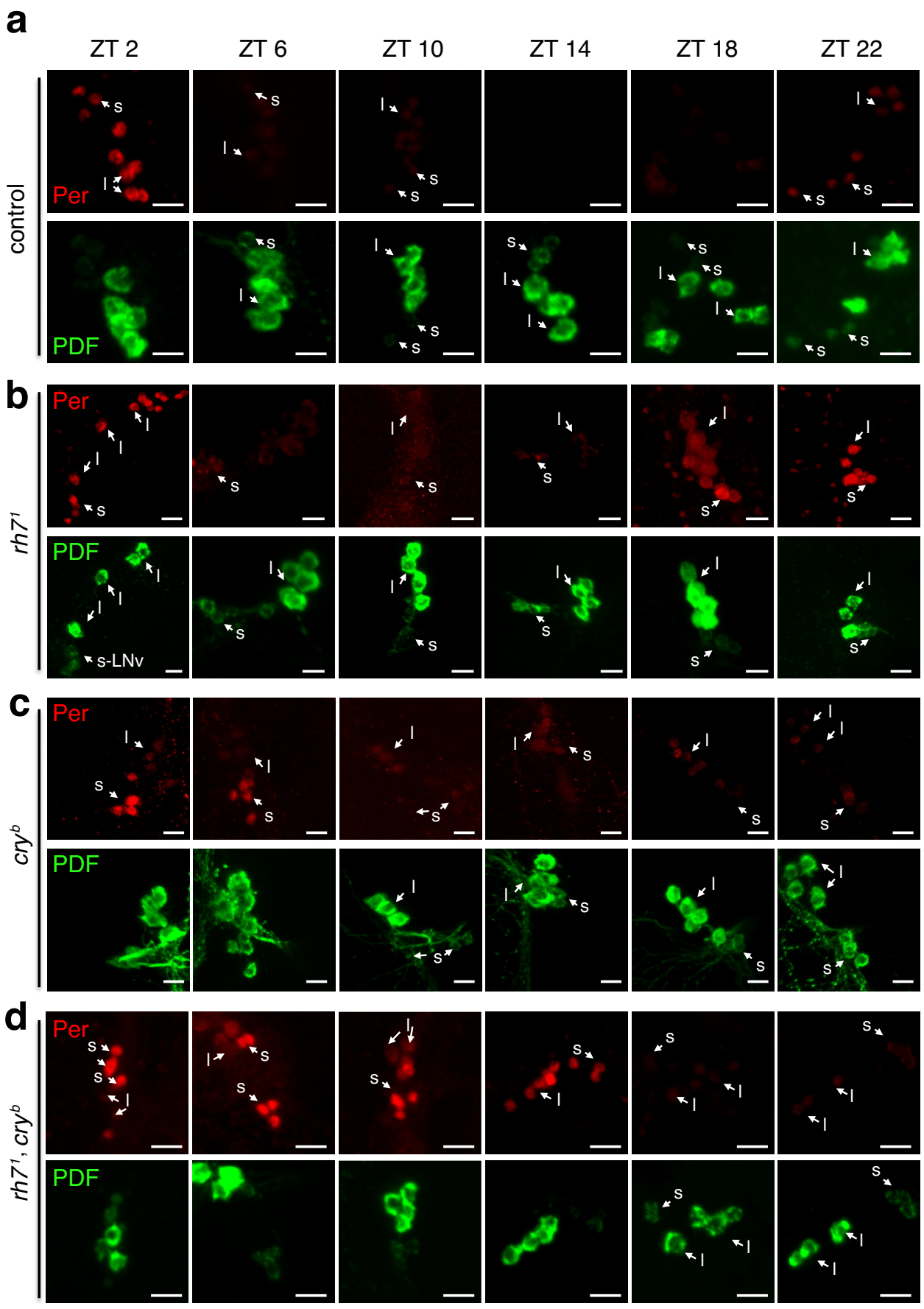

Extended Data Figure 9. Per oscillates in control, *cry^{b}*, *rh7^{1}* and *rh7^{1}*,*cry^{b}* flies. Flies were entrained under L/D cycles for 4 days and the brains were dissected on the 5th day. The ZT times indicate when the brains were fixed and dissected for staining with anti-Per (Per, upper rows, red) and anti-PDF (PDF, lower rows, green) as indicated. At least 1 s-LNV (s) and 1 l-LNV (l) are labeled in the images of each ZT point to facilitate identification of LNVs. **a**, control. **b**, *rh7^{1}*. **c**, *cry^{b}*. **d**, *rh7^{1}*,*cry^{b}*. The scale bars indicate 10 μm.

Extended Data Figure 10

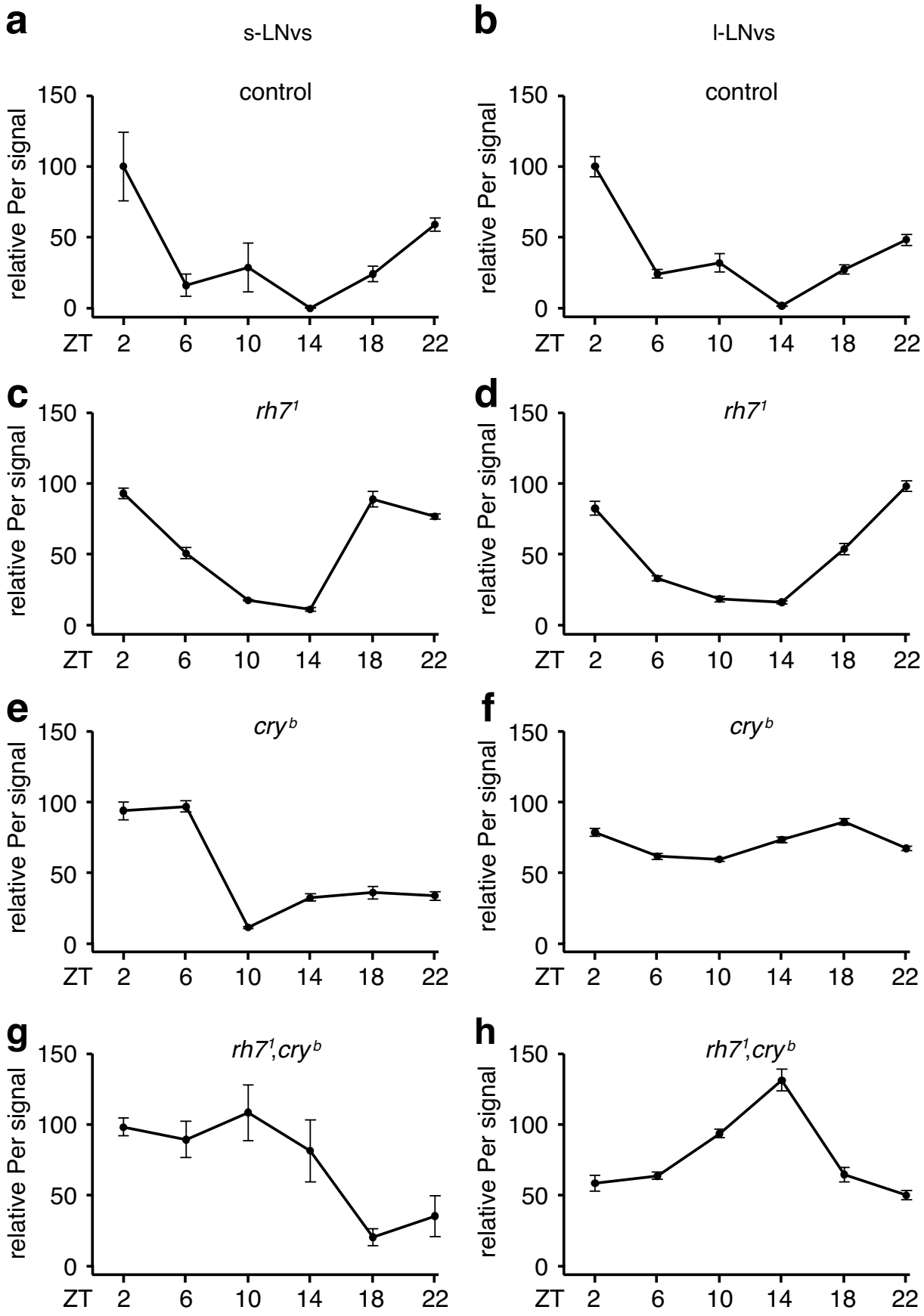

Extended Data Figure 10. Quantification of Per fluorescent intensities in PDF-positive neurons. The image quantification was performed using ImageJ. The Y-axes indicate relative Per intensities in s-LNVs and l-LNVs. The Per intensities in ZT2 of the control flies were designated as 100. For control flies, ZT10, n=6; ZT22, n=8, and n=5 for all other time points. For *rh7*^{1}, ZT2, n=9; ZT6, n=8; ZT10, n=6; ZT14, n=8; ZT18, n=8; ZT22, n=7. For *cry*^{b}, ZT2, n=8; ZT6, n=9; ZT10, n=8; ZT14, n=7; ZT18, n=10; ZT22, n=8. For *rh7*^{1},*cry*^{b}, n=5 for all time points. The error bars indicate S.E.M.s.

Extended Data Figure 11

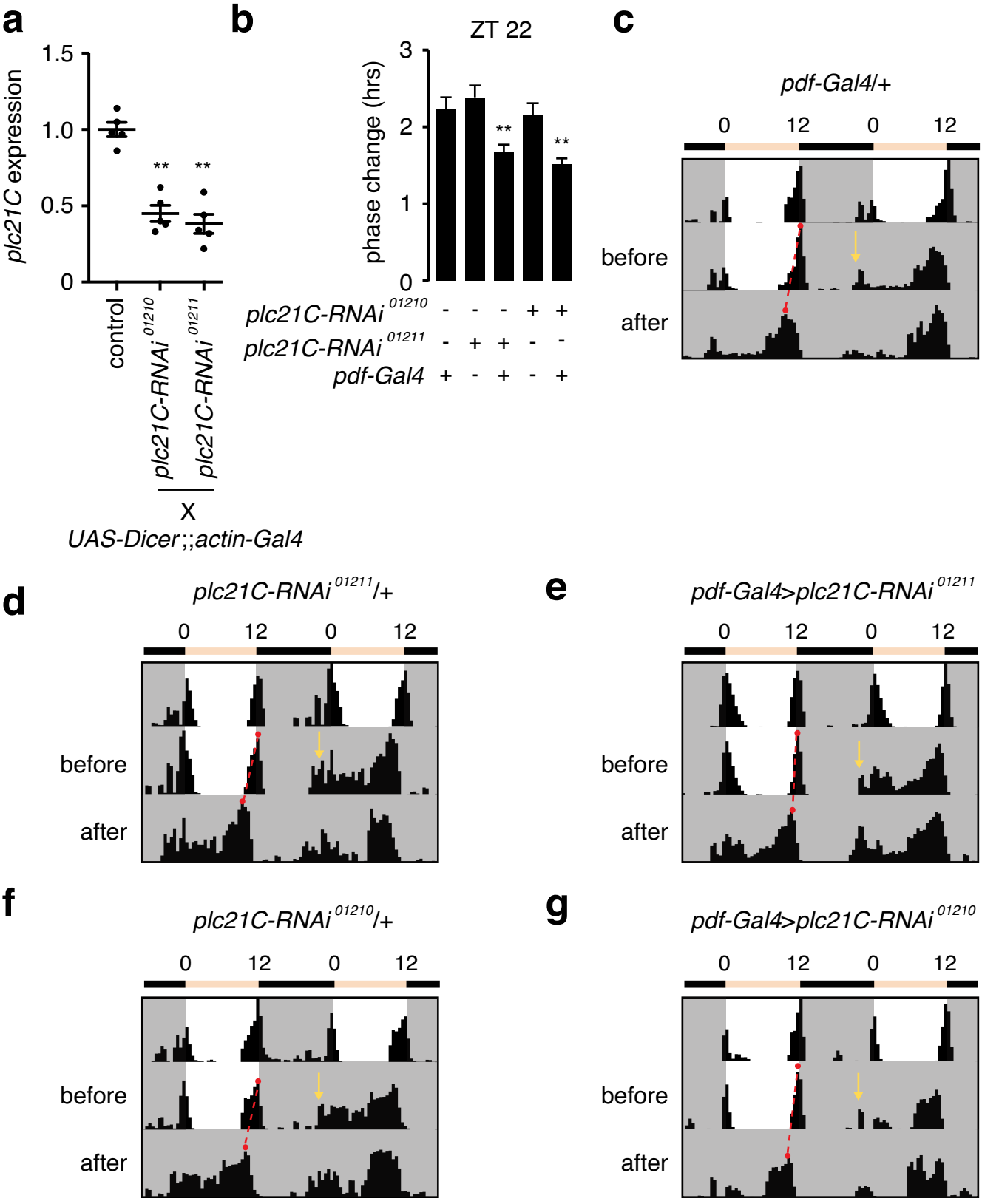

Extended Data Figure 11. Knockdown of *plc21C* in PDF-positive neurons impaired circadian phase response. a, Quantitative real-time PCR analysis of *plc21C* mRNA using RNA prepared from whole adults. The *plc21C* expression levels in each sample were normalized using *rp49* expression. The control was w^{1118}. **b**, Phase response of the indicated genotypes to a 5-min white light stimulation at ZT22. One-away ANOVA test (Kruskal-Wallis test) followed by the Dunn's test. $^{**}p<0.01$. *pdf-Gal4*/+, n=32; *plc21C-RNAi*^{01211}/+, n=31; *pdf-Gal4>plc21C-RNAi*^{01211}, n=37; *plc21C-RNAi*^{01210}/+, n= 15; *pdf-Gal4>plc21C-RNAi*^{01210}, n=32. The error bars indicate S.E.M.s. **c**—**g**, Examples of behavior before and after the 5-minute light pulse. The yellow arrows indicate the times of the 5-minute white light pulses (~600 lux). The red dots connected by the dashed red lines indicate the evening peaks before and after the light pulse.

Extended Data Figure 12

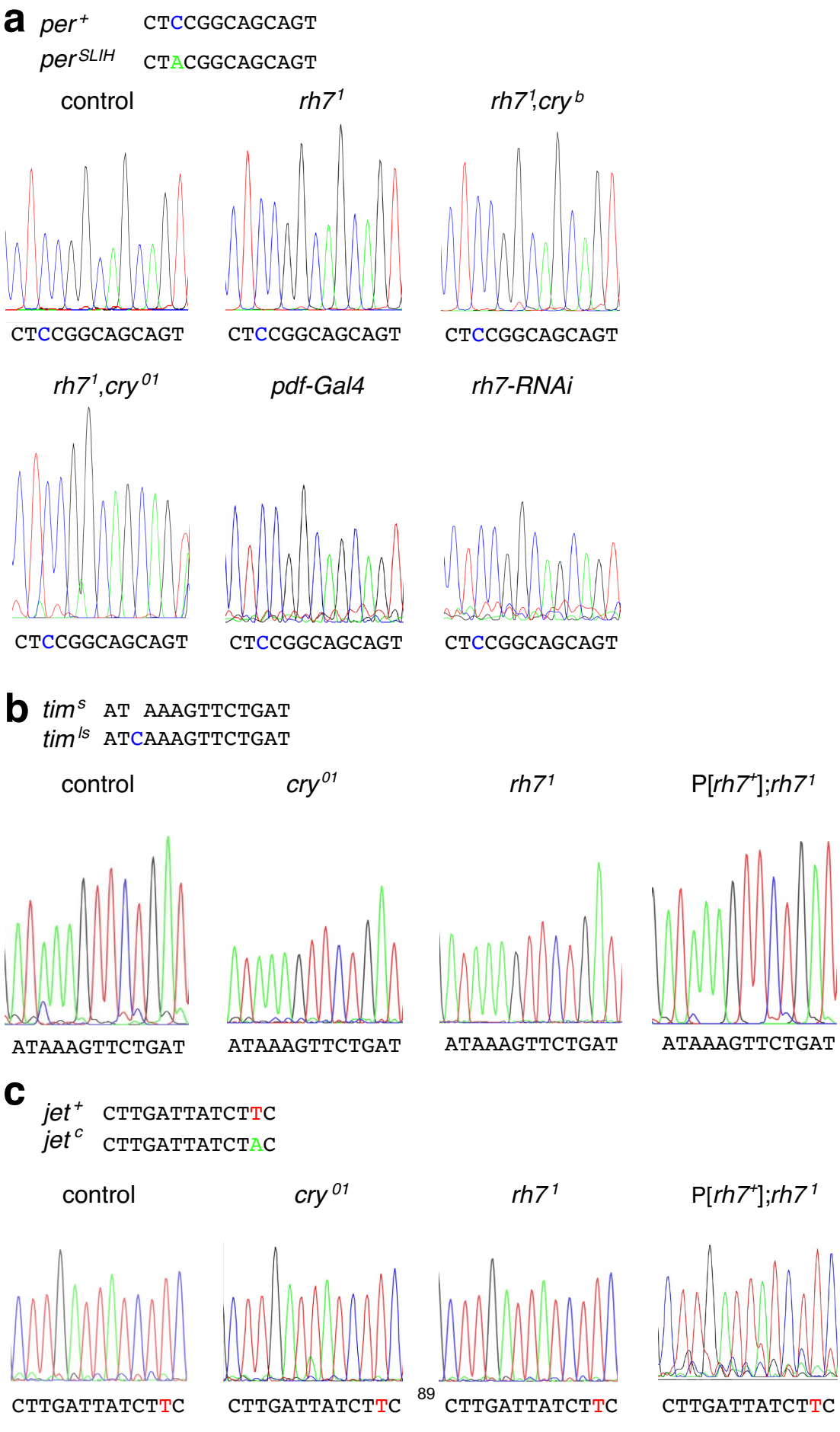

Extended Data Figure 12. Genotyping of *per*, *jet* and *tim* alleles. a, The genomic DNA sequences for per^{+} and per^{SLIH} are indicated. Shown are the sequencing results for the genomic region spanning the site of the C to A substitution in per^{SLIH}. **b**, The genomic DNA sequences for tim^{ls} and tim^{s} are indicated. Shown are the sequencing results spanning the genomic region where there is a polymorphism between tim^{s} and tim^{ls}. **c**, The genomic DNA sequences for jet^{+} and jet^{c} are indicated. Shown are the sequencing results covering the genomic region where jet^{c} allele has an A to T substitution.

Chapter 3: Coordinated activity of sleep and arousal neurons for stabilizing sleep/wake states in Drosophila

(This work is in preparation for publication as: Coordinated activity of sleep and arousal neurons for stabilizing sleep/wake states in Drosophila. **Jinfei D. Ni**, Tyler H. Ogunmowo, Hannah Hackbart, Andrew A. Verdegaal and Craig Montell[*])

Introduction

The output arm of the sleep homeostat in Drosophila is a group of neurons with projections to the dorsal fan-shaped body (dFSB) of the central complex in the brain. However, interactions between other sleep-regulating neurons and the sleep homeostat remain poorly understood. Using neurogenetic approaches combined with *in vivo* Ca^{2+} imaging, we identify two groups of sleep-regulatory neurons, which modulate the activity of the sleep homeostat in opposite directions. Sleep-promoting neurons activate the sleep homeostat with glutamate, while the arousal-promoting neurons down-regulate the sleep homeostat's output with

dopamine. Co-activating these two inputs leads to frequent swings between sleep and wake states, suggesting a temporally segregated activity profile for sleep and arousal-promoting neurons under physiology conditions. We also identify GABA as the essential neurotransmitter released by the sleep homeostat neurons and these neurons inhibit octopaminergic arousal neurons. Taken together, we suggest coordinated neuronal activity is essential for stabilizing sleep/wake states.

Results

Activation of *allatostatin-A* neurons promotes sleep independent of effects of temperature

To dissect the neuronal circuits that regulate sleep in *Drosophila,* we used a variety of *Gal4* drivers to express the warm-activated TRPA1 channel (*UAS-trpA1*) in different subsets of putative peptidergic neurons. TRPA1 is activated at 29° but not 22°C {Viswanath, 2003 #1892}. Therefore, if we drive TRPA1 expression in sleep-promoting neurons and increase the ambient temperature to 29°C, the

animals would display an increase in sleep relative to 22°C. On the other hand, if a *Gal4* line drives *UAS-trpA1* expression in neurons that promote arousal, total sleep would decline at the higher temperature (29°C).

We identified three independent *Gal4* lines that promote sleep upon thermal activation by TRPA1 (Figure. S1A; 39351, 51978, 51979). All three lines were expressed under the transcriptional control of the gene encoding the neuropeptide Allatostatin-A (AstA)(Hergarden et al., 2012). Given the similar effects of these lines, we focused on one *AstA-Gal4* line (39351) to conduct the following investigation. Control flies (*UAS-trpA1*/+ and *AstA-Gal4*/+) exhibit small increases in total sleep time after shifting the temperature from 22°C to 29°C (Figures 1A, 1B and 1D). In contrast, we found that activating *AstA-Gal4*+ neurons in *AstA>trpA1* flies by increasing the temperature to 29°C drastically increased the amount of total sleep (Figures 1C and 1D), similar to results previously reported {Chen, 2016 #5650}.

To assess the effects of depolarizing *AstA-Gal4*+ neurons in the absence of a temperature change, we used two approaches. First, we expressed NaChBac, a bacterial Na^+ channel(Nitabach et al., 2006) in *AstA-Gal4*+neurons. Compared to the controls (*AstA-Gal4*/+ and *UAS-NaChBac*/+), flies that expressed *UAS-NaChBac* under control of the *AstA-Gal4* (*AstA>NaChBac* flies) showed a substantial increase in sleep, which was most profound during the day (Figures 1E—1H). Nighttime sleep was also enhanced (Figure 1I), although the change was less pronounced since flies sleep extensively at night. Depolarizing *AstA-Gal4*+ neurons did not appear to impair the flies' locomotor ability because *AstA>NachBac* flies were as active as the control flies during the wake periods (Figure 1J).

In a second temperature independent approach, we expressed a red-light activated channel-rhodopsin, CsChrimson(Klapoetke et al., 2014) in *AstA-Gal4*+ neurons. We entrained flies using a 12-hour blue-light/dark paradigm, which did not activate CsChrimson, and then employed a red-light/dark cycle. We observed

a large increase in daytime sleep upon neuronal activation with red light (Figures 1J and 1K). Following the daytime activation of *AstA-Gal4+* neurons, the amount of sleep during the following night declined (Figures 1J and 1L), possibly as part of a homeostatic mechanism.

Sleep is regulated in part by the circadian clock(Harbison et al., 2009). To determine if chronic activation of *AstA-Gal4+* neurons disrupts circadian behavior, we entrained *AstA>NaChBac* and control flies under 12-hour light/12-hour dark cycles for 4 days and maintained them under constant darkness. These flies exhibited normal rhythmic locomotion with morning and evening anticipation under light-dark cycles. When the flies were transferred to constant darkness, the *AstA>NaChBac* files continued to show normal rhythmicity and periodicity (Figures S1B—S1E).

Requirement for AstA (SLP) neurons for promoting sleep

To identify the sleep-promoting neurons labeled by the *AstA-Gal4*, we first characterized the expression pattern of *AstA-Gal4* by expressing a membrane-tagged GFP (*UAS-mCD8::GFP*) and performed whole-mount immunofluorescence of the fly brain. GFP labeled several regions in the Drosophila brain(Ito et al., 2014), including neurons that innervate the medulla layer of the optical lobe (med), neurons innervating the primary gustatory center, the subesophageal zone (SEZ), 3 neurons located at lateral posterior region of the brain (LPN), and neurons that project to the superior lateral protocerebrum (SLP; Figures 2A and 2B).

The position of the 3 neurons at lateral posterior region of the brain resembles the lateral posterior circadian pacemaker neurons (LPNs). We generated a know-in reporter ($AstA^{lexA}$) by replace *AstA* coding region with *lexA* using CRISPR mediated homologous recombination. We expressed GFP with this $AstA^{lexA}$ reporter and found it also labeled 3 LPNs (Figures 2C). We confirmed the identity

of LPN neurons by co-staining with Tim, one of the core clock proteins expressed in the circadian pacemaker neurons. Indeed, Tim stains LPNs labeled by *AstA* reporters (*AstA>mCD8-GFP;* Figures 2D and 2E). These LPNs also express AstA neuropeptide (Figures 2F and 2G).

To identify which subsets of the *AstA-Gal4*+ neurons are sleep-promoting neurons, we used a genetic "*Flp-out*" approach to generate flies expressing *trpA1* (tagged with mCherry) in different subgroups of neurons labeled by the *AstA-Gal4* (Figure S2A). To induce stochastic expression of TRPA1 in subsets of *AstA-Gal4*+ neurons, we heat-shocked flies during the 3rd instar larval period. After eclosion, we monitored the sleep of individual flies and plotted the histogram of sleep changed exhibited by individual flies at 22°C (no TRPA1 activation) and at 29°C (TRPA1 activation) (Figure S2B).. Without inducing Flpase expression, flies exhibited a similar level of sleep regardless of whether the temperature was 22° or 29°C (*AstA>flpout-trpA1::mCherry* no heat shock).

To visualize the key sleep-promoting neurons, we compared the expression patterns of TRPA1-mCherry in the brains of flies that did not show an increase in total sleep, with the staining patterns in flies that showed significant increases in sleep upon thermoactivation. For comparison, we also expressed GFP by *AstA-Gal4*. Neurons located in the optical lobe medullar layer (med) and SEZ did not show differential expression between the two groups of flies. This indicates these neurons are not the sleep-promoting neurons, consistent with their innervation in brain areas for sensory processing. LPN neurons stained strongly with mCherry in flies that showed significant increases in sleep and are weakly stained with mCherry in flies that did not show an increase in sleep. However, of significance here, we found that mCherry stained neurons that project to SLP only in the flies with an increase of sleep (Figures S2D and S2E). These data suggest that SLP neurons (and possibly LPN neurons) are sleep-promoting neurons.

To test if LPN neurons are able to promote sleep, we expressed *CsChrimson* by $AstA^{lexA}$ reporter. $AstA^{lexA}$ reporter labels LPN, but not SLP neurons (Figures

2C). Activation of LPN neurons by red light leads to an increase of daytime sleep, compared to control flies without expression of CsChrimson. The sleep-promoting effect is diminished when tetanus toxin (TNT) is expressed with *AstA-Gal4* (also labels LPN neuron, Figures 2B; but not other neurons labled by $AstA^{lexA}$ reporter), indicating that LPN neurotransmission is required to promote sleep.

To test whether the SLP neurons promote sleep, we restricted *AstA-Gal4* induction of *UAS-NaChBac* using transgenic lines that express the Gal4 inhibitor, Gal80(Lee and Luo, 1999). We expressed Gal80 in LPN neurons by $AstA^{lexA}$ and therefore excluding NaChBac expression by *AstA-Gal4* in LPN neurons. We found these flies also sleep more than control flies. However, the sleep-promoting effect is smaller than expressing NachBac in all *AstA-Gal4*+ neurons.

Combining *AstA-Gal4* with *tsh-Gal80* abolished the sleep-promoting effect of *UAS-trpA1* induced by *AstA-Gal4* (Figure S2F). The sleep-promoting effect due to NaChbac was also deminished (Figure S2G). In contrast, combining *AstA-Gal4* with either the *Cha-Gal80* or the *Vglut-Gal80* retained sleep-promoting effect of

both *trpA1* and Nachbac induced by AstA-Gal4. We examined the expression patter of *AstA-Gal4* in combination with the above Gal80s. We found that *AstA-Gal4* labeling of LPN and SLP neurons is eliminated by *tsh-Gal80,* but retained when in combination with either the *ChaT-Gal80* or the *Vglut-Gal80* (Figures S2H—S2J) . These data support the proposal that SLP and LPN neurons are the sleep-promoting neurons labled by *AstA-Gal4*.

AstA1R1-Gal4 labels sleep-promoting neurons projecting to the fan-shaped body

To identify sleep-promoting neurons that could potentially function post-synaptic to the neurons labeled by *AstA-Gal4*, we expressed *NaChBac* under the control of a collection of *AstA receptor 1* (*AstAR1*) *Gal4*s. Among 25 different *AstAR1-Gal4* lines, 23E10 had the strongest effect, and resembled the sleep-promoting phenotype of *AstA>NaChBac* flies (Figures 3A—3F). Hereafter, we refer to this line as the *AstAR1-Gal4*. This phenotype was not due to a general

defect in locomotion since the overall activity of *AstAR1-Gal4>NaChBac* flies were not decreased relative to control flies (Figure 3G). We also expressed *CsChrimson* in *AstAR1-Gal4* neurons, and found that activating these neurons by shifting the light from blue to red drastically increased the daytime sleep in *AstAR1>CsChrimson*, but not the control flies (*AstAR1-Gal4*/+ and *UAS-CsChrimson*/+) (Figure S3A—S3E).

We examined the expression pattern of the *AstAR1-Gal4* and found that it labels neurons innervating the dorsal region of the fan-shaped body (dFSB) (Figure 3H). The dFSB is part of the central complex in the Drosophila brain, and is proposed to be one of the sleep-regulating centers (ref). The *AstAR1-Gal4* also sparsely labeled neurons innervating the SEZ and the ventral nerve code (VNC; Figure 3H)

To identify which groups of neurons labeled by the *AstAR1-Gal4* promotes sleep, we applied a genetic intersection method by combining different *Gal80*s into *AstAR1>trpA1* flies. The sleep-promoting effect in *AstAR1>trpA1* flies was

preserved when the *AstAR1-Gal4* was combined with either the *tsh-Gal80* or choline acetyltransferase (*Chat*)-*Gal80* or both (Figure 3I), which eliminate most reporter staining except for the dFSB (Figures 3J and 3K and Figures S3F—S3H). The increased sleep was abolished by introduction of the *vesicular GABA transporter* (*VGAT*)-*Gal80* (Figure 3F), which eliminates expression in dFSB neurons (Figure 3L).

AstA-Gal4+ and dFSB neurons form close associations

Since activating dFSB neurons labeled by the *AstAR1-Gal4* phenocopies the sleep- promoting effect of neuronal activation using the *AstA-Gal4*, we tested whether or not the projections of these two groups of neurons form close associations, which would occur if they formed synapses. As a first approach, we expressed dendritic (DenMark) and axonal (syt-eGFP) markers(Nicolai et al., 2010) to image the relative dendritic and axonal locations of these neurons. Neurons labeled with the *AstA-Gal4* extend axonal projections into the superior

medial protocerebrum (SMP) region of the brain (Figures 4A and 4B), whereas the *AstAR1-Gal4*+ dFSB neurons send dendrites near the SMP (Figure 4C). In addition, the axonal terminals (labeled by syt-eGFP) of the *AstAR1-Gal4*+ neurons are primarily in the dFSB (Figure 4D).

To visualize the relative positions of the *AstA-Gal4* and *AstAR1-Gal4* projections, we labeled the neurons with GFP and tdTomato respectively. We found that the SMP region was innervated by both SLP neurons (labeled by *AstA-Gal4* driven GFP) and dFSB neurons (labeled by *AstAR1-lexA* driven mCherry; Figure 4E). We also performed double labeling of LPN neurons (labeled by $AstA^{lexA}$ driven GFP) and dFSB neurons (labeled by *AstAR1-Gal4* driven mCherry); Figure 4F) and found they innervated a common SMP region.

We used GFP Reconstitution Across Synaptic Partners (GRASP) (Gordon and Scott, 2009) to probe for close associations that could be due to synaptic connections between these two sets of sleep-promoting neurons (Figure 4G),. Consistent with close associations, we detected GFP fluorescence in the SMP

region of the brain (Figure 4H), where both *AstA-Gal4+* and dFSB neurons send their projections.

***AstAR1-Gal4+* dFSB neurons function downstream of *AstA-Gal4+* neurons to promote sleep**

To test whether or not synaptic transmission is required for the sleep-promoting effect of *AstA-Gal4+* neurons, we co-expressed transgenes encoding a temperature-sensitive dynamin (Ikeda et al., 1976)(*UAS-shi^{ts}*) and *trpA1* (*UAS-trpA1*) under control of the *AstA-Gal4*. In the absence of *shi^{ts}*, thermoactivation of the *AstA-Gal4+* neurons at 29°C promotes sleep; however, blocking neurotransmission with the *shi^{ts}* transgene at the non-permissive temperature (29°C) prevents the sleep promoting-effect of neuronal activation by TRPA1(Figure S3I).

Anatomical close association between *AstA-Gal4+* neurons and dFSB neurons suggest possible synaptic transmission between them. We therefore investigate if

AstAR1-Gal4+ dFSB neurons function downstream of *AstA-Gal4+* neuron to promote sleep. We expressed CsChrimson with an *AstA-LexA* driver made with the same regulatory sequence as *AstA-Gal4*. In *AstA-LexA*>CsChrimson flies, neuronal activation by red light promotes daytime sleep (Figures 4I, 4J, 4L and 4M). However, if TNT is expressed in dFSB neurons (*AstAR1-Gal4>TNT*) to block their neurotransmission, activating *AstA-lexA+* neurons by CsChrimson no longer promotes sleep (Figures 4K, 4L and 4M). *AstA-lexA+* neuronal activation also consolidates daytime sleep into longer bouts (Figure 4O), and this effect is also abolished when dFSB neuronal transmission is blocked (Figure 4P).

Glutamate is the sleep-promoting neurotransmitter from *AstA-Gal4+* neurons to activate sleep-promote dFSB neurons

To identify the neurotransmitter released by the *AstA-Gal4+* neurons to enhance sleep, we used RNAi to knock-down genes essential for the synthesis or for the packaging of various neurotransmitters. We performed RNAi in

AstA>NaChBac flies such that the *AstA-Gal4+* neurons were constitutively activated, thereby causing an elevation in sleep. We found that the sleep-promoting effect of due to activation of *AstA-Gal4+* neurons was reduced (Figures 5A, 5F and 5G) when RNAi was directed against the gene encoding the vesicular glutamate transporter (VGLUT)(Daniels et al., 2006). However, when we performed RNAi on genes required for the synthesis of other major neurotransmitters, including acetylcholine (*ChAT*)(Itoh et al., 1986), GABA(Jackson et al., 1990) (*GAD1*) and biogenic amines (*Vmat*)(Greer et al., 2005), the sleep-promoting effect of NaChBac were unaffected (Figures 5B—G). These observations suggest an important role for glutamate for conferring the sleep-promoting effect of *AstA-Gal4+* neurons.

To test whether the *AstAR1-Gal4+* dFSB neurons respond to glutamate, we employed an *ex-vivo* brain preparation so that we can image neuronal activity in freshly dissected brains. We expressed *UAS-GCaMP6f*(Chen et al., 2013) using the *AstAR1-Gal4* and imaged the soma of dFSB neurons after applying glutamate

to the bath. We found that addition of glutamate caused increases in GCaMP6f fluorescence (Figures 5H and 5I). In contrast, the dFSB Gal4 neurons did not respond to acetylcholine, the other major excitatory neurotransmitter in the Drosophila brain (Figures 5J—5K).

GABA is required in dFSB neurons to promote sleep

We attempted to identify the neurotransmitter released by the sleep-promoting dFSB neurons. Thermoactivation of dFSB neurons (*AstAR1>trpA1*) promotes sleep (Figures 5A, 5B, 5D and 5E). However, this effect was eliminated when we used RNAi to knockdown *Gad1* in dFSB neurons (*AstAR1>trpA1*) (Figures 5C and 5F). In contrast, we still observed significant sleep-promoting effects resulting from activation of dFSB neurons when we used RNAi to reduce production of other major neurotransmitters (Figures 5G—5I). These results indicate that GABA is a critical sleep-promoting neurotransmitter synthesized in dFSB neurons (Figures, S4A—S5B).

dFSB sleep-promoting neurons inhibit arousal neurons

Octopamine (OA) is an arousal factor in *Drosophila*. Elevating octopaminergic signaling by feeding OA(Crocker and Sehgal, 2008) or by activating TDC2 (Tyrosine decarboxylase 2) expressing neurons (*tdc2-Gal4>NaChBac*)(Crocker et al., 2010) reduces nighttime sleep (Figures S5A). Nighttime sleep in *tdc2-Gal4>Nachbac* flies was fragmented, as the number of sleep bouts increased dramatically, and the average length of each nighttime sleep bout was significantly reduced (Figures, S5B—S5C).

We wondered whether dFSB neurons might down-regulate the activity of TDC2 positive arousal (OA) neurons. As a first test, we investigated for possible synaptic connections between these two sets of neurons by labeling them with different fluorescent proteins. We found that that the TDC2 reporter labeled neurons that project to multiple layers of the dFSB, including a layer where dFSB neurons also project (Figure S5D). We expressed dendritic (Denmark) and axonal

(syt-eGFP) markers under control of the *tdc2-Gal4* to visualize the potential input and output sites of the TDC2+ (OA) neurons. The majority of the OA neuronal projections in the dFSB were axonal (syt-eGFP; Figure S5E). In addition, there was a single dendritic layer in the dFSB labeled with Denmark (dsRed; Figure S5E). To determine whether OAA and dFSB neurons were in close contact, we performed GRASP analysis. Of note, the OAA neurons formed contacts with the output sites of dFSB sleep-promoting neurons (Figure S5F).

To determine if activation of dFSB neurons inhibited OAA neurons, we expressed the ATP-activated cation channel P2X2 in OAA neurons, and imaged activity with GCaMP3(Yao et al., 2012). After applying ATP, we observed a dramatic reduction in GCaMP3 fluorescence (Figures S5G—S5H). These data indicate that dFSB sleep-promoting neurons inhibit OAA arousal neurons.

Inhibition of dFSB sleep-promoting neurons by dopaminergic arousal neurons.

A dopaminergic arousal circuit projects to the dFSB(Liu et al., 2012), raising the possibility that dopaminergic arousal neurons (DA neurons) negatively regulate dFSB sleep-promoting neurons. We analyzed the anatomical relationship of dFSB and DA neurons by labeling the dFSB neurons with GFP and the DAA neurons with antibodies that recognize TH (tyrosine hydroxylase), an enzyme required for dopamine biosynthesis. Consistent with the idea that DAA neurons regulate dFSB neurons, the anti-TH and anti-GFP labeled neighboring neurons in the dFSB (Figures S6A).

To image the relative innervation patterns of the two classes of neurons, we labeled the dFSB neurons with tdTomato (*AstAR1-lexA>tdTomato*) and the DA neurons with a GFP reporter (*TH-Gal4>GFP*; Figure 7A), which is expressed in a majority of neurons stained with anti-TH (Figures S6B and S6C)(Friggi-Grelin et al., 2003; Liu et al., 2012). We found that the DA neurons project to two layers within the dFSB. The dorsal layer overlaps with the projections from dFSB

neurons (Figure 7B), suggesting possible synaptic connection between these two groups of neurons.

We used GRASP to assess whether the DAA and dFSB neuronal membranes were in close proximity—a prerequisite for forming synaptic connections. We expressed *UAS-mCD4-spGFP1-10* and *LexAop-mCD4-spGFP11* under the control of the *TH-Gal4* and *AstAR1-LexA*, respectively. We observed GRASP signals in regions of the brain containing the receptive field of the dFSB neuronal projections (Figure 7C).

To address whether dopamine inhibits dFSB neurons, we expressed *UAS-GCaMP6f* using the *AstAR1-Gal4* and imaged the soma of neurons with projections that extend to the dFSB. After applying dopamine to the buffer, there was a large reduction in GCaMP6f fluorescence (Figures 7D and 7E), indicating that dopamine inhibits sleep-promoting dFSB neurons.

To test if activation of DAA neurons inhibit dFSB neurons, we expressed the ATP-activated cation channel P2X2 in DA neurons (*TH-Gal4>P2X2*) and

examined for changes in the activity of dFSB neurons activity with GCaMP3 (*AstAR1-lexA>Gcamp3*). After applying ATP (2.5 mM final concentration), we observed a reduction in GCaMP3 fluorescence (Figure S6D). As a control, when P2X2 was co-expressed with GCaMP3 in dFSB neurons (*AstAR1-Gal4* plus *UAS-P2X2* and *UAS-GCaMP3*), application of ATP increased fluorescence (Figure S6E).

Simultaneous activation of dFSB **and DAA neurons reveals "push-pull" regulation**

Sleep-promoting dFSB neurons receive input from in the SMP (SLP neurons) and transmit output through projections to other neurons in the dFSB (OA neurons). Our GRASP data indicated that DAA neurons form connections with sleep-promoting dFSB neurons at multiple projection areas, including the SMP and dFSB. On the other hand, glutamate inputs are restricted primarily to the SMP, and are not detected in the dFSB.

We wondered if dopamine suppresses Ca^{2+} dynamics of sleep-promoting dFSB neurons at their axonal terminals, thereby negatively regulating their output. To test this, we used sytGCaMP (Cohn et al., 2015), which consists of GCaMP6s fused to synaptotagmin—a vesicular synaptic protein located in close proximity to the Ca^{2+} microdomain at axonal terminals. Immunofluorescent staining of the sytGCaMP reporter in dFSB neurons confirmed its localization at terminals in the dFSB (Figure S6F).

We imaged Ca^{2+} dynamics at the axonal terminals of sleep-promoting dFSB neurons using an *ex vivo* brain preparation. Consistent with the ability of glutamate to activate these neurons, application of glutamate to the bath solution resulted in a large elevation of Ca^{2+} (Figures 7F and 7G). When we applied dopamine to the bath, we observed a reduction of Ca^{2+} levels at the axonal terminals of the dFSB neurons (Figures 7H and 7I). Applying either of two other biogenic amines (octopamine and tyramine) did not change the Ca^{2+} dynamics (Figure S6G).

Since SLP and DA neurons are two opposite regulatory inputs acting on dFSB sleep-promoting neurons, we tested the effects on sleep when dFSB and DA neurons were activated simultaneously. Activating DA neurons lead to a drastic reduction in total sleep time (158 ±37 min; *TH-Gal4* and *UAS-NaChBac*), relative to the *UAS-NaChBac* only control (849 ±32 min ; Figures,7J and 7K). As described above, activating dFSB neurons promotes sleep (Figures 7J and 7K; 1343±36 min). Of significance, co-activating DA and dFSB neurons with NaChBac lead to a level of total sleep time (881±2 min) similar to the control flies (880±41 min; Figures 7J and 7K).

To characterize the consequences of co-activating DA and *AstA-Gal4+* neurons in greater detail, we analyzed two features of the sleep patterns: sleep bout number and bout length. When we activated *AstA-Gal4+* neurons alone (*AstA>NaChBac*), sleep bout was significantly lengthened in flies (Figure S6J). Conversely, activating DA neurons (*TH>NaChBac*) resulted in fragmented sleep, with a significantly reduced sleep bout length (Figure S6J). When *AstA-Gal4+* and

DA neurons were activated simultaneously, the flies sleep bouts were shorter than exhibited by the *UAS-NaChBac* only control, but were comparable to flies in which only the DA neurons were activated (*TH>NaChBac*; Figure S7J). Additionally, activating both the *AstA-Gal4+* and DA neurons caused the flies to initiate significantly more sleep episodes (Figure S6K).

We then compared the episodes of wakefulness of these flies. In the control flies, wake bout length is longer during the day than the night (day time, 48.9 ±5.1 min.; night time, 9.3 ±1.1 min; Figures S6L-S6M). Activating sleep-promoting dFSB neurons lead to a reduction of the bout length of daytime wakefulness, while activating arousal-promoting DAA neurons increased the bout length of nighttime wakefulness (Figures S7L-S6M). When the two groups of neurons were activated simultaneously, both daytime and nighttime activities were fragmented (Figures S6L-S6M).

Discussion

A regular sleep pattern is achieved through coordinated activation of sleep promoting neurons and suppression of arousal neurons. However, the underlying neuronal circuit that achieves this synchronization is poorly understood. Nevertheless, neurons projecting to the dFSB of the central complex are proposed to be the effecter arm of the sleep homeostat(Donlea et al., 2014; Liu et al., 2016). In our study, we identified multiple sleep and arousal neurons that comprise a neuronal network that coordinates with dFSB neurons, thereby enable flies to achieve regular sleep pattern.

We identified a group of sleep-promoting neurons located in the SLP region that use glutamate as the neurotransmitter. Glutamate receptors are proposed to promote sleep in Drosophila(Tomita et al., 2015). Yet the specific synaptic sites of sleep-promoting glutaminergic neurontransmission remains unclear. Our results pinpoint one such sleep-promoting synapse. Using the GRASP technique, we found that axons extending from SLP neurons form close associations with dendrites of dFSB sleep-promoting neurons. Based on *ex vivo* Ca^{2+} imaging

experiments, we found that glutamate acts as an excitatory neurotransmitter to activate dFSB neurons.

Dopamine is an arousal neuromodulator is both Drosophila and mammals(Liu et al., 2012; Ueno et al., 2012), and can switch dFSB neurons from an active to a quiescent state(Pimentel et al., 2016). Our GRASP analyses reveal that dopaminergic arousal (DAA) neurons form close associations at various locations along the dendritic and axonal regions of dFSB neurons. These include the SMP region where dFSB neurons receive glutaminergic input. In addition, based on staining of dendritic and axonal makers, we propose that DA neurons form synapses with axons of dFSB neurons. In support of this latter conclusion, we performed Ca^{2+} imaging and found that dopamine down-regulates Ca^{2+} levels at the axonal terminals of dFSB neurons. Thus, we propose that dopamine also contributes to arousal by suppressing the synaptic output of sleep promoting dFSB neurons.

dFSB neurons receive both sleep-promoting glutaminergic and arousal-promoting dopaminergic inputs. We found that simultaneous activation of these opposing input neurons causes the flies to rapidly swing between sleep and wake states. Consequently, the flies are unable to experience long sleep bouts at night or stay awake for long periods during the day. Our observations argue for a requirement for temporal segregation of the activity of AstA-positive sleep-promoting SLP neurons and TH positive DA arousal neurons on dFSB neurons.

An additional question is the mechanism through which dFSB neurons, which make up the effector arm of the Drosophila sleep-homeostatic circuit(Donlea et al., 2014; Liu et al., 2016), promotes sleep. GABA is an inhibitory neurotransmitter, and has been linked to sleep promotion in flies and mammals (refs). We demonstrate that dFSB use GABA as the sleep-promoting neurotransmitter. Moreover, we found that a key target for GABA are arousal-promoting octopaminergic (OAA) neurons. On the basis of GRASP analysis, we found that

dFSB neurons and OAA neurons are in close association, and may form synapses. Moreover, activating dFSB neurons inhibits OAA neurons. This inhibitory effect that is mediated by GABA might serve to maintain long sleep bouts at night, since activating OAA neurons leads to fragmentation of nighttime sleep. Finally, given that the dFSB is part of the central complex, which integrates different types of sensory information (Wolff et al., 2015), we suggest that the GABA released by dFSB neurons provides inhibitory modulation that increases the threshold for sensory responses in sleeping animals.

Author contributions

J.N. and C.M designed the experiments, interpreted the data and wrote the manuscript with the input from T.O. J.N. performed most of the experiments. T.O. contributes to Ca^{2+} imaging and immunohistochemistry. H.H and A.V. contributed to the initial screen and characterization of the reporter expression pattern.

Acknowledgments

The work was supported by a grant to C.M. from the National Institute on Deafness and other Communication Disorders (DC007864). We thank Drs. Orie Shafer and Julie Simpson for transgenic flies, Drs. Mark Wu and Sha Liu for guidance for performing sleep assays and Dr. William Joiner for sharing sleeplab software. We also thank the Bloomington Stock Center for providing fly stocks.

Experimental Model and Subject Details

Animals

Flies (Drosophila Melanogaster) were cultured on cornmeal-agar-molasses medium under 12 hour light/dark cycle at room-temperature and ambient humidity. Detailed information regarding specific stains and genotypes are provided in the Key Resources Table section.

Methods Details

Immunohistochemistry

For whole-mount brain immunohistochemistry, fly brains are dissected in PBS+0.3%tritonX100 (PBST), fixed with 4%PFA in PBST at room temperature for 20 minutes. Brains were briefly washed with PBST and blocked with PBST+5% normal goat serum (NGS) at 4C for 1 hour. Primary antibodies diluted in PBST+5%NGS were incubated with the brain for over-night. After three washes with PBST, secondary antibodies diluted in PBST+5%NGS were incubated with the brain for over-night. Brains were washed three times and mounted in vectashield (Vector labs) on glass slides. To imaging GRASP signal, we dissected the fly brains in PBST, fixed with 4%PFA in PBST at room temperature for 20 minutes and were briefly washed to get rid of the PFA before mounting. Brain images were taken with an upright Zeiss LSM700 confocal miscroscope with 20X, 40X (oil) or 63X (oil) lens.

Ca^{2+} imaging in brains

Flies subject to whole-brain Ca^{2+} imaging were anaesthetized on ice and dissected in AHL buffer (Recipe:) and transferred to a imaging chamber with a glass bottom made from cover slides (brand). Brains were immobilized with a harp (brand) and imaged using an inverted Zeiss LSM800 confocal microscope. Neuron soma or neutrophils to imaging were first found and bring to focus using mercury lamp and scanned with time-lapse mode for Ca^{2+} imaging. >30 cycle were imaged for base line measurement before adding relative chemicals to the bath. Chemicals were added to the imaging chamber in less than 5 seconds during the imaging. The average intensity during the 10 cycles before adding the chemical is used as the baseline (F) to calculate ΔF.

Behavior

To measure fly sleep, we use 3-7 day old female flies. Individual flies were loaded into glass tubes (provided with the Drosophila Actometer assay platform provided by Trikinetics) with 5%sucrose + 1% agarose as food source at one end and a small cotton plug at the other end. Flies were entrained for at least two days

before activity data were collected for analysis. Activity data were collect in one-minute bin for further process using sleeplab software. If no activity was detected by the Drosophila Actometer assay platform for more than 5 minutes, the fly was considered to be in a sleep status. Sleep assay were performed under 25C with white LED light unless otherwise mentioned. For optogenetic stimulation, flies were cultured in regular food supplied with all-trans retinal in dark for 24 hours before loaded into glass tubes for activity measurement.

Quantification and Statistical Analysis

For analysis sleep behavior, multiple animals were tested and sleep index of individual animals were quantified independently. Numbers of animals tested are all biological replicates with n numbers indicated in all figure legends. Err bars indicates SEM with indicated P values for statistical analysis. * indicates $p<0.05$ and ** indicates $p<0.01$. Specific statistical methods are stated in all figure legends.

References

Borbely, A.A. (1982). A two process model of sleep regulation. Human neurobiology 1, 195-204.

Bussell, J.J., Yapici, N., Zhang, S.X., Dickson, B.J., and Vosshall, L.B. (2014). Abdominal-B neurons control Drosophila virgin female receptivity. Curr Biol 24, 1584-1595.

Chen, J., Reiher, W., Hermann-Luibl, C., Sellami, A., Cognigni, P., Kondo, S., Helfrich-Förster, C., Veenstra, J.A., and Wegener, C. (2016). Allatostatin A signalling in Drosophila regulates feeding and sleep and Is modulated by PDF. PLoS Genet 12, e1006346.

Chen, T.W., Wardill, T.J., Sun, Y., Pulver, S.R., Renninger, S.L., Baohan, A., Schreiter, E.R., Kerr, R.A., Orger, M.B., Jayaraman, V., et al. (2013). Ultrasensitive fluorescent proteins for imaging neuronal activity. Nature 499, 295-300.

Clyne, J.D., and Miesenbock, G. (2008). Sex-specific control and tuning of the pattern generator for courtship song in Drosophila. Cell 133, 354-363.

Cohn, R., Morantte, I., and Ruta, V. (2015). Coordinated and Compartmentalized Neuromodulation Shapes Sensory Processing in Drosophila. Cell 163, 1742-1755.

Crocker, A., and Sehgal, A. (2008). Octopamine regulates sleep in drosophila through protein kinase A-dependent mechanisms. The Journal of neuroscience : the official journal of the Society for Neuroscience 28, 9377-9385.

Crocker, A., Shahidullah, M., Levitan, I.B., and Sehgal, A. (2010). Identification of a neural circuit that underlies the effects of octopamine on sleep:wake behavior. Neuron 65, 670-681.

Daniels, R.W., Collins, C.A., Chen, K., Gelfand, M.V., Featherstone, D.E., and DiAntonio, A. (2006). A single vesicular glutamate transporter is sufficient to fill a synaptic vesicle. Neuron 49, 11-16.

Donlea, J.M., Pimentel, D., and Miesenbock, G. (2014). Neuronal machinery of sleep homeostasis in Drosophila. Neuron 81, 860-872.

Friggi-Grelin, F., Coulom, H., Meller, M., Gomez, D., Hirsh, J., and Birman, S. (2003). Targeted gene expression in Drosophila dopaminergic cells using regulatory sequences from tyrosine hydroxylase. Journal of neurobiology 54, 618-627.

Gordon, M.D., and Scott, K. (2009). Motor control in a Drosophila taste circuit. Neuron 61, 373-384.

Greer, C.L., Grygoruk, A., Patton, D.E., Ley, B., Romero-Calderon, R., Chang, H.Y., Houshyar, R., Bainton, R.J., Diantonio, A., and Krantz, D.E. (2005). A splice variant of the Drosophila vesicular monoamine transporter contains a conserved trafficking domain and functions in the storage of dopamine, serotonin, and octopamine. Journal of neurobiology 64, 239-258.

Griffith, L.C. (2013). Neuromodulatory control of sleep in Drosophila melanogaster: integration of competing and complementary behaviors. Current opinion in neurobiology 23, 819-823.

Harbison, S.T., Mackay, T.F., and Anholt, R.R. (2009). Understanding the neurogenetics of sleep: progress from Drosophila. Trends Genet 25, 262-269.

Hergarden, A.C., Tayler, T.D., and Anderson, D.J. (2012). Allatostatin-A neurons inhibit feeding behavior in adult Drosophila. Proceedings of the National Academy of Sciences of the United States of America 109, 3967-3972.

Ikeda, K., Ozawa, S., and Hagiwara, S. (1976). Synaptic transmission reversibly conditioned by single-gene mutation in Drosophila melanogaster. Nature 259, 489-491.

Iranzo, A. (2016). Sleep in Neurodegenerative Diseases. Sleep medicine clinics 11, 1-18.

Ito, K., Shinomiya, K., Ito, M., Armstrong, J.D., Boyan, G., Hartenstein, V., Harzsch, S., Heisenberg, M., Homberg, U., Jenett, A., et al. (2014). A systematic nomenclature for the insect brain. Neuron 81, 755-765.

Itoh, N., Slemmon, J.R., Hawke, D.H., Williamson, R., Morita, E., Itakura, K., Roberts, E., Shively, J.E., Crawford, G.D., and Salvaterra, P.M. (1986). Cloning of Drosophila choline acetyltransferase cDNA. Proceedings of the National Academy of Sciences of the United States of America 83, 4081-4085.

Jackson, F.R., Newby, L.M., and Kulkarni, S.J. (1990). Drosophila GABAergic systems: sequence and expression of glutamic acid decarboxylase. Journal of neurochemistry 54, 1068-1078.

Kayser, M.S., Yue, Z., and Sehgal, A. (2014). A critical period of sleep for development of courtship circuitry and behavior in Drosophila. Science 344, 269-274.

Kitamoto, T. (2002). Conditional disruption of synaptic transmission induces male-male courtship behavior in Drosophila. Proceedings of the National Academy of Sciences of the United States of America 99, 13232-13237.

Klapoetke, N.C., Murata, Y., Kim, S.S., Pulver, S.R., Birdsey-Benson, A., Cho, Y.K., Morimoto, T.K., Chuong, A.S., Carpenter, E.J., Tian, Z., et al. (2014). Independent optical excitation of distinct neural populations. Nature methods 11, 338-346.

Kondo, S., and Ueda, R. (2013). Highly improved gene targeting by germline-specific Cas9 expression in Drosophila. Genetics 195, 715-721.

Lee, T., and Luo, L. (1999). Mosaic analysis with a repressible cell marker for studies of gene function in neuronal morphogenesis. Neuron 22, 451-461.

Liu, Q., Liu, S., Kodama, L., Driscoll, M.R., and Wu, M.N. (2012). Two dopaminergic neurons signal to the dorsal fan-shaped body to promote wakefulness in Drosophila. Current biology : CB 22, 2114-2123.

Liu, S., Liu, Q., Tabuchi, M., and Wu, M.N. (2016). Sleep Drive Is Encoded by Neural Plastic Changes in a Dedicated Circuit. Cell 165, 1347-1360.

Myers, M.P., Wager-Smith, K., Rothenfluh-Hilfiker, A., and Young, M.W. (1996). Light-induced degradation of TIMELESS and entrainment of the Drosophila circadian clock. Science 271, 1736-1740.

Nicolai, L.J., Ramaekers, A., Raemaekers, T., Drozdzecki, A., Mauss, A.S., Yan, J., Landgraf, M., Annaert, W., and Hassan, B.A. (2010). Genetically encoded dendritic marker sheds light on neuronal connectivity in Drosophila. Proceedings of the National Academy of Sciences of the United States of America 107, 20553-20558.

Nitabach, M.N., Wu, Y., Sheeba, V., Lemon, W.C., Strumbos, J., Zelensky, P.K., White, B.H., and Holmes, T.C. (2006). Electrical hyperexcitation of lateral ventral pacemaker neurons desynchronizes downstream circadian oscillators in the fly circadian circuit and induces multiple behavioral periods. The Journal of neuroscience : the official journal of the Society for Neuroscience 26, 479-489.

Parisky, K.M., Agosto, J., Pulver, S.R., Shang, Y., Kuklin, E., Hodge, J.J., Kang, K., Liu, X., Garrity, P.A., Rosbash, M., et al. (2008). PDF cells are a GABA-responsive wake-promoting component of the Drosophila sleep circuit. Neuron 60, 672-682.

Pimentel, D., Donlea, J.M., Talbot, C.B., Song, S.M., Thurston, A.J., and Miesenbock, G. (2016). Operation of a homeostatic sleep switch. Nature 536, 333-337.

Ren, X., Sun, J., Housden, B.E., Hu, Y., Roesel, C., Lin, S., Liu, L.P., Yang, Z., Mao, D., Sun, L., et al. (2013). Optimized gene editing technology for Drosophila melanogaster using germ line-specific Cas9. Proceedings of the National Academy of Sciences of the United States of America 110, 19012-19017.

Sehgal, A., and Mignot, E. (2011). Genetics of sleep and sleep disorders. Cell 146, 194-207.

Sehgal, A., Price, J.L., Man, B., and Young, M.W. (1994). Loss of circadian behavioral rhythms and per RNA oscillations in the Drosophila mutant timeless. Science 263, 1603-1606.

Shafer, O.T., Helfrich-Forster, C., Renn, S.C., and Taghert, P.H. (2006). Reevaluation of Drosophila melanogaster's neuronal circadian pacemakers reveals new neuronal classes. The Journal of comparative neurology 498, 180-193.

Sweeney, S.T., Broadie, K., Keane, J., Niemann, H., and O'Kane, C.J. (1995). Targeted expression of tetanus toxin light chain in Drosophila specifically eliminates synaptic transmission and causes behavioral defects. Neuron 14, 341-351.

Tomita, J., Ueno, T., Mitsuyoshi, M., Kume, S., and Kume, K. (2015). The NMDA Receptor Promotes Sleep in the Fruit Fly, Drosophila melanogaster. PloS one 10, e0128101.

Tsuneki, H., Sasaoka, T., and Sakurai, T. (2016). Sleep Control, GPCRs, and Glucose Metabolism. Trends in endocrinology and metabolism: TEM 27, 633-642.

Ueno, T., Tomita, J., Tanimoto, H., Endo, K., Ito, K., Kume, S., and Kume, K. (2012). Identification of a dopamine pathway that regulates sleep and arousal in Drosophila. Nature neuroscience 15, 1516-1523.

Viswanath, V., Story, G.M., Peier, A.M., Petrus, M.J., Lee, V.M., Hwang, S.W., Patapoutian, A., and Jegla, T. (2003). Opposite thermosensor in fruitfly and mouse. Nature 423, 822-823.

Weber, F., and Dan, Y. (2016). Circuit-based interrogation of sleep control. Nature 538, 51-59.

Westermann, J., Lange, T., Textor, J., and Born, J. (2015). System consolidation during sleep - a common principle underlying psychological and immunological memory formation. Trends in neurosciences 38, 585-597.

Wolff, T., Iyer, N.A., and Rubin, G.M. (2015). Neuroarchitecture and neuroanatomy of the Drosophila central complex: A GAL4-based dissection of

protocerebral bridge neurons and circuits. The Journal of comparative neurology 523, 997-1037.

Yao, Z., Macara, A.M., Lelito, K.R., Minosyan, T.Y., and Shafer, O.T. (2012). Analysis of functional neuronal connectivity in the Drosophila brain. Journal of neurophysiology 108, 684-696.

Yu, Z., Ren, M., Wang, Z., Zhang, B., Rong, Y.S., Jiao, R., and Gao, G. (2013). Highly efficient genome modifications mediated by CRISPR/Cas9 in Drosophila. Genetics 195, 289-291.

Figure 1

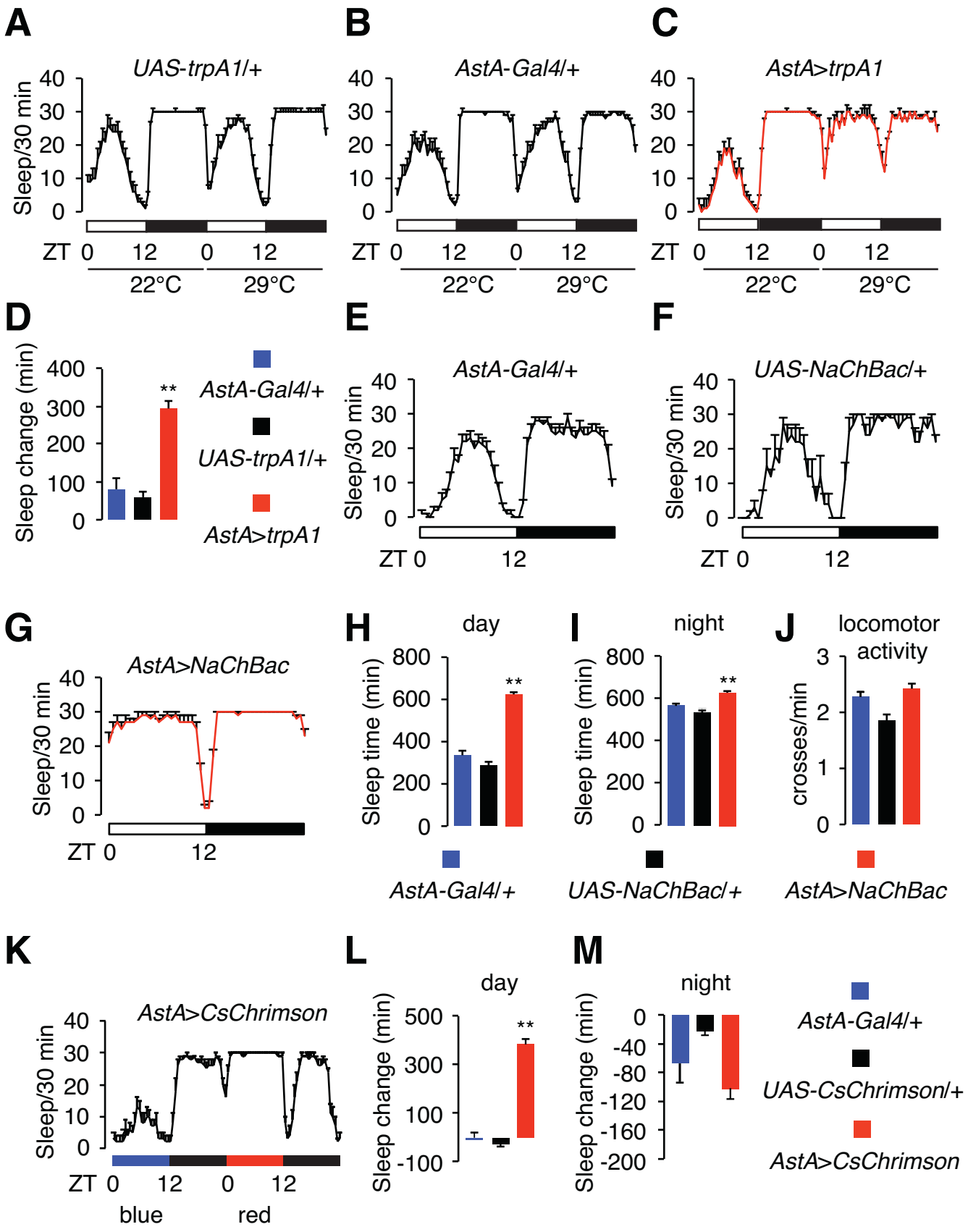
A
UAS-trpA1/+
Sleep/30 min
40
30
20
10
0
ZT 0 12 0 12
22°C 29°C
B
AstA-Gal4/+
C
AstA>trpA1
D
Sleep change (min)
400
300
200
100
0
**
AstA-Gal4/+
UAS-trpA1/+
AstA>trpA1
E
AstA-Gal4/+
ZT 0 12
F
UAS-NaChBac/+
G
AstA>NaChBac
H
day
Sleep time (min)
800
600
400
200
0
**
AstA-Gal4/+
I
night
UAS-NaChBac/+
J
locomotor activity
crosses/min
3
2
1
0
AstA>NaChBac
K
AstA>CsChrimson
blue red
L
day
Sleep change (min)
500
300
100
-100
**
M
night
0
-40
-80
-120
-160
-200
AstA-Gal4/+
UAS-CsChrimson/+
AstA>CsChrimson

Figure legends

Figure 1. Activation *AstA-Gal4* neuron promotes sleep. (**A-C**) Sleep profile of control flies (*UAS-trpA1*/+ and *AstA-Gal4*/+) and flies expressed *UAS-trpA1* under the control of the *AstA-Gal4* (*AstA>trpA1*). Light/dark bar beneath the sleep profile indicates the day and night. ZT0 indicate the time when the light turned on. Experimental temperature is indicated below the light/dark bar. Sleep time is plotted in 30-min bins. (**D**) Quantification of warm temperature induced sleep change (24-hour total sleep time at 29ºC - 24-hour total sleep time at 22ºC). n=23-78; ±SEMs; **p<0.01, one way ANOVA with Dunnett's test. (**E-G**) Sleep profile of control flies (*AstA-Gal4*/+ and *UAS-NaChBac*/+) and *AstA>NaChbac* flies. (**H-I**) Quantification of daytime sleep and nighttime sleep of indicated flies. (**J**) Quantification of locomotion activity of indicated flies during wakefulness. N=16-68; err bar, SEM; **p<0.01, one way ANOVA with Dunnett's test. (**K**) Acute activation of *AstA-Gal4* neurons by CsChrimson leads to increase of sleep. Flies were entrained with 12-hour blue light/dark cycle for 3 days and shifted to red light/dark cycle on the fourth day. Sleep profiles with blue light (non-activation condition) and red light (Cschrimson activation condition) were plotted. (**L-M**) Quantification of daytime and nighttime sleep change induced by CsChrimson activation. *AstA-Gal4/+* and *UAS-CsChrimson/+* serves as controls. n = 32-70; err bar, SEM; **p<0.01, one way ANOVA with Dunnett's test.

Figure 2

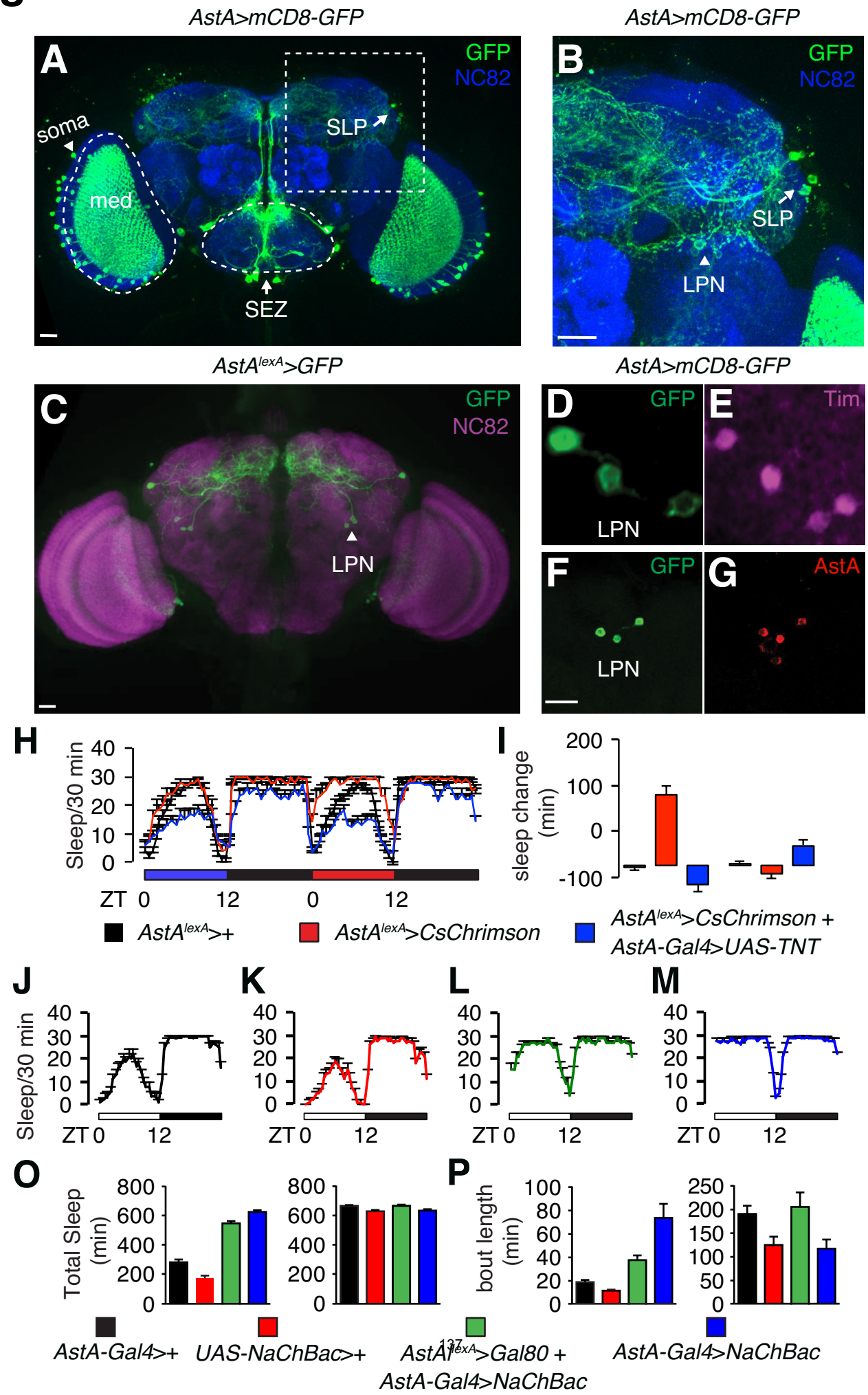
AstA>mCD8-GFP
A
GFP
NC82
soma
med
SLP
SEZ
AstA>mCD8-GFP
B
GFP
NC82
SLP
LPN
AstA^lexA>GFP
C
GFP
NC82
LPN
AstA>mCD8-GFP
D
GFP
LPN
E
Tim
F
GFP
LPN
G
AstA
H
Sleep/30 min
40
30
20
10
0
ZT 0
12
0
12
AstA^lexA>+
AstA^lexA>CsChrimson
I
sleep change (min)
200
100
0
-100
AstA^lexA>CsChrimson + AstA-Gal4>UAS-TNT
J
K
L
M
Sleep/30 min
ZT 0
12
O
Total Sleep (min)
800
600
400
200
0
AstA-Gal4>+
UAS-NaChBac>+
P
bout length (min)
100
80
60
40
20
0
250
200
150
100
50
0
AstA^lexA>Gal80 + AstA-Gal4>NaChBac
AstA-Gal4>NaChBac

Figure 2. Identification of a subset of neurons labeled by *AstA-Gal4* as the sleep-promoting neurons. (**A**) Immunohistochemistry of the whole-mount Drosophila (*AstA>mCD8-GFP*) brain. Green: anti-GFP, Blue: anti-NC82. (**B**) Zoom-in view of boxed region in A. Arrow indicates SLP neurons and arrowhead indicates the LPN neurons. The scale bars represents 20*μ*m. (**C**) Immunohistochemistry of the whole-mount Drosophila (*AstA^{lexA}>GFP*) brain. Green: anti-GFP, Magenta: anti-NC82. The scale bars represents 20*μ*m. (**D-G**) Immunohistochemistry of the whole-mount Drosophila (*AstA>mCD8-GFP*) brain. D and E show the co-staining of GFP and Tim in LPN neurons. F and G show the co-staining GFP and AstA in LPN neurons. The scale bars represents 20*μ*m. **(H)** Sleep profiles of indicated flies with blue light (non-activation condition) and red light (Cschrimson activation condition) were plotted. Sleep time is plotted in 30-min bins. **(I)** Quantification of daytime and nighttime sleep change induced by CsChrimson activation. *AstA^{lexA}/+* serves as controls. n = 10-32; err bar, SEM; **p<0.01, one way ANOVA with Dunnett's test. Note that red light induced sleep-promoting effect of *AstA^{lexA}>CsChrimson* is abolished when in combination with *AstA-Ga4>UAS-TNT*. **(J-K)** Sleep profile of control flies (*AstA-Gal4/+* and *UAS-NaChBac/+*), *AstA>NaChBac* flies and *AstA>NaChbac + AstA^{lexA}>Gal80* flies. **(O)** Quantification of daytime sleep and nighttime sleep of indicated flies. **(P)**

Quantification of daytime sleep and nighttime sleep-bout length of indicated flies. Note that the genotypes of flies tested in J-P are indicated with corresponding color. n = 23-32; err bar, SEM; **p<0.01, one way ANOVA with Dunnett's test.

Figure 3

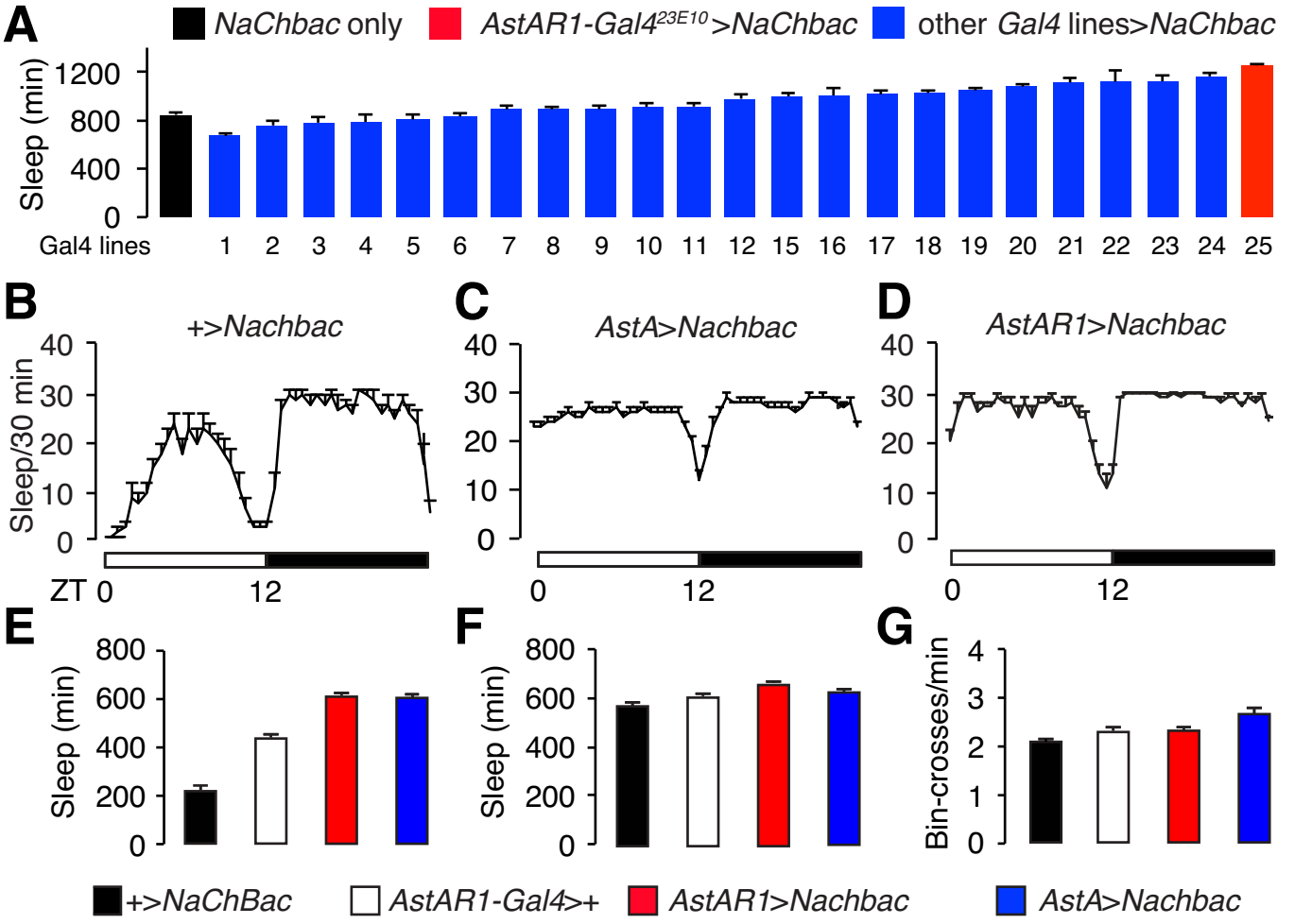
A
NaChbac only
AstAR1-Gal4^23E10>NaChbac
other Gal4 lines>NaChbac
Sleep (min)
1200
800
400
0
Gal4 lines
1 2 3 4 5 6 7 8 9 10 11 12 15 16 17 18 19 20 21 22 23 24 25
B
+>Nachbac
C
AstA>Nachbac
D
AstAR1>Nachbac
Sleep/30 min
40
30
20
10
0
ZT 0
12
E
F
G
Sleep (min)
800
600
400
200
0
Bin-crosses/min
4
3
2
1
0
+>NaChBac
AstAR1-Gal4>+
AstAR1>Nachbac
AstA>Nachbac

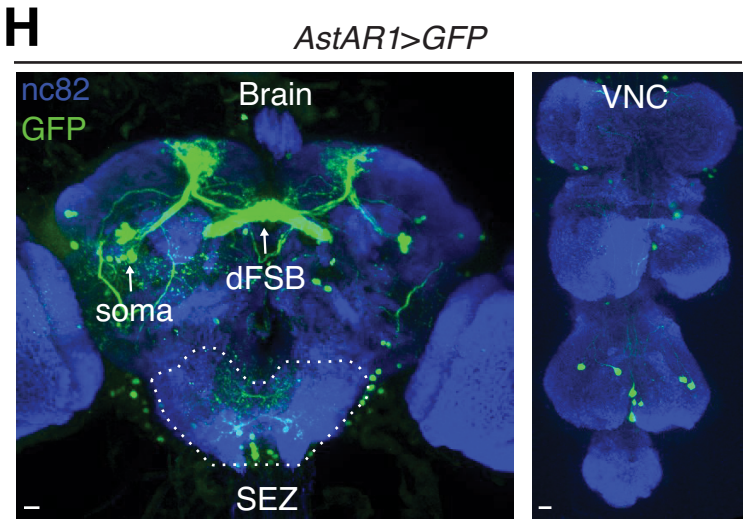
H
AstAR1>GFP
nc82
GFP
Brain
VNC
dFSB
soma
SEZ

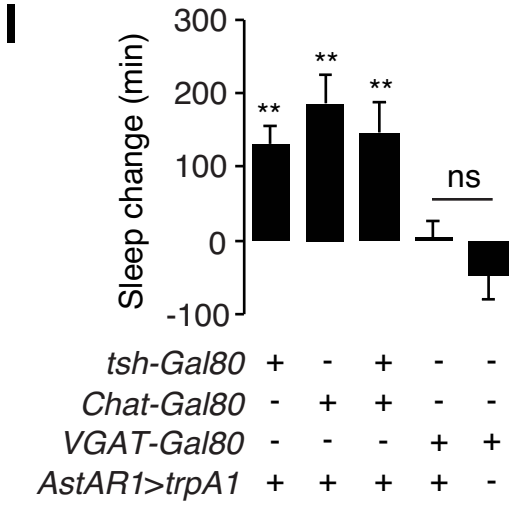
I
Sleep change (min)
300
200
100
0
-100
**
**
**
ns
tsh-Gal80 + - + - -
Chat-Gal80 - + + - -
VGAT-Gal80 - - - + +
AstAR1>trpA1 + + + + -

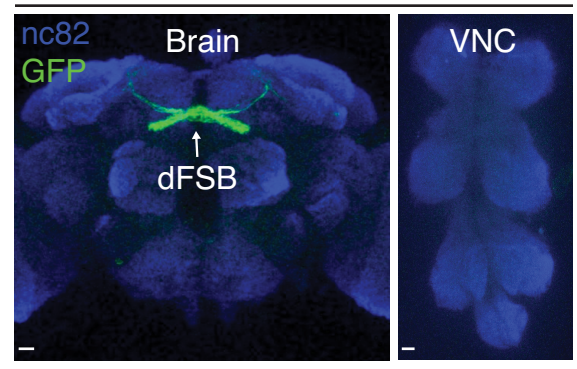
J
AstAR1>GFP + tsh-Gal80
nc82
GFP
Brain
dFSB
VNC

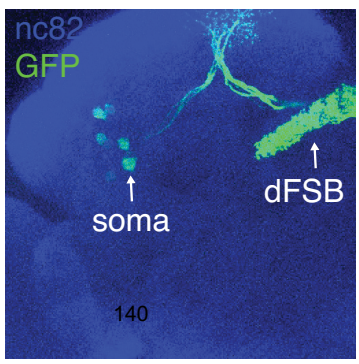
K
AstAR1>GFP + tsh-Gal80
nc82
GFP
soma
dFSB
140

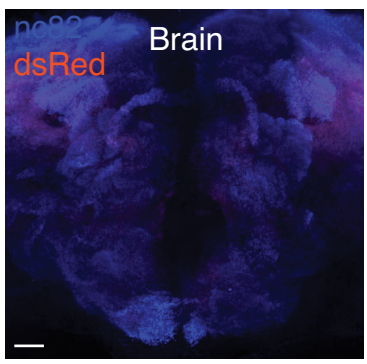
L
AstAR1>dsRed+VGAT-Gal80
dsRed
Brain

Figure 3. dFSB sleep-promoting neurons labeled by an *AstAR1-Gal4* reporter. (**A**) Screen for sleep-promoting neurons labeled by different *AstAR1-Gal4*s. Total sleep times of a 24-hour light/dark cycle are quantified; (n=8-53). We focused on one line (23E10) and named this line *AstAR1-Gal4* hereafter. (**B-D**) Sleep profile of *UAS-NaChbac*/+, *AstA>NaChbac* and *AstAR1>NaChbac* flies. (**E-F**) Quantification of daytime sleep and nighttime sleep of indicated flies. (**G**) Quantification of locomotion activity of indicated flies during wakefulness (n=16-48). err bar, SEM; **p<0.01, one way ANOVA with Dunnett's test. (**H**) Immunohistochemistry of the whole-mount Drosophila (*AstAR1>GFP*) brain. Green: anti-GFP, Blue: anti-NC82. (**I**) Quantification of warm temperature induced sleep change (n=18-33). err bar, SEM; **p<0.01, one way ANOVA with Dunnett's test. (**J-K**) Brain Immunohistochemistry *AstAR1>GFP* Drosophila after suppressed by *tsh-Gal80*. **(L)** Brain Immunohistochemistry *AstAR1>dsRed* flies after suppressed by *VGAT-Gal80*. The scale bars in all panels represent 20μm.

Figure 4

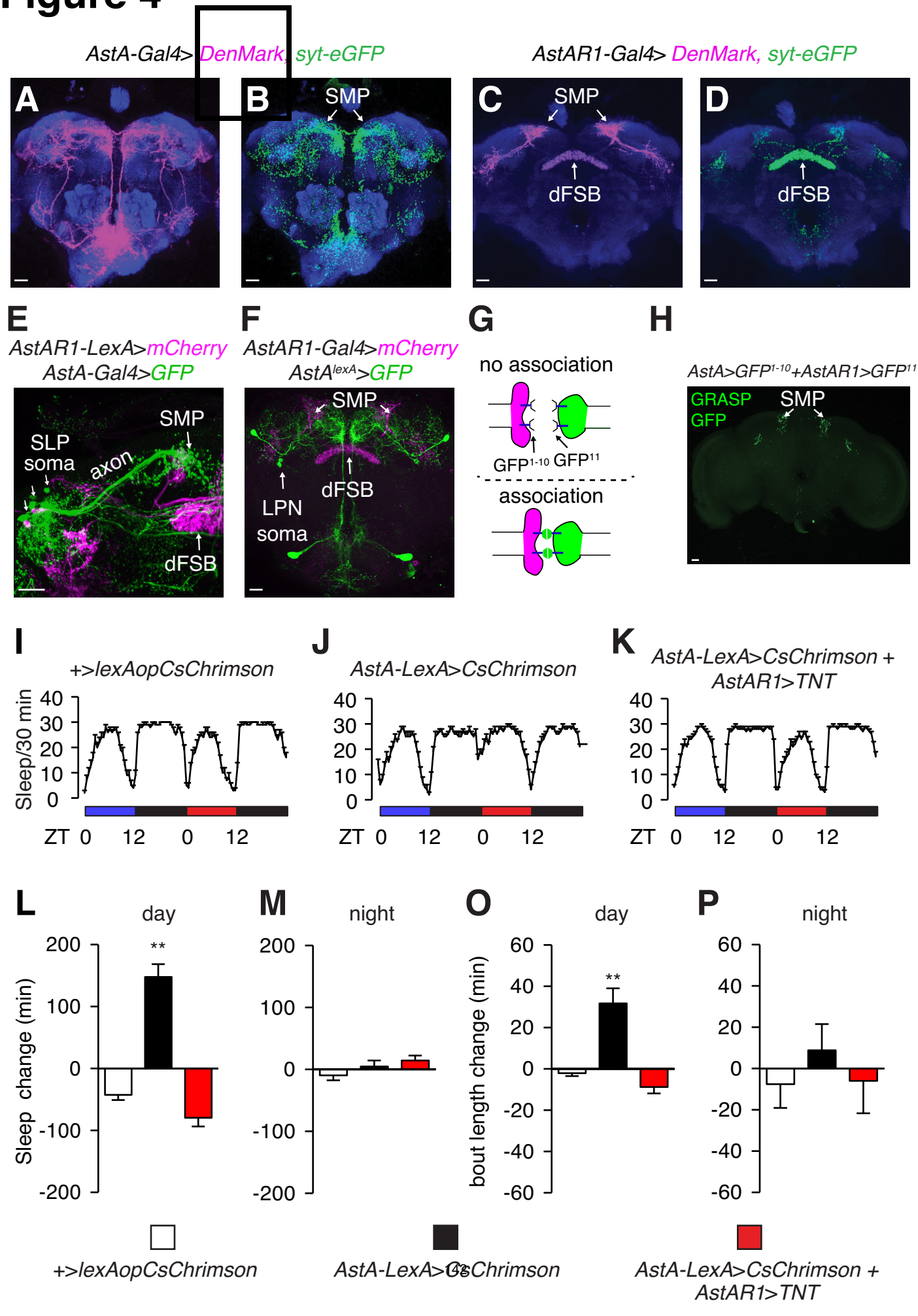
AstA-Gal4> DenMark, syt-eGFP
AstAR1-Gal4> DenMark, syt-eGFP
A
B
SMP
C
SMP
dFSB
D
dFSB
E
AstAR1-LexA>mCherry
AstA-Gal4>GFP
SMP
SLP
soma
axon
dFSB
F
AstAR1-Gal4>mCherry
AstA^lexA>GFP
SMP
dFSB
LPN
soma
G
no association
GFP1-10 GFP11
association
H
AstA>GFP1-10+AstAR1>GFP11
GRASP
GFP
SMP
I
+>lexAopCsChrimson
Sleep/30 min
40
30
20
10
0
ZT 0 12 0 12
J
AstA-LexA>CsChrimson
40
30
20
10
0
ZT 0 12 0 12
K
AstA-LexA>CsChrimson +
AstAR1>TNT
40
30
20
10
0
ZT 0 12 0 12
L
day
Sleep change (min)
200
100
0
-100
-200
**
M
night
200
100
0
-100
-200
O
day
bout length change (min)
60
40
20
0
-20
-40
-60
**
P
night
60
40
20
0
-20
-40
-60
+>lexAopCsChrimson
AstA-LexA>CsChrimson
AstA-LexA>CsChrimson +
AstAR1>TNT

Figure 4. Anatomical and functional connectivity between *AstA-Gal4+* and dFSB sleep-promoting neurons.

(**A-B**) Immunohistochemistry of whole-mount brains of *AstA-Gal4>DenMark, syt-eGFP* flies. (**C-D**) Immunohistochemistry of whole-mount brains of *AstAR1-Gal4>DenMark, syt-eGFP* flies. The scale bars represent 20*μ*m. (**E**) Immunohistochemistry of whole-mount brains of *AstAR1* reporter (*AstAR1-LexA>tdTomato*) and *AstA* reporter (*AstA-Gal4>GFP*). Both reporters showed innervation near SMP region of the brain. (**F**) Immunohistochemistry of whole-mount brains of *AstAR1* reporter (*AstAR1-Gal4>mCherry*) and *AstA* reporter ($AstA^{lexA}$*>GFP*). Both reporters showed innervation near SMP region of the brain. The scale bars represent 20*μ*m. **(G-H**) Image of GRASP GFP fluorescence revealing anatomical close association between *AstA-Gal4* and *AstAR1-Gal4* neurons in the fly brain. (**I**-**K**) Sleep profiles of indicated flies under 12-hour blue light/dark and red light /dark. (**L-M**) Quantification of CsChrimson activation induced change of daytime and nighttime sleep. (**O-P**) Quantification of CsChrimson activation induced change of daytime and nighttime sleep bout length. n=15-31, err bar, SEM; **p<0.01, one way ANOVA with Dunnett's test.

Figure 5

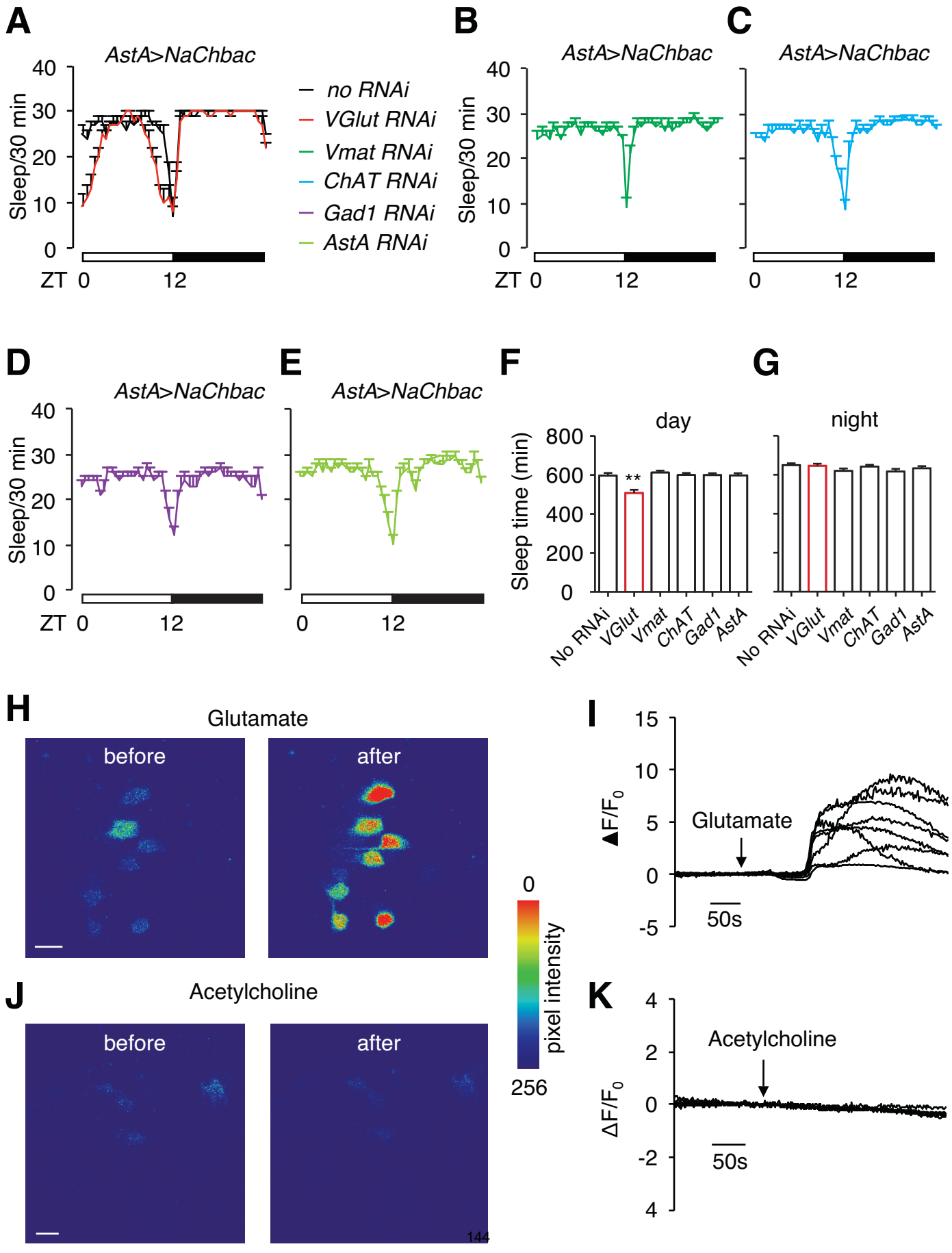
A
AstA>NaChbac
Sleep/30 min
40
30
20
10
0
ZT 0
12
no RNAi
VGlut RNAi
Vmat RNAi
ChAT RNAi
Gad1 RNAi
AstA RNAi
B
AstA>NaChbac
C
AstA>NaChbac
D
AstA>NaChbac
E
AstA>NaChbac
F
day
night
Sleep time (min)
800
600
400
200
0
**
No RNAi
VGlut
Vmat
ChAT
Gad1
AstA
G
H
Glutamate
before
after
0
pixel intensity
256
I
ΔF/F0
15
10
5
0
-5
Glutamate
50s
J
Acetylcholine
before
after
K
4
2
0
-2
4
Acetylcholine
50s
144

Figure 5. Glutamate is the excitatory neurotransmitter in *AstA-Gal4+* neurons to activate dFSB neurons and promote sleep.

(**A**) Sleep profile of *AstA>Nachbac* flies with or without *Vglut* RNAi. (**B-E**) Sleep profile of *AstA>Nachbac* flies expressing *Vmat-RNAi*, *ChAT-RNAi Gad1-RNAi*, or *AstA-RNAi* transgenes. (**F-G**) Quantification of daytime sleep and nighttime sleep of indicated flies. n=29-55; err bar, SEM; **p<0.01, one way ANOVA with Dunnett's test. (**H**) Representative image of Gcamp6f fluorescence before the after bath application of 50mM Glutamate. (**I**) Representative traces of change of Gcamp6 fluorescence ($\Delta F/F_0$) upon bath application of 50mM Glutamate. (**J**) Representative image of Gcamp6f fluorescence before the after bath application of 50mM Acetylcholine. (**K**) Representative traces of change of Gcamp6 fluorescence ($\Delta F/F_0$) upon bath application of 50mM Glutamate. The scale bars in panel H and J represents 20μm.

Figure 6

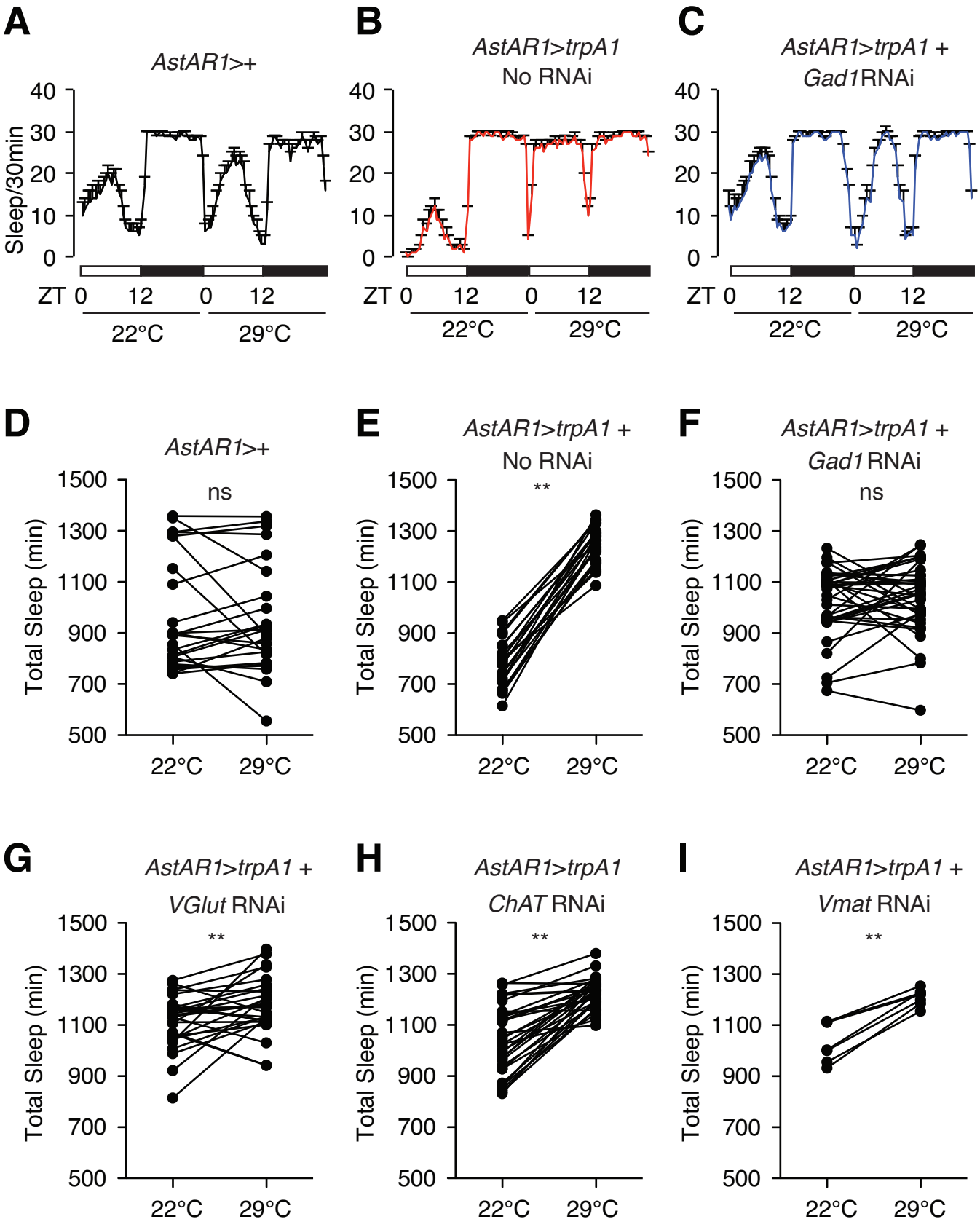
A
AstAR1>+
B
AstAR1>trpA1
No RNAi
C
AstAR1>trpA1 +
Gad1RNAi
Sleep/30min
40
30
20
10
0
ZT 0 12 0 12
22°C 29°C
D
AstAR1>+
ns
E
AstAR1>trpA1 +
No RNAi
**
F
AstAR1>trpA1 +
Gad1 RNAi
ns
Total Sleep (min)
1500
1300
1100
900
700
500
22°C 29°C
G
AstAR1>trpA1 +
VGlut RNAi
**
H
AstAR1>trpA1
ChAT RNAi
**
I
AstAR1>trpA1 +
Vmat RNAi
**

Figure 6. GABA is the required in *AstAR1-Gal4* neurons to promote sleep.

(**A-C**) Sleep profile of control flies (*AstAR1-Gal4/+)* and *AstAR1>trpA1* flies with or without *Gad1* RNAi. (**D-I**) Quantification of total sleep-time of one combined light/dark cycle at 22°C and 29°C of control flies and *AstAR1>trpA1* flies with or without RNAi directed to genes required for neurotransmitter synthesis or package. **p<0.01, pair-wise student t-test.

Figure 7

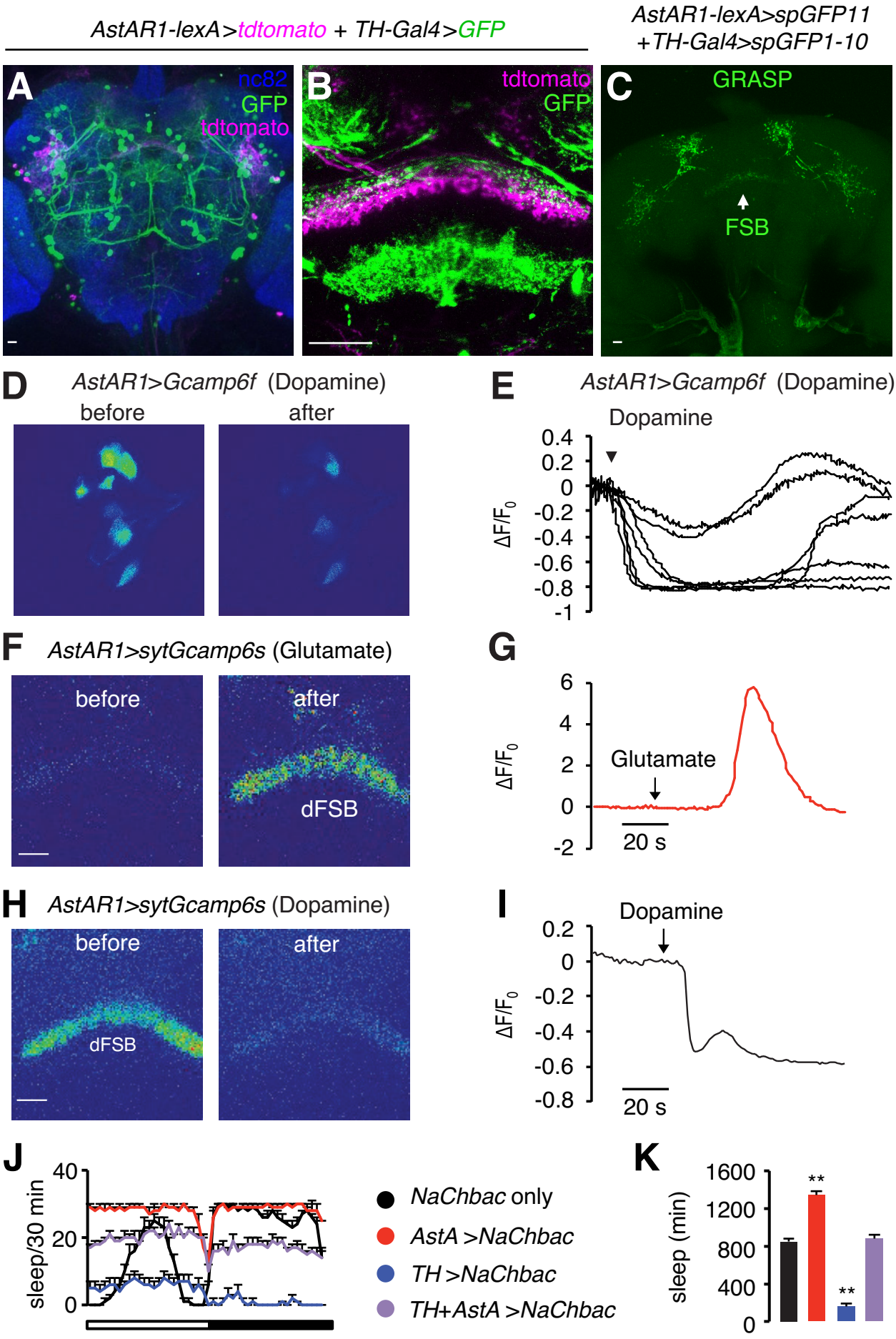
AstAR1-lexA>tdtomato + TH-Gal4>GFP
AstAR1-lexA>spGFP11
+TH-Gal4>spGFP1-10
A
nc82
GFP
tdtomato
B
tdtomato
GFP
C
GRASP
FSB
D
AstAR1>Gcamp6f (Dopamine)
before
after
E
AstAR1>Gcamp6f (Dopamine)
Dopamine
ΔF/F0
0.4
0.2
0
-0.2
-0.4
-0.6
-0.8
-1
F
AstAR1>sytGcamp6s (Glutamate)
before
after
dFSB
G
ΔF/F0
6
4
2
0
-2
Glutamate
20 s
H
AstAR1>sytGcamp6s (Dopamine)
before
after
dFSB
I
Dopamine
ΔF/F0
0.2
0
-0.2
-0.4
-0.6
-0.8
20 s
J
sleep/30 min
40
20
0
NaChbac only
AstA >NaChbac
TH >NaChbac
TH+AstA >NaChbac
K
sleep (min)
1600
1200
800
400
0
**
**

Figure 7. Dopaminergic neurons inhibit the activity of sleep-promoting dFSB neurons neurons. (**A**) Immunostaining of a fly brain expressing both a Dopaminergic neurons reporter (*TH-Gal4>GFP*, in green) and sleep-promoting dFSB neuron reporter (*AstAR1-lexA>tdTomato,* in red). Anti-NC82 in blue for background staining. (**B**) High magnitude image of the fly brain expressing the two reporters, showing innervating of the two reporters at fan-shaped body region (dFSB and vFSB). (**C**) Image of GRASP GFP fluorescence revealing anatomical association between sleep-promoting dFSB neurons and Dopaminergic neurons in the fly brain. The scale bars represents 20μm. (**D**) Representative image of GCaMP6f fluorescence before the after bath application of 10 mM Dopamine. The scale bars represents 20 μm. (**E**) Representative traces of change of Gcamp6 fluorescence ($\Delta F/F_0$) upon bath application of 10 mM Dopamine. (**F**) Representative images of syt-Gcamp6s fluorescence in *AstAR1-Gal4* neuron's axonal terminal before the after bath application of 50 mM Glutamate. (**G**) Representative trace showing the change in sytGCaMP fluorescence ($\Delta F/F_0$) upon bath application of 50 mM glutamate. (**H**) Representative images of syt-Gcamp6s fluorescence in *AstAR1-Gal4* neuron's axonal terminal before the after bath application of 10 mM Dopamine. The scale bars represents 20μm. (**I**) Representative trace showing the change in syt-GCaMP fluorescence ($\Delta F/F_0$) upon bath application of 10 mM dopamine. (**J-K**) Activation of dopaminergic

neurons antagonizes the sleep-promoting effect of *AstA-Gal4* neuronal activation. (**H**) Sleep profiles of flies with indicated genotypes. (**K**) Quantification of total sleep time of one combined light/dark cycle. n = 12-24; err bar, SEM; *p<0.05, **p<0.01 one way ANOVA with Dunnett's test.

Figure S1

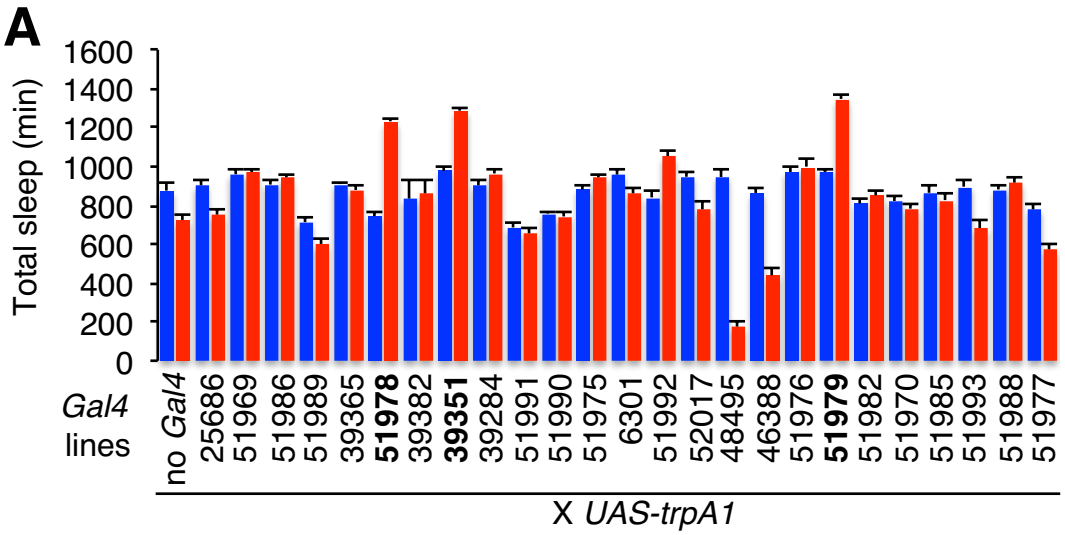
A
Total sleep (min)
1600
1400
1200
1000
800
600
400
200
0
Gal4 lines
no Gal4
25686
51969
51986
51989
39365
51978
39382
39351
39284
51991
51990
51975
6301
51992
52017
48495
46388
51976
51979
51982
51970
51985
51993
51988
51977
X UAS-trpA1

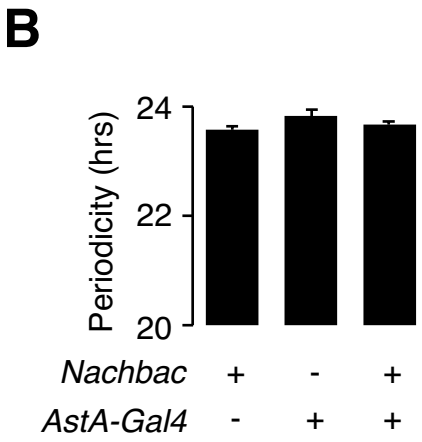
B
Periodicity (hrs)
24
22
20
Nachbac + - +
AstA-Gal4 - + +

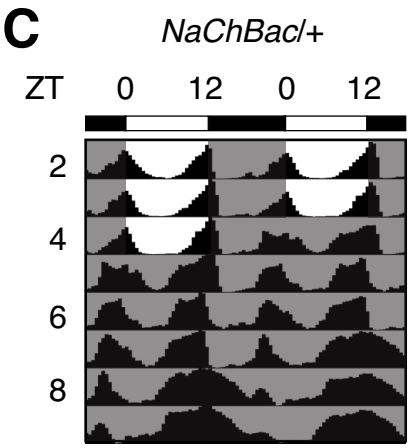
C
NaChBac/+
ZT 0 12 0 12
2
4
6
8

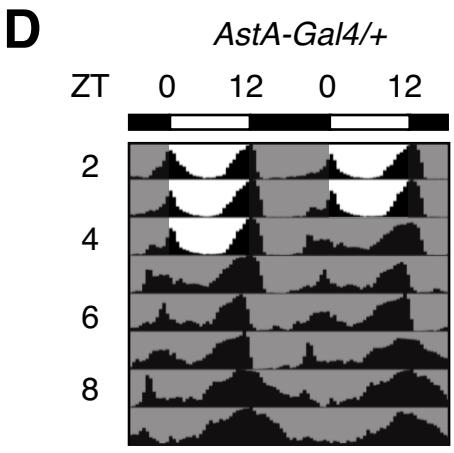
D
AstA-Gal4/+
ZT 0 12 0 12
2
4
6
8

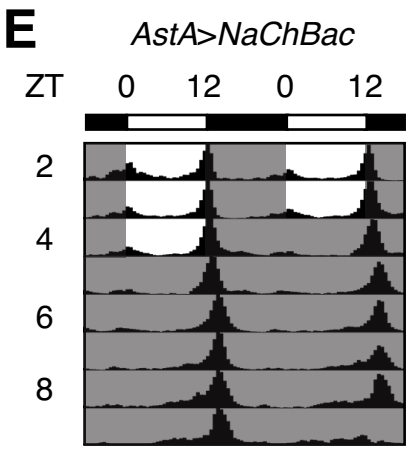
E
AstA>NaChBac
ZT 0 12 0 12
2
4
6
8

Supplemental Figure legends

Figure S1. Identification of *AstA-GAL4* lines that label sleep-promoting neurons

(**A**) Activation of neurons labeled by a panel of candidate *Gal4* lines by expressing a heat-activated channel *trpA1*. Total sleep-time in a 24-hour day is quantified at 22°C (non-activating temperature) and 29°C (activating temperature). Gal4 lines are labeled with their Bloomington stock numbers. (**B**) Periodicity of flies with indicated genotypes. n = 16; err bar, SEM (**C-E**) Actogram of flies with indicated genotypes. ZT0 refers to when the light is turned on.

Figure S2

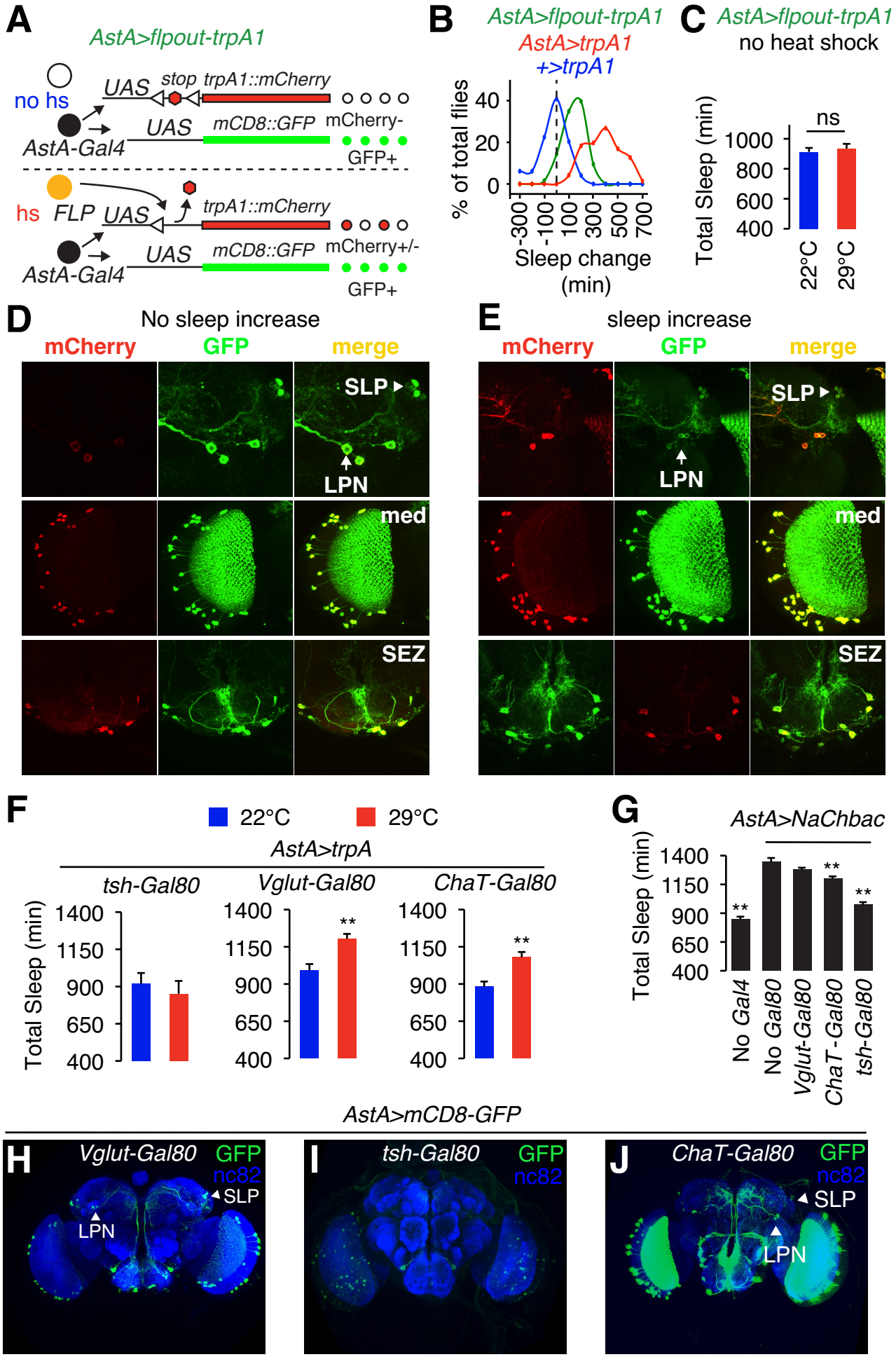
A
AstA>flpout-trpA1
no hs
UAS
stop
trpA1::mCherry
AstA-Gal4
UAS
mCD8::GFP
mCherry-
GFP+
hs
FLP
UAS
trpA1::mCherry
AstA-Gal4
UAS
mCD8::GFP
mCherry+/-
GFP+
B
AstA>flpout-trpA1
AstA>trpA1
+>trpA1
% of total flies
40
20
0
-300
-100
100
300
500
700
Sleep change (min)
C
AstA>flpout-trpA1
no heat shock
Total Sleep (min)
1000
800
600
400
ns
22°C
29°C
D
No sleep increase
mCherry
GFP
merge
SLP
LPN
med
SEZ
E
sleep increase
mCherry
GFP
merge
SLP
LPN
med
SEZ
F
22°C
29°C
AstA>trpA
tsh-Gal80
Vglut-Gal80
ChaT-Gal80
Total Sleep (min)
1400
1150
900
650
400
**
G
AstA>NaChbac
Total Sleep (min)
1400
1150
900
650
400
**
No Gal4
No Gal80
Vglut-Gal80
ChaT-Gal80
tsh-Gal80
AstA>mCD8-GFP
H
Vglut-Gal80
GFP
nc82
SLP
LPN
I
tsh-Gal80
GFP
nc82
J
ChaT-Gal80
GFP
nc82
SLP
LPN

Figure S2. SLP neurons are the sleep-promoting neurons labeled by *AstA-Gal4*.

(A) Diagram of the flip-out method to generate TRPA1::mCherry positive *AstA-Gal4* neurons. The flies used in this analysis were termed *AstA>flpout-trpA1.* (**B**) Histogram showing the distribution of flies with indicated sleep change upon thermo-activation by TRPA1. Vertical dashed line marks no sleep change. (**C**) No increase of total sleep time in *AstA-Gal4>flipout- trpA1* flies without inducing *trpA1* expression by heat shock. n=16; err bar, SEM; (**D**) Brain Immunostaining of fly no increase of sleep. All *AstA-Gal4* neurons are labeled with GFP, while *trpA1* expressing *AstA-Gal4* neurons are labeled with mCherry. *trpA1* expression is induced in almost all *AstA-Gal4* neurons located in the optical lobe medullar (med), neurons in SEZ and LPN neurons, but not in neurons located in SLP. (**E**) Brain Immuno-fluorescence staining of flies with increase of sleep. Note that *trpA1* is induced in neurons located in SLP. **(F)** Quantification of total sleep-time at 22°C and 29°C of *AstA>trpA1* flies carrying different *Gal80* transgenes. n=20-30; err bar, SEM; **p<0.01, pair-wise student t-test. **(G)** Quantification of total sleep-time of control flies and *AstA>NaChBac* flies with or without indicated *Gal80* transgenes, n=12-24; err bar, SEM; **p<0.01, one way ANOVA with Dunnett's test using *AstA>NaChBac* as control. (**H-J**) Immunohistochemistry of *AstA>GFP* fly whole-mount brains carrying indicated *Gal80* transgenes.

Figure S3

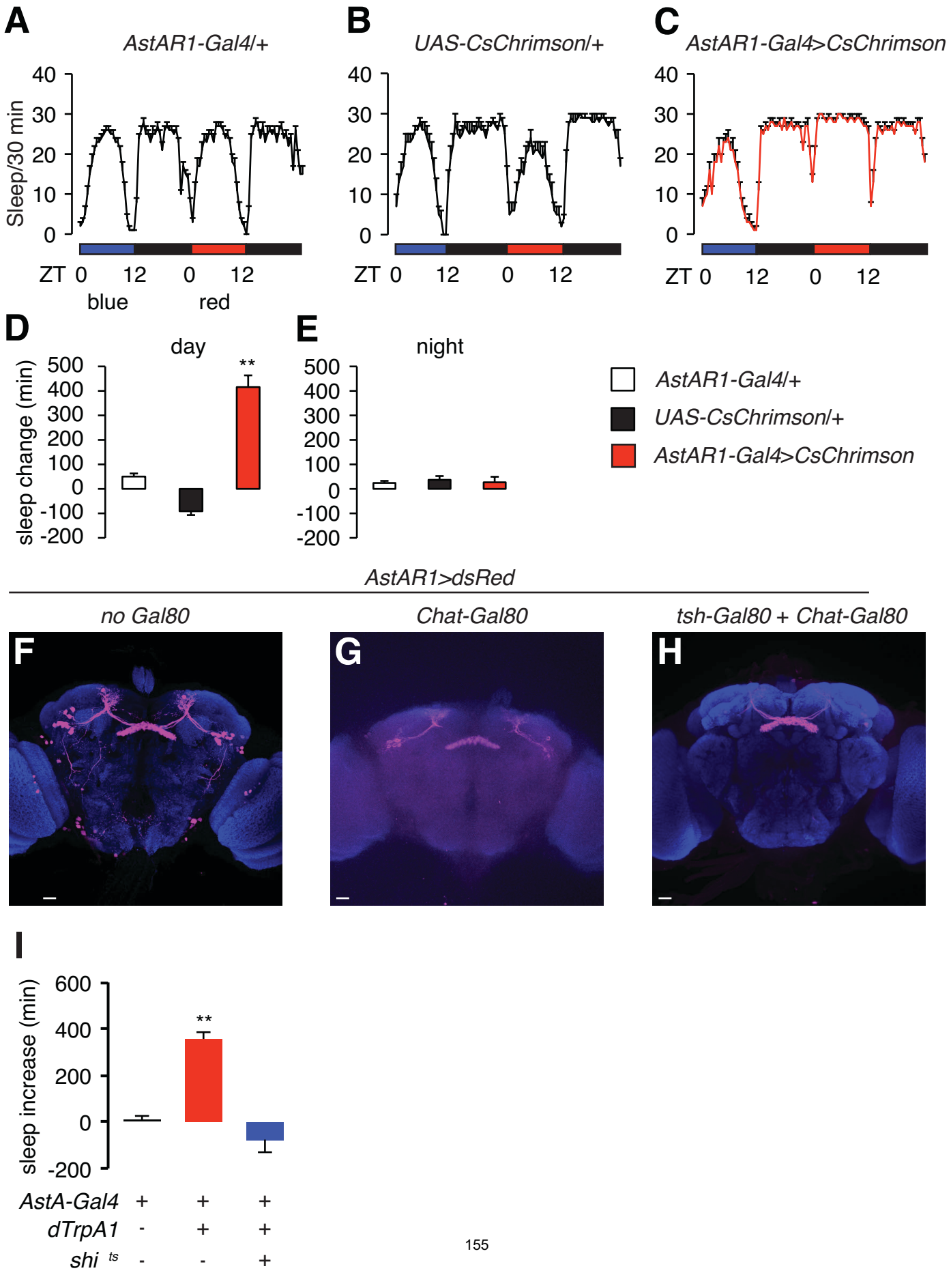
A
AstAR1-Gal4/+
B
UAS-CsChrimson/+
C
AstAR1-Gal4>CsChrimson
Sleep/30 min
40
30
20
10
0
ZT 0 12 0 12
blue
red
D
day
E
night
sleep change (min)
500
400
300
200
100
0
-100
-200
**
AstAR1-Gal4/+
UAS-CsChrimson/+
AstAR1-Gal4>CsChrimson
AstAR1>dsRed
no Gal80
Chat-Gal80
tsh-Gal80 + Chat-Gal80
F
G
H
I
sleep increase (min)
600
400
200
0
-200
**
AstA-Gal4 + + +
dTrpA1 - + +
shi ts - - +

Figure S3. A subset of *AstAR1-Gal4* neurons project to dorsal fan-shaped body promote sleep.

(**A-C**) Sleep profile of indicated flies under blue-light (non-activating condition) and red-light (activating condition). **(D-E)** Quantification of Sleep-promoting effect of *AstAR1-Gal4* neuronal activation by CsChrimson. Sleep increase measures the difference of sleep time during red light and blue light. (**F-H**) Immunohistochemistry of *AstAR1>dsRed* fly whole-mount brains carrying indicated *Gal80* transgenes. (**I)** Quantification of sleep increase by *AstA-Gal4* neurons activation with or without shi^{ts}. n = 20-23; err bar, SEM; **p<0.01, one way ANOVA with Dunnett's test.

Figure S4

A

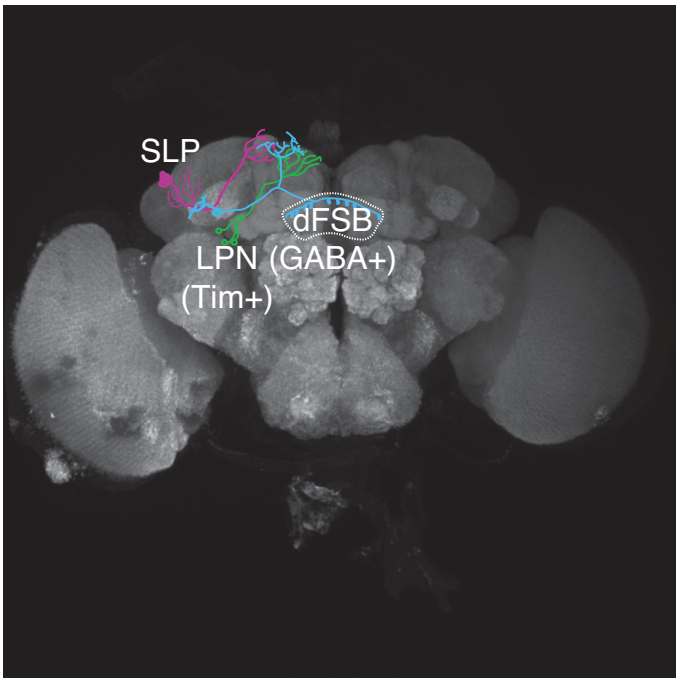
SLP
dFSB
LPN (GABA+)
(Tim+)

B

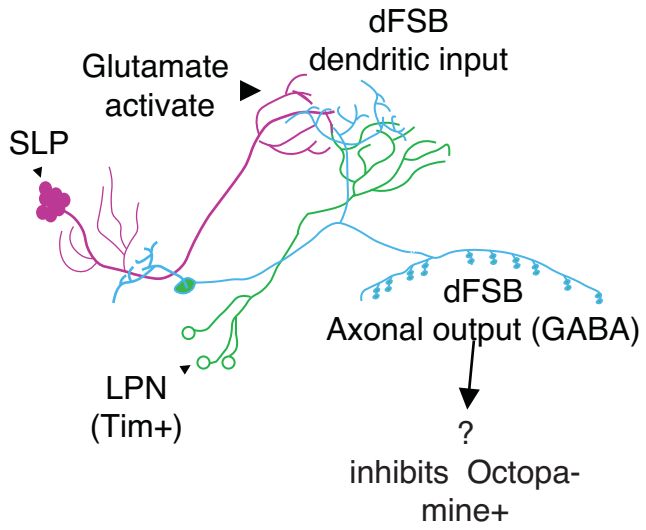
dFSB
dendritic input
Glutamate
activate
SLP
dFSB
Axonal output (GABA)
LPN
(Tim+)
?
inhibits Octopa-
mine+

Figure S4. Schematic model of *AstA-Gal4+* — dFSB sleep promoting neuronal circuit.

(A) Illustration of *AstA-Gal4+* — dFSB sleep-promoting neurons in Drosophila brain. *AstA-Gal4+* sleep-promoting neurons are colored in green (Tim+ LPN neurons) and magenta (SLP neurons) while dFSB sleep-promoting neurons (GABAnergic neurons) are colored in cyan. **(B)** a detailed illustration showing the connections and neurotransmitters used by *AstA-Gal4+* — dFSB sleep-promoting neurons.

Figure S5

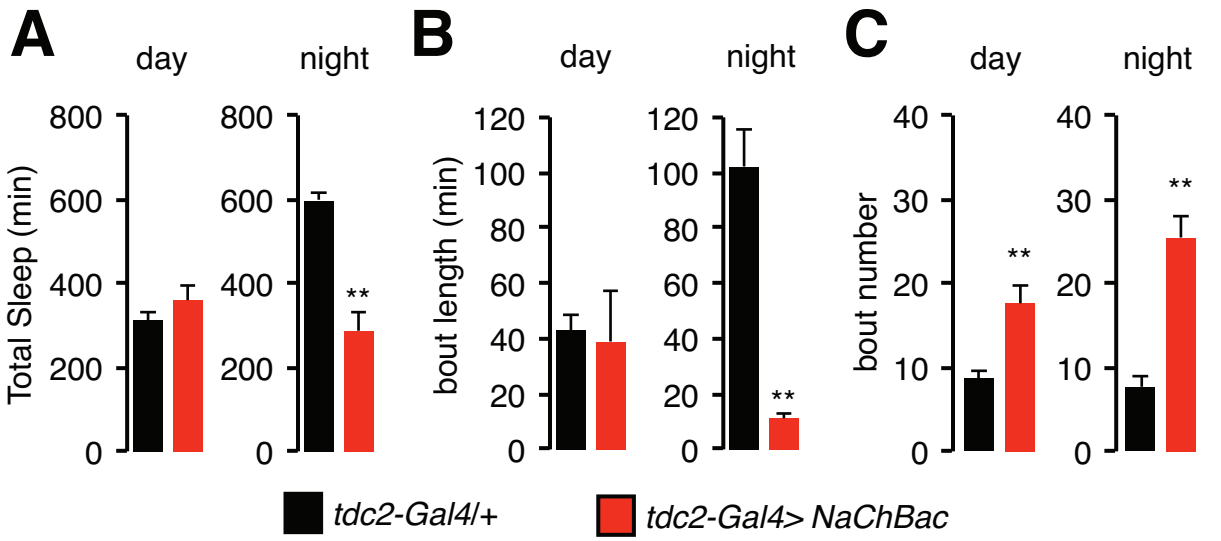
A
day
night
Total Sleep (min)
800
600
400
200
0
**
B
bout length (min)
120
100
80
60
40
20
C
bout number
40
30
20
10
tdc2-Gal4/+
tdc2-Gal4> NaChBac

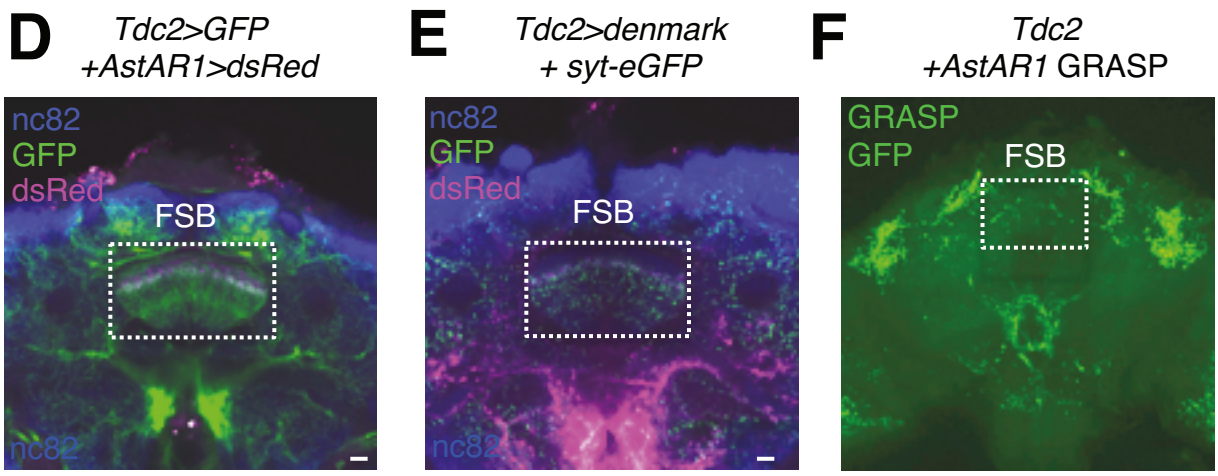
D
Tdc2>GFP
+AstAR1>dsRed
nc82
GFP
dsRed
FSB
E
Tdc2>denmark
+ syt-eGFP
F
Tdc2
+AstAR1 GRASP
GRASP
GFP

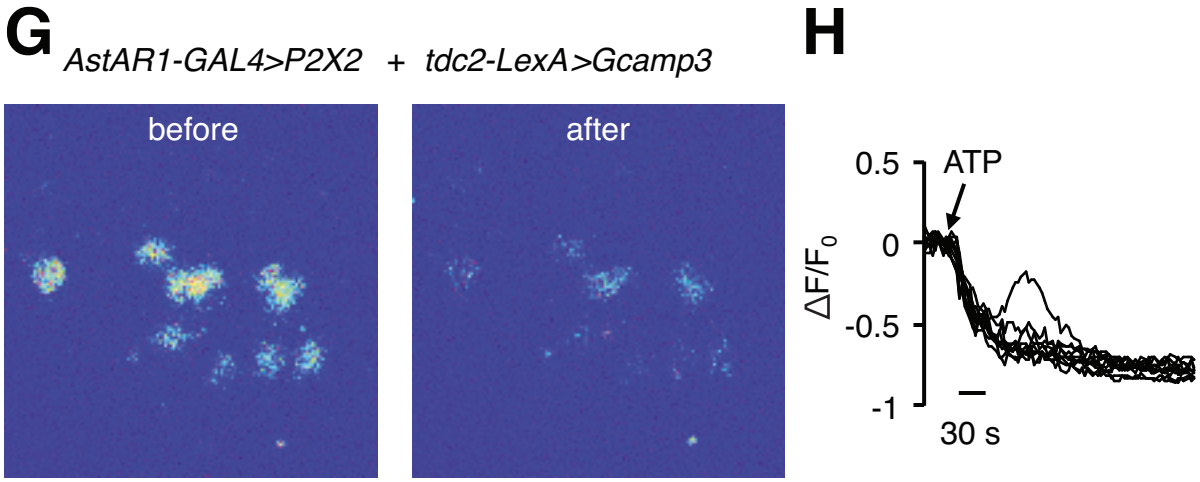
G
AstAR1-GAL4>P2X2 + tdc2-LexA>Gcamp3
before
after
H
ATP
0.5
0
-0.5
-1
ΔF/F0
30 s

Figure S5. *AstAR1-Gal4* sleep-promoting neurons inhibit octopaminergic arousal neurons.

(A) Quantification of daytime and nighttime sleep (**B**) Quantification of daytime and nighttime sleep bout length (**C**) Quantification of daytime and nighttime bout number. n = 16; err bar, SEM. (**D**) Immunohistochemistry of fly whole-mount brains co-expressing *AstAR1* and *Tdc2* reporters. (**E**) Immunohistochemistry of whole-mount brains of *Tdc2>DenMark, syt-eGFP* flies. The scale bars represents 20μm. (**F**) Image of GRASP GFP fluorescence revealing anatomical synaptic connection between *Tdc2* and *AstAR14* neurons in the fly brain. Boxed region contains dFSB. (**G**) Representative image of Gcamp3 fluorescence before the after bath application of 2.5 mM ATP. The scale bars represents 20μm. (**H**) Representative traces of change of Gcamp3 fluorescence ($\Delta F/F_0$) upon bath application of 2.5 mM ATP.

Figure S6

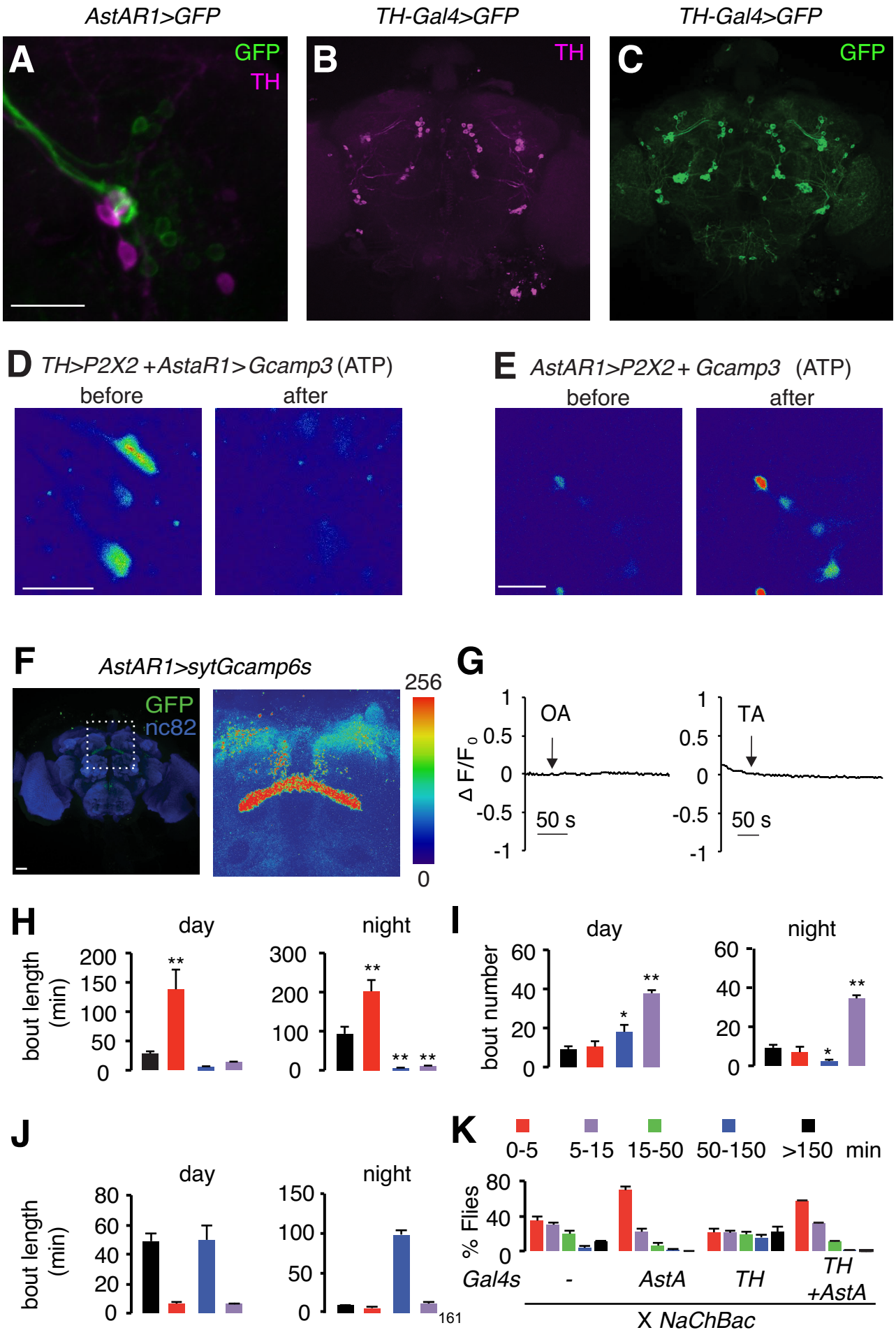
AstAR1>GFP
TH-Gal4>GFP
TH-Gal4>GFP
A
GFP
TH
B
TH
C
GFP
D TH>P2X2 +AstaR1>Gcamp3 (ATP)
before
after
E AstAR1>P2X2+ Gcamp3 (ATP)
before
after
F AstAR1>sytGcamp6s
GFP
nc82
256
0
G
OA
TA
ΔF/F0
1
0.5
0
-0.5
-1
50 s
H
day
night
bout length (min)
200
150
100
50
0
300
200
100
0
**
I
day
night
bout number
60
40
20
0
*
**
J
day
night
bout length (min)
80
60
40
20
0
150
100
50
0
K
0-5
5-15
15-50
50-150
>150
min
% Flies
80
40
0
Gal4s
-
AstA
TH
TH +AstA
X NaChBac
161

Figure S6. Compartmentalized regulation of *AstAR1-Gal4+* sleep-promoting neurons by Glutamate and dopamine.

(A) Immunohistochemistry of Drosophila whole-mount brains expressing *AstAR1* reporter *(AstAR1>GFP)*. The brain was stained with TH antibody to label dopaminergic neurons (in red). **(B-C)** Immunohistochemistry of Drosophila whole-mount brains expressing *TH* reporter *(TH-Gal4>GFP)*. The brain was stained with TH antibody (B) and GFP (C). **(D)** Representative image of Gcamp3 fluorescence in dFSB neurons before the after bath application of ATP (2.5mM). The scale bar represents 20μm. ATP activated P2X2 cation channel was expressed in TH+ neurons. **(E)** Representative image of Gcamp3 fluorescence in *AstA-Gal4+* dFSB neurons before the after bath application of ATP (2.5mM). The scale bar represents 20μm. ATP activated P2X2 cation channel was expressed also in dFSB neurons. **(F)** Immunohistochemistry of the whole-mount fly (AstAR1>syt-Gcamp6s) brain. In right panel, High magnitude image of the boxed region in B showing the intensities of syt-Gcamp6s signal in a heat map. The scale bars represents 20μm. (**G**) Representative traces of change of syt-Gcamp6s fluorescence ($\Delta F/F_0$) upon bath application of Octopamine. (**H**) Representative traces of change of syt-Gcamp6s fluorescence ($\Delta F/F_0$) upon bath application of Tyramine. (**J-K**) Quantification of sleep bout length (**J**) and bout number (**K**) of flies with indicated genotypes. n = 12-24; err bar, SEM; *p<0.05, **p<0.01 one way ANOVA with Dunnett's test. (**L**) Quantification of average wake bout length and (**M**) distribution of length of wake period of flies with indicated genotype. n = 12-24; err bar, SEM.

Chapter 4: The Drosophila visual cycle and *de novo* chromophore synthesis depends on *rdhB*

(This work is published as J Neurosci. 2012 Mar 7;32(10):3485-91. doi: 10.1523/JNEUROSCI.5350-11.2012.)

Introduction

Rhodopsin is comprised of a protein subunit, the opsin, and a light-sensitive retinylidene chromophore (Wald, 1968; Palczewski, 2006). Light activates the visual pigments by inducing a *cis* to *trans* isomerization of the protein-bound chromophore, whereupon in vertebrate rod and cone photoreceptor cells, all-*trans* retinal is released from the protein subunit, the opsin. The 11-*cis* retinal is then regenerated through an enzymatic pathway known as the visual or retinoid cycle. This regeneration pathway, as well as the *de novo* synthesis of the chromophore, depends on multiple retinol dehydrogenases (RDHs), which catalyze the interconversion between retinol and retinal (Liden et al., 2003; Travis et al., 2007).

In *Drosophila* photoreceptor cells, the chromophore does not appear to release from the opsin following photoisomerization (Hamdorf, 1979). Rather, a

second photon of light promotes the regeneration of the inactive, *cis* form, which is 3-hydroxy-11-*cis* retinal (3-OH-11-*cis*-retinal). A similar stable interaction is thought to occur between the visual pigment, melanopsin, and the chromophore in mammalian intrinsically photosensitive retinal ganglion cells (Berson, 2007; Hankins et al., 2008).

Despite the stability of the chromophore/opsin interaction in fly photoreceptor cells, an enzymatic visual cycle is used in *Drosophila*, and functions to recycle the chromophore that is liberated following endocytosis of rhodopsin, and degradation of the opsin (Wang et al., 2010). This enzymatic pathway allows the flies to maintain chromophore levels under conditions of nutrient deprivation when dietary carotenoids are unavailable. The first step in the *Drosophila* visual cycle pathway depends on a retinol dehydrogenase, PDH, which is expressed in the retinal pigment cells (RPCs) (Wang et al., 2010). The function and juxtaposition of RPCs to photoreceptor cells is reminiscent of the cells in the mammalian retinal pigment epithelium (RPE) (Travis et al., 2007). Other than PDH, the RDHs responsible either for the visual cycle or *de novo* synthesis of the chromophore are unknown.

Here we report the identification of a gene encoding a protein homologous to known retinol dehydrogenases, and which is highly expressed in RPCs (RDHB;

Retinal Pigment Cell Dehydrogenase). We created *rdhB*^{1} null mutant flies by homologous recombination, and found that RDHB promoted the visual cycle and synthesis of 3-OH-11-*cis*-retinal from dietary sources. The *rdhB*^{1} flies displayed visual impairment and progressive retinal degeneration. This work allows for a refinement of the enzymes and cellular requirement for the *Drosophila* visual cycle (Wang et al., 2010).

Results

Expression of *rdhB* in retinal pigment cells

RDHs belong to the short-chain dehydrogenase/reductase (SDR) family, which also includes alcohol dehydrogenases and other proteins that act in cell types that are not associated with the visual system (Liden et al., 2003; Travis et al., 2007). Therefore, to identify RDHs that were required for recycling or for *de novo* synthesis of the chromophore, we focused on SDR proteins that were expressed primarily in the eye. We took advantage of a previous genome-wide gene expression analysis that compared the relative levels of mRNA expression in heads isolated from wild-type and eyeless flies (Xu et al., 2004). The most eye-enriched gene is *pdh* (>220 fold) (Xu et al., 2004), which is required for

recycling of the chromophore (Wang et al., 2010). The second most eye-enriched SDR family member (*CG7077*; 43-fold enrichment) has not been characterized functionally.

Since an RDH could function in the eye either in the photoreceptor cells or in RPCs, we examined the cellular distribution of the CG7077 protein. The fly compound eye is comprised of ~800 ommatidia, which includes seven out of the eight photoreceptor cells in coronal sections (Fig. 1*A*). Each photoreceptor cell contains a microvillar portion referred to as the rhabdomere, which is the functional equivalent of the outer segments of vertebrate rods and cones. The photoreceptor cells are surrounded by six secondary retinal pigment cells (RPCs). The vertices of the hexagonally shaped ommatidia consist of either tertiary RPCs or mechanosensory bristle cells arranged in an alternating pattern.

To examine the spatial distribution of CG7077, we expressed a CG7077-Myc fusion protein under control of the *CG7077* promoter using the *GAL4*/*UAS* system (Brand and Perrimon, 1993) and stained coronal eye sections with anti-Myc. As a marker for the rhabdomeres of the R1-6 photoreceptor cells, we co-stained the sections with antibodies specific for the major rhodopsin, Rh1. The anti-Myc signal was restricted to cells situated between ommatidia, and which encircle the

R1-6 rhabdomeres labeled by anti-Rh1 (Fig. 1*B—D*). Since this expression pattern was consistent with secondary RPCs, and CG7077 was required for chromophore production (see below), we referred to CG7077 as RDHB (Retinal Pigment Cell Dehydrogenase).

In flies, maturation of rhodopsin is dependent on binding to the chromophore, 3-OH-11-*cis*-retinal. Without the chromophore, rhodopsin is trapped in the endoplasmic reticulum and eventually gets degraded (Harris et al., 1977; Ozaki et al., 1993). Thus, we would expect that an RDH that is required for chromophore synthesis would be expressed at a time earlier than the initial appearance of rhodopsin, which takes place about 80 – 90 hours after puparium formation (APF; Fig. 1*E*). To characterize the temporal expression pattern of RDHB, we raised RDHB antibodies and probed a Western blot containing extracts prepared at various times during pupal development. RDHB expression initiated during early pupal development, ~40 hours APF, and continued to be expressed throughout the rest of pupal development, and in the adult (Fig. 1*E*). We performed immunostaining on pupal eyes, and detected the anti-RDHB signal exclusively in secondary and tertiary RPCs (Fig. 1*F,G*).

Defects in chromophore synthesis during pupal stage in *rdhB* mutant flies

To investigate the requirements for RDHB *in vivo*, we generated *rdhB* mutant flies (*rdhB*^{1}) by ends-out homologous recombination (Fig. 2*A*). The RDHB protein was eliminated in the *rdhB*^{1}, as assessed by probing Western blots with RDHB antibodies (Fig. 2*B*), and by immunostaining pupal eyes (Fig. 1*F,G*). Since maturation of fly rhodopsin is dependent on binding to the chromophore (Ozaki et al., 1993), mutations that interfere with *de novo* synthesis or recycling of the chromophore cause a reduction in rhodopsin levels. To test for a requirement for RDHB for chromophore production, we raised larvae on retinoid-deficient food, with or without retinoid supplementation. We then prepared head extracts from newly-eclosed flies, and probed Western blots for expression of Rh1. Wild-type or *rdhB*^{1} animals raised on retinoid-deficient food were impaired in the production of Rh1 (Fig. 2*C,D*). Addition of b-carotene restored production of Rh1 (Fig. 2*C,D*). During *de novo* synthesis of the chromophore carotenoids are cleaved into two copies of retinaldehyde through activity of the NINAB (Neither Inactivation Nor Afterpotential B) □,□'-carotene-15,15'-dioxgenase (von Lintig et al., 2001) (Fig. 3). Since NINAB also possesses intrinsic light-independent isomerase activity, some of the 3-OH-all-*trans*-retinal is directly converted into 3-OH-11-*cis*-retinal

(Oberhauser et al., 2008; Voolstra et al., 2010), which can be used as the chromophore without a requirement for an RDH (Fig. 3). Supplementation of retinoid deficit food with either all-*trans*-retinal or all-*trans*-retinol, which are rapidly converted to their 3-OH derivatives in the eyes (Seki et al., 1998), restored the ability of wild-type animals to synthesize rhodopsin (Fig. 2*C,D*). However, the *rdhB*^{1} mutant was unable to produce Rh1 after feeding on food containing either all-*trans*-retinal or all-*trans*-retinol (Fig. 2*C,D*).

To directly assay the effect of deleting the *rdhB* gene on chromophore synthesis during the pupal stage, we profiled chromophore levels in wild-type and *rdhB*^{1} flies using high performance liquid chromotography (HPLC). Beginning during the 2nd instar period, we raised the animals on retinoid-deficient food that was supplemented with either all-*trans*-retinal or all-*trans*-retinol, and assayed retinoid levels in one-day old flies. We detected only a small amount of chromophore in head extracts isolated from *rdhB*^{1} flies (Fig. 2E). These data indicate that RDHB functions subsequent to the generation of all-*trans*-retinol.

RDHB functioned in adult flies for rhodopsin production

To address whether RDHB contributed to chromophore biosynthesis in adult

flies, we raised larvae on retinoid-free food, and then supplied newly eclosed flies with b-carotene, all-*trans*-retinol, or all-*trans*-retinal. Wild-type adult flies were able to use any of these supplements to synthesize Rh1 (Fig. 4*A*). The *rdhB*^{1} flies also synthesized normal levels of Rh1 after being placed on the diet supplemented with b-carotene (Fig. 4*A*). However, in contrast to wild-type, the levels of Rh1 were reduced significantly in *rdhB*^{1} after feeding on either all-*trans*-retinal or all-*trans*-retinol (Fig. 4*A*). These results indicate that RDHB also functions in adult flies for chromophore biosynthesis.

Adult flies rely on the visual cycle as the principle pathway for maintaining chromophore levels in light-exposed flies (Wang et al., 2010). This pathway is not necessary in the dark since it is used to recycle the chromophore that is released from following light-induced internalized rhodopsin. If RDHB functions in the visual cycle, we would anticipate there would be an age dependent reduction in rhodopsin in *rdhB*^{1} if the mutants were maintained under a light-dark cycle, but not in the dark. Therefore, we raised wild-type and *rdhB*^{1} flies on retinoid-containing corn meal food, and quantified Rh1 levels after they were exposed to a light-dark cycle or kept in the dark. After 1 day of a light-dark cycle the Rh1 levels in wild-type and *rdhB*^{1} were similar (Fig. 4*B*). However, there was a subsequent age-

and light dependent decline in Rh1 in *rdhB*^{1}. After 7 and 25 days under a light-dark cycle the concentration of Rh1 in *rdhB*^{1} was reduced 2.3- and 11.2-fold, respectively, while the Rh1 levels were maintained if the mutant flies were dark-reared for 25 days (Fig. 4*B*).

Visual impairment and retinal degeneration in *rdhB*^{1} flies

A reduction in functional rhodopsin levels causes an electrophysiological phenotype that is revealed by performing electroretinogram (ERG) recordings. ERGs are extracellular recordings that measure the summed light response of the retina. After exposure to bright blue light and conversion of the inactive *cis*-retinal to the active all-*trans* form, the light-stimulated metarhodopsin remains in the active state in the dark. This causes a prolonged depolarization afterpotential (PDA) since the active all-*trans*-retinal does not absorb blue light, but must absorb a second photon (e.g. orange light) to restore the *cis*-retinal and terminate the PDA. In addition, metarhodopsin activity is quenched by binding to arrestin, which is present at ~20% the concentration of Rh1 in wild-type flies (Dolph et al., 1993). A PDA can only be produced when functional rhodopsin is in a molar excess over arrestin (Dolph et al., 1993), as in 2 day old wild-type and *rdhB*^{1} flies, and in

25-day old wild-type (Fig. 5*A—C*). Consistent with the 90% decrease in Rh1 in 25-day old *rdhB*^{1} (Fig 4*B,D*), bright blue light did not produce a PDA in the mutant (Fig 5*D*). We rescued this phenotype by expression of a wild-type *rdhB* cDNA under the control of the *rdhB* promoter (Fig 5*E*).

To determine whether the *rdhB*^{1} mutation caused retinal degeneration, we aged flies under a light-dark cycle or in complete darkness, and examined tangential sections by transmission EM. Wild-type flies displayed the full set of seven intact rhabdomeres even after 30 days under a light-dark cycle (Fig. 6*A,D*). When the *rdhB*^{1} mutant was incubated for 30 days under a light-dark cycle, the rhabdomeres were either smaller than in wild-type or were missing (4.5 $^{\pm}$0.4 rhabdomeres/ommatidium; Fig. 6*B,D*). All seven rhabdomeres were present if the mutant flies were incubated in the dark for 30 days (Fig. 6*C,D*). These data demonstrated that the *rdhB*^{1} caused light- and age-dependent retinal degeneration.

Discussion

Dual role for RDHB in the visual cycle and for *de novo* chromophore synthesis

An enzymatic visual cycle is used in flies, and is the main mode for maintaining chromophore levels in the adult (Wang et al., 2010). This pathway is required for recycling the released chromophore after rhodopsin undergoes light-induced endocytosis, and the opsin is degraded. Thus, in the dark there is no need for this enzymatic cycle. We propose that RDHB functions in the visual cycle since RDHB is expressed in adult RPCs, and elimination of RDHB causes an age-dependent decline in rhodopsin in the adult, but only if the flies are maintained under a light-dark cycle. This loss of rhodopsin occurs in the presence of carotenoid rich food, highlighting the greater importance of the visual cycle over *de novo* synthesis in adult flies.

The first step in the visual cycle, the reduction of 3-OH-all-*trans*-retinal to all-*trans*-retinol, requires an RDH, referred to as PDH. As a result, *pdh* mutants can synthesize the chromophore from all-*trans*-retinol but not all-*trans*-retinal (Wang et al., 2010). We suggest that RDHB promotes the last step in this pathway, the oxidation of 3-OH-11-*cis*-retinol to 3-OH-11-*cis*-retinal. This step is the only RDH-dependent step that appears to be required for both *de novo* synthesis of the chromophore from all-*trans*-retinoids as well as for the regeneration of the chromophore through the visual cycle (Fig. 3). Accordingly, our analyses showed

that RDHB was also required for *de novo* synthesis, which is primary mechanism for generating the chromophore during the pupal stage. In further support of the proposal that RDHB functions in the final oxidation step, chromophore production in *rdhB*^{1} was severely diminished if the dietary retinoids were limited to either all-*trans*-retinal or all-*trans*-retinol. The other step that is common to the visual cycle and *de novo* synthesis is isomerization of 3-OH-all-*trans*-retinol to 3-OH-11-*cis*-retinol. We suggest that RDHB catalyzes the final oxidation step rather than the isomerization since the protein is homologous to known RDHs but not to retinoid isomerases.

An additional RDH may function in concert with RDHB during the visual cycle

The *rdhB*^{1} mutant undergoes light- and age-dependent retinal degeneration, consistent with a role for RDHB in the visual cycle. However the retinal degeneration in *rdhB*^{1} was mild compared to that in *pdh* mutant flies (Wang et al., 2010). The relatively weak retinal degeneration associated with *rdhB*^{1}, combined with the finding that the concentration of Rh1 is reduced but not eliminated in 25 day-old *rdhB*^{1} mutant flies suggests that there exist one or more RDHs that are

partially redundant with RDHB. A similar phenomenon of functional redundancy occurs in the mouse retina, as the severity of the retinal degeneration associated with single mutants affecting some *RDH* genes is less severe than the combined mutations (Maeda et al., 2007). Additional genes encoding SDRs are highly expressed in the eye relative to other tissues (e.g. *CG40485* and *CG40486*), and therefore represent candidate RDHs. It will be of interest to generate mutations in these genes, and characterize the phenotypes individually and in combination with $rdhB^{1}$.

Entire visual cycle may function in the RPCs

RDHB could function either in the RPCs or the photoreceptor cells. RDHB is most likely required in RPCs since we detected expression of the *rdhB* reporter (*rdhB -GAL4*) and the RDHB protein in secondary and tertiary pigment cells and not in photoreceptor cells. Moreover, introduction of wild-type *rdhB* transgene in RPCs rescues the mutant phenotype. Thus, *rdhB* acts cell autonomously in RPCs. These data also support the model that the oxidation of 3-OH-11-*cis*-retinol takes place in the RPCs.

Given that PDH is also expressed and required in RPCs (Wang et al., 2010),

we propose that all of the enzymatic steps in the visual cycle occur in the RPCs. The mammalian RPE also functions in *de novo* synthesis of the chromophore, and in the visual cycle, further indicating functional similarities between the RPCs and the RPE. However, in contrast to the *Drosophila* pathway, the visual cycle in the mammalian rods and cones includes enzymatic reactions in both photoreceptor cells and the RPE or Müller cells, respectively (Travis et al., 2007).

The finding that flies use a visual cycle, and that the enzymatic steps appear to take place exclusively in RPCs raises questions concerning the physiology of mammalian melanopsin. This latter visual pigment, which has non-image forming functions in photosensitive retinal ganglion cells, bears greater sequence and biophysical similarities to the *Drosophila* rhodopsins than rod and cone visual pigments (Berson, 2007; Hankins et al., 2008). As is the case for the fly rhodopsins, melanopsin may be a bistable photopigment (Berson, 2007; Hankins et al., 2008). However, it remains to be determined whether melanopsin depends on a visual cycle, and if so, the cellular sites for this pathway.

Abbreviations

After puparium formation, APF; ERG, electroretinogram; HPLC, high

performance liquid chromatography; NINAB, Neither Inactivation nor afterpotential B; PDA, prolonged depolarization afterpotential; PDH, Pigment Cell Dehydrogenase; RDH, retinol dehydrogenase; Rh1, rhodopsin 1; RPCs, retinal pigment cells; RDHB, Retinal Dehydrogenase B; RPE, retinal pigment epithelium; SDR, short-chain dehydrogenase/reductase.

Materials and Methods

Fly Stocks and Media for Feeding

We used the following stocks obtained from the Bloomington Stock center: *bw*^{1};*st*^{1}, *ninaE*^{I17} and the *y,w*;P[*70FLP*]*11* P[*70I-SceI*]*2B nocSco*/CyO flies. We raised the flies at 25°C on standard cornmeal-yeast medium under a 12 hour light/12 hour dark cycle unless indicated otherwise. For retinoid feeding during the larval stages, we placed embryos for four days on retinoid-deficient medium (Wang et al., 2010) and transferred 2nd instar larvae to the retinoid-deficient medium containing one type of retinoid: 5 mM β-carotene (Sigma), 500 μM all-*trans*-retinal (Sigma) or all-*trans*-retinol (Sigma). For retinoid feeding using adult flies, we reared the larvae on retinoid-free food, and then transferred newly-eclosed flies to retinoid-deficient medium containing one of the following

retinoids for 48-72 hours before performing Western blots: 5 mM β-carotene, 500 μM all-*trans*-retinal or all-*trans*-retinol.

Generation of *rdhB*^{1} knockout flies

We generated the *rdhB* knockout flies (*rdhB*^{1}) by ends-out homologous recombination (Gong and Golic, 2003). The targeting construct deleted a ~500-bp region encompassing the second to last exon and the translation termination site. Two ~3 kb genomic fragments were inserted into the *NotI* site and the *BamHI* site of pw35 (Gong and Golic, 2003), respectively. Transgenic flies carrying the targeting construct on the 2nd chromosome were crossed to *y,w;P*[*70FLP*]*11* P[*70I-SceI*]*2B nocSco*/*CyO* flies, and the progeny were screened for gene targeting by PCR.

Generation of Transgenic Flies

To generate the *UAS-rdhB::myc* flies, we subcloned the *rdhB* cDNA (GH05294, BDGP DGC clone), between the *NotI* and *XbaI* sites of pUAST (Brand and Perrimon, 1993), and added the sequence encoding a 6x Myc tag to the 3' end of

the cDNA. The construct was introduced into w^{1118} flies by germline transformation.

Generation of Recombination Proteins and anti-PDH Antibodies

To generate RDHB antibodies, an *rdhB* cDNA fragment encoding the N-terminal 120 residues was subcloned into the pGEX5X-1 vector (GE Healthcare). We expressed the GST-fusion protein in *Escherichia coli* BL21 codon-plus (Stratagene) and purified it using glutathione agarose beads (GE Healthcare). The protein was introduced into rabbits (Covance) to create the RDHB antibodies.

Western Blots

We prepared fly head extracts by homogenizing the heads directly in 1×SDS sample buffer with a pellet pestle (Kimble-Kontes). The extracts were fractionated by 4-10% SDS-PAGE (Bio-Rad) and transferred to Immobilon-P transfer membranes (Millipore) in Tris-glycine buffer. The primary antibodies used for probing were mouse anti-tubulin and mouse anti-Rh1 from Developmental Studies Hybridoma Bank, or rabbit anti-RDHB. The secondary antibodies used

were peroxidase conjugated anti-mouse or rabbit IgG secondary antibody (Sigma). The signals were detected using ECL reagents (GE Healthscience). For quantification of the Western blots we used LICOR-Odyssey secondary antibodies (anti-mouse IRDye 680, or anti-rabbit IRDye 800) and detected the signals using the LI-COR Odyssey Imaging System.

Immunolocalization

Immunofluorescent stainings of dissected fly pupae retinas were performed as described previously (Walther and Pichaud, 2006). The primary antibodies were rabbit anti-RDHB. The secondary antibodies were anti-rabbit IgG conjugated with Alexa Fluor 568 (Molecular Probes). The primary antibodies used for staining adult eye sections were anti-Myc and anti-Rh1. The samples were examined using a laser-scanning microscope (Zeiss LSM510-Zeta, Carl Zeiss MicroImaging Inc.) with plan-apochromat 20x objectives. The images were acquired using a Carl Zeiss LSM imaging system and transferred into Adobe Photoshop 7.0 for analysis.

Electroretinogram recordings

ERG recordings were performed as described previously (Wes et al., 1999). Briefly, two glass microelectrodes filled with Ringer's solution were inserted into small drops of electrode cream placed on the surfaces of the compound eye and the thorax, respectively. A Newport light projector (model 765) was used for stimulation. The ERG signals were amplified with a Warner electrometer IE-210 and recorded with a MacLab/4s A/D converter and the Chart v3.4/s program (A/D Instruments). We used 5 second pulses of orange (580) or blue (480) light with 7 second intervals in the following order: orange, blue, blue, orange, orange.

High performance liquid chromatography (HPLC)

Dissected fly heads were homogenized in a glass homogenizer in 200 ml 2 M NH_2OH (pH 6.8) and 600 ml methanol. After 10 minutes, we added 600 ml acetone, 250 ml diethyl ether and 250 ml petroleum benzene. To extract retinoids the samples were vortexed three times for 10 seconds, centrifuged (2000xg, 25°C, 15 seconds) and the organic phases were collected. The extraction was repeated two times with 400 ml petroleum benzene and the collected organic phases were

dried under a nitrogen stream. Lipophilic compounds were dissolved in 100 ml HPLC-solvent and subjected to quantitative HPLC analysis as described previously (Oberhauser et al., 2008). All steps were carried out under a dim red safety light.

Characterization of retinal degeneration by transmission electron microscopy

Dissected fly heads were fixed in glutaraldehyde and embedded in LR White resin as described (Porter et al., 1992). Thin sections (50 nm) prepared at a depth of 30 mm were examined using a Zeiss (Oberkochen) FEI Tecnai 12 transmission electron microscope. The images were acquired using a Gatan (Pleasanton) camera (model 794) and Gatan Digital Micrograph software and converted into tiff files.

Statistics

Unpaired Student's *t* -tests were used for quantification of Western blot data ($n \geq 3$). ANOVA was used for determining significant differences in rhabdomere

numbers. *p<0.05.

References

Berson DM (2007) Phototransduction in ganglion-cell photoreceptors. Pflugers Arch 454:849-855.

Brand AH, Perrimon N (1993) Targeted gene expression as a means of altering cell fates and generating dominant phenotypes. Development 118:401-415.

Dolph PJ, Ranganathan R, Colley NJ, Hardy RW, Socolich M, Zuker CS (1993) Arrestin function in inactivation of G protein-coupled receptor rhodopsin in vivo. Science 260:1910-1916.

Gong WJ, Golic KG (2003) Ends-out, or replacement, gene targeting in *Drosophila*. Proc Natl Acad Sci USA 100:2556-2561.

Hamdorf K (1979) The physiology of invertebrate visual pigment. In: Handbook of Sensory Physiology vol. VII/6A (Autrum H, ed), pp 145-224. Berlin: Springer-Verlag.

Hankins MW, Peirson SN, Foster RG (2008) Melanopsin: an exciting photopigment. Trends Neurosci 31:27-36.

Harris WA, Ready DF, Lipson ED, Hudspeth AJ, Stark WS (1977) Vitamin A deprivation and *Drosophila* photopigments. Nature 266:648-650.

Liden M, Tryggvason K, Eriksson U (2003) Structure and function of retinol dehydrogenases of the short chain dehydrogenase/reductase family. Mol Aspects Med 24:403-409.

Maeda A, Maeda T, Sun W, Zhang H, Baehr W, Palczewski K (2007) Redundant and unique roles of retinol dehydrogenases in the mouse retina. Proc Natl Acad Sci USA 104:19565-19570.

Oberhauser V, Voolstra O, Bangert A, von Lintig J, Vogt K (2008) NinaB combines carotenoid oxygenase and retinoid isomerase activity in a single polypeptide. Proc Natl Acad Sci USA 105:19000-19005.

Ozaki K, Nagatani H, Ozaki M, Tokunaga F (1993) Maturation of major Drosophila rhodopsin, ninaE, requires chromophore 3-hydroxyretinal. Neuron 10:1113-1119.

Palczewski K (2006) G protein-coupled receptor rhodopsin. Annu Rev Biochem 75:743-767.

Porter JA, Hicks JL, Williams DS, Montell C (1992) Differential localizations of and requirements for the two Drosophila *ninaC* kinase/myosins in photoreceptor cells. J Cell Biol 116:683-693.

Seki T, Isono K, Ozaki K, Tsukahara Y, Shibata-Katsuta Y, Ito M, Irie T, Katagiri M

(1998) The metabolic pathway of visual pigment chromophore formation in *Drosophila melanogaster*--all-*trans* (*3S*)-3-hydroxyretinal is formed from all-*trans* retinal via (*3R*)-3-hydroxyretinal in the dark. Eur J Biochem 257:522-527.

Travis GH, Golczak M, Moise AR, Palczewski K (2007) Diseases caused by defects in the visual cycle: retinoids as potential therapeutic agents. Annu Rev Pharmacol Toxicol 47:469-512.

von Lintig J, Dreher A, Kiefer C, Wernet MF, Vogt K (2001) Analysis of the blind *Drosophila* mutant *ninaB* identifies the gene encoding the key enzyme for vitamin A formation *in vivo*. Proc Natl Acad Sci USA 98:1130-1135.

Voolstra O, Oberhauser V, Sumser E, Meyer NE, Maguire ME, Huber A, von Lintig J (2010) NinaB is essential for *Drosophila* vision but induces retinal degeneration in opsin-deficient photoreceptors. J Biol Chem 285:2130-2139.

Wald G (1968) The molecular basis of visual excitation. Nature 219:800-807.

Walther RF, Pichaud F (2006) Immunofluorescent staining and imaging of the pupal and adult Drosophila visual system. Nat Protoc 1:2635-2642.

Wang X, Wang T, Jiao Y, von Lintig J, Montell C (2010) Requirement for an enzymatic visual cycle in *Drosophila*. Curr Biol 20:93-102.

Wes PD, Xu X-ZS, Li H-S, Chien F, Doberstein SK, Montell C (1999) Termination of phototransduction requires binding of the NINAC myosin III and the PDZ protein INAD. Nat Neurosci 2:447-453.

Xu H, Lee SJ, Suzuki E, Dugan KD, Stoddard A, Li HS, Chodosh LA, Montell C (2004) A lysosomal tetraspanin associated with retinal degeneration identified via a genome-wide screen. EMBO J 23:811-822.

Figure 1

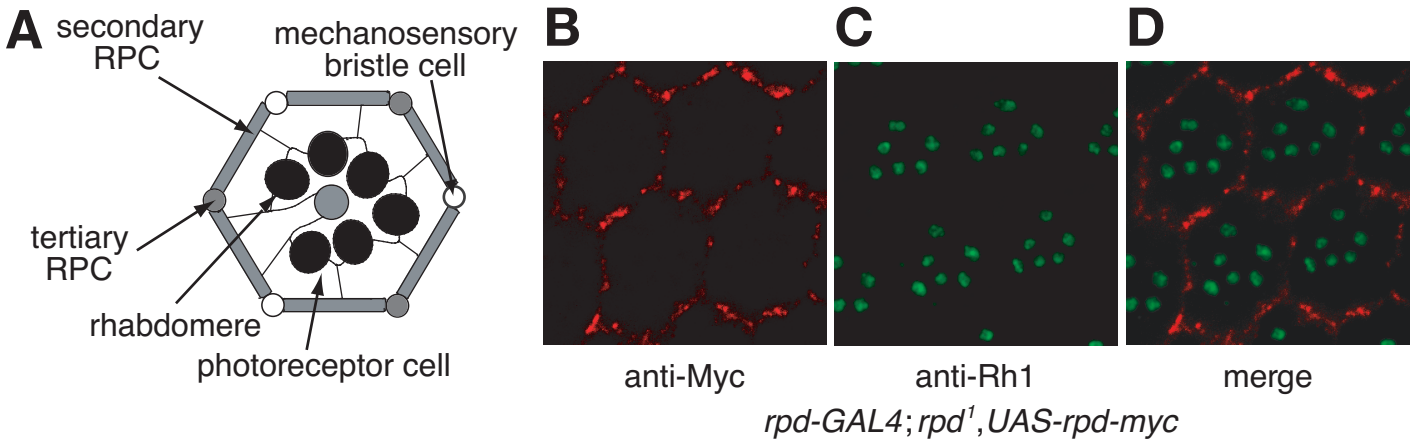
A
secondary RPC
mechanosensory bristle cell
tertiary RPC
rhabdomere
photoreceptor cell
B
C
D
anti-Myc
anti-Rh1
merge
rpd-GAL4;rpd1,UAS-rpd-myc
E
hours after puparium formation (APF)
adult (days)
0 24 40 45 50 60 65 70 80 85 90 95 <1 7 30
26
17
34
26
55
RPD
Rh1
Tub
F
wt (anti-RPD)
45 APF
G
rpd1 (anti-RPD)
45 APF

Figure Legends

Figure 1. Spatial and temporal expression of RDHB. ***A,*** Schematic diagram of a cross-sectional view of a single ommatidium from a *Drosophila* compound eye. ***B – D,*** Immunostaining of a 0.5 μm head section from an *rdhB -GAL4*;*rdhB*^{1}, *UAS-rdhB -myc* fly. ***B,*** Myc antibodies (red). ***C,*** Rhodopsin (Rh1) antibodies (green). ***D,*** Merged image. ***E,*** Developmental Western blots probed with antibodies to RDHB, Rh1 and tubulin (Tub). Samples were prepared from flies at the indicated pupal times and from adult flies of the indicated ages. ***F,G,*** Immunostaining of dissected pupae eyes (~45 hours after puparium formation) with rabbit anti-RDHB. ***F,*** wild-type. The arrows indicate labeling of tertiary pigment cells. ***G,*** *rdhB*^{1}.

Figure 2

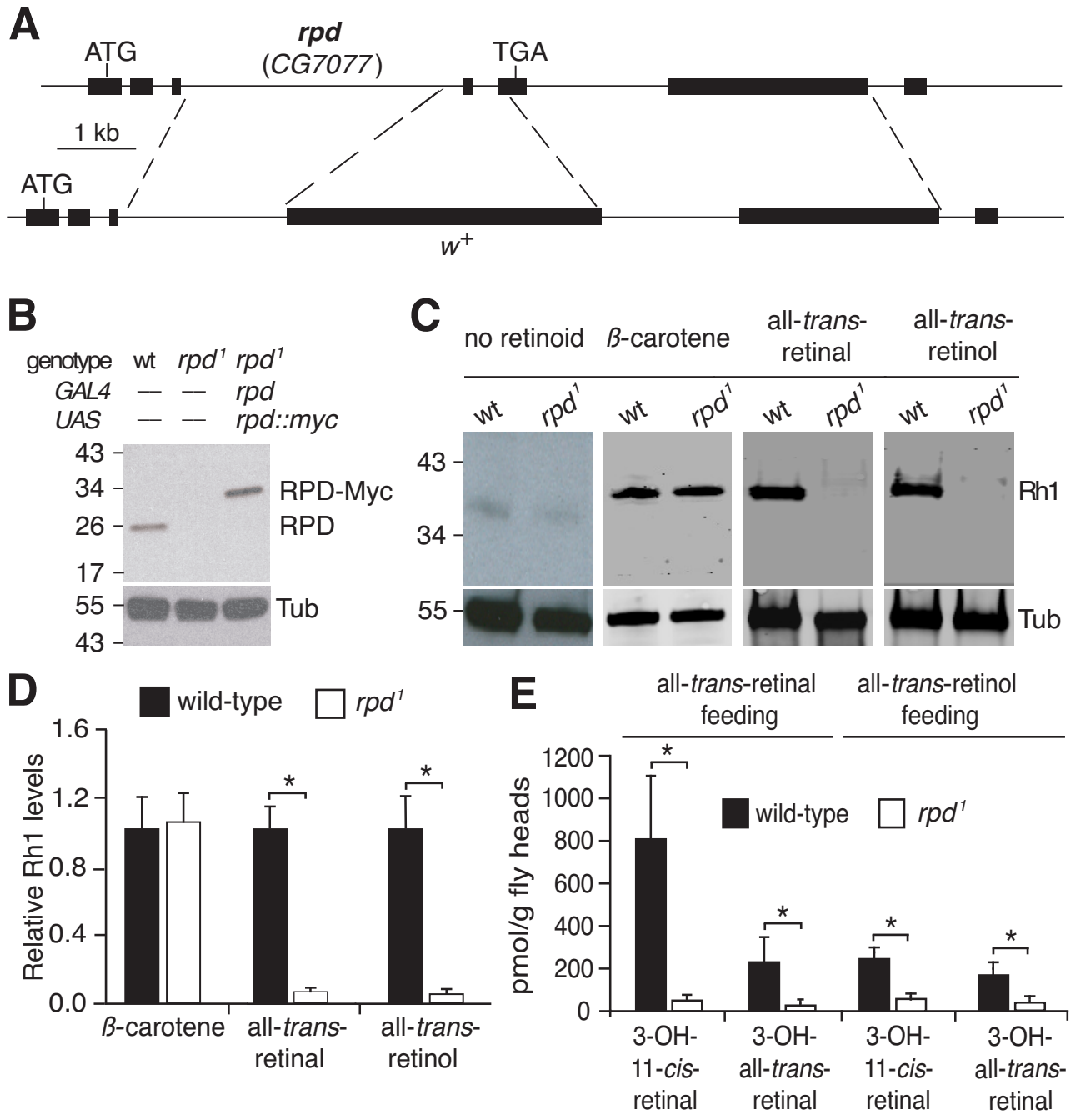
A
ATG
rpd
(CG7077)
TGA
1 kb
ATG
w+
B
genotype wt rpd1 rpd1
GAL4 — — rpd
UAS — — rpd::myc
43
34
26
17
55
43
RPD-Myc
RPD
Tub
C
no retinoid
ß-carotene
all-trans-retinal
all-trans-retinol
wt
rpd1
43
34
55
Rh1
Tub
D
wild-type
rpd1
Relative Rh1 levels
1.6
1.2
0.8
0.4
0.0
ß-carotene
all-trans-retinal
all-trans-retinol
E
all-trans-retinal feeding
all-trans-retinol feeding
pmol/g fly heads
1200
1000
800
600
400
200
0
wild-type
rpd1
3-OH-11-cis-retinal
3-OH-all-trans-retinal
3-OH-11-cis-retinal
3-OH-all-trans-retinal

Figure 2. Generation of *rdhB*^{1} and effects of mutation on chromophore and Rh1 production during the pupal period. ***A,*** Schematic illustration of the *rdhB* (*CG7077*) gene and generation of the *rdhB* knock-out (*rdhB*^{1}) by ends-out homologous recombination. ***B,*** Western blot containing head extracts from the indicated flies probed with anti-RDHB and reprobed with anti-Tubulin (Tub). ***C,*** Western blot of head extracts from ≤1 day-old wild-type and *rdhB*^{1}. The flies were raised from the 2nd instar larval stage on retinoid-free medium supplemented with 5 mM β-carotene or 500 μM all-*trans*-retinal or all-*trans*-retinol. The flies were kept under a 12 hour light/12 hour dark cycle. ***D,*** Quantification of Western blot results shown in *C*. n≥3. ***E,*** Decreased chromophore levels in *rdhB*^{1} flies fed all-*trans*-retinal or all-*trans*-retinol. The flies were ≤1 day-old and raised as indicated in *C*. n=3.The concentration of 3-OH-11-*cis*-retinal and 3-hydroxy-all-*trans*-retinal were measured by HPLC. Error bars represent $^{\pm}$SEMs. *p<0.05. Unpaired Student's *t*-tests.

Figure 3

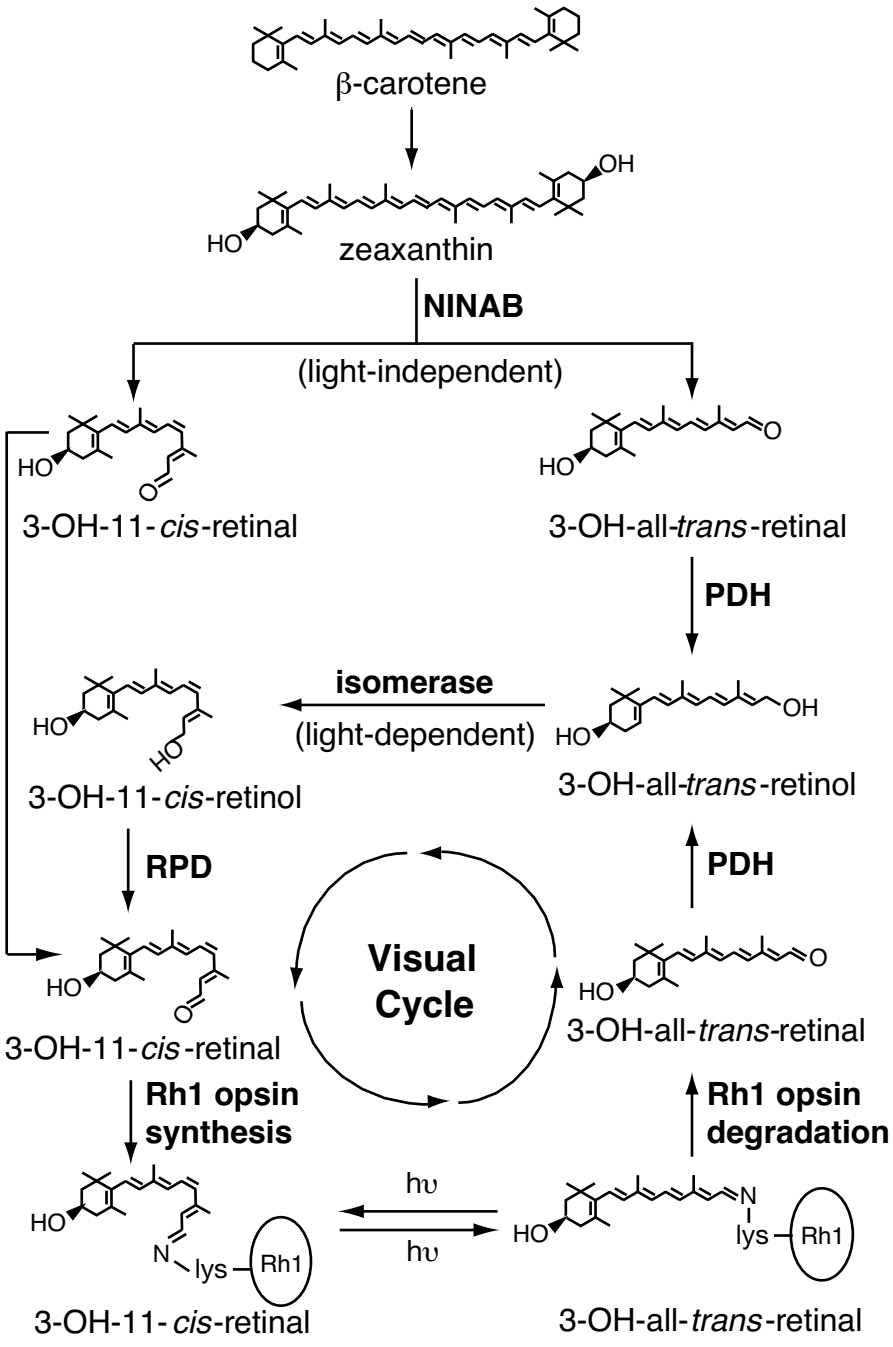
β-carotene
zeaxanthin
NINAB
(light-independent)
3-OH-11-*cis*-retinal
3-OH-all-*trans*-retinal
PDH
isomerase
(light-dependent)
3-OH-11-*cis*-retinol
3-OH-all-*trans*-retinol
RPD
PDH
Visual Cycle
3-OH-11-*cis*-retinal
3-OH-all-*trans*-retinal
Rh1 opsin synthesis
Rh1 opsin degradation
hυ
hυ
lys
Rh1
3-OH-11-*cis*-retinal
3-OH-all-*trans*-retinal

Figure 3. Proposed pathways for *de novo* synthesis of the chromophore and for the visual cycle. The proposed function for RDHB is indicated.

Figure 4

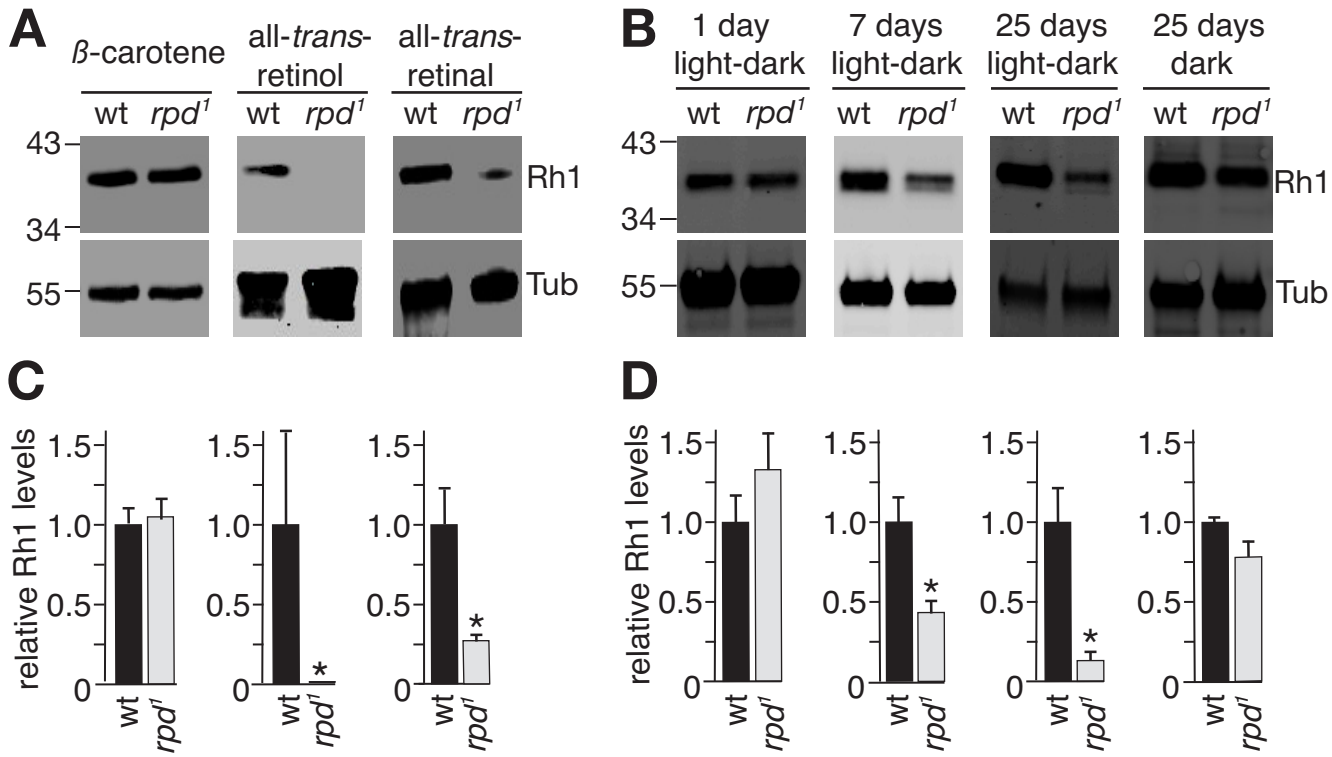
A
ß-carotene
all-trans-retinol
all-trans-retinal
wt
rpd1
43
34
55
Rh1
Tub
B
1 day light-dark
7 days light-dark
25 days light-dark
25 days dark
C
D
relative Rh1 levels
1.5
1.0
0.5
0
*

Figure 4. RDHB was required to maintain Rh1 levels in adult flies. ***A,*** Western blot of head extracts from 2-3 day old wild-type and *rdhB*^{1} flies. The flies were raised on retinoid-free medium during the larval stages. Newly eclosed flies were maintained on retinoid-free medium supplemented with 5 mM β-carotene, 500 μM all-*trans*-retinal or all-*trans*-retinol or. The flies were kept under a 12 hour light/12 hour dark cycle for 48 hours before performing the Western blots. ***B,*** Western blot of head extracts obtained from wild-type and *rdhB*^{1} flies of the indicated ages, and under the indicated light conditions. The flies were raised on normal retinoid containing fly food (corn meal and molasses) and kept under a 12 hour light/12 hour dark cycle. ***C-D,*** Quantification of Western blot data shown in *A* and *B*. Error bars represent $^{\pm}$SEMs. $^{*}p<0.05$. Unpaired Student's *t* test. n≥3.

Figure 5

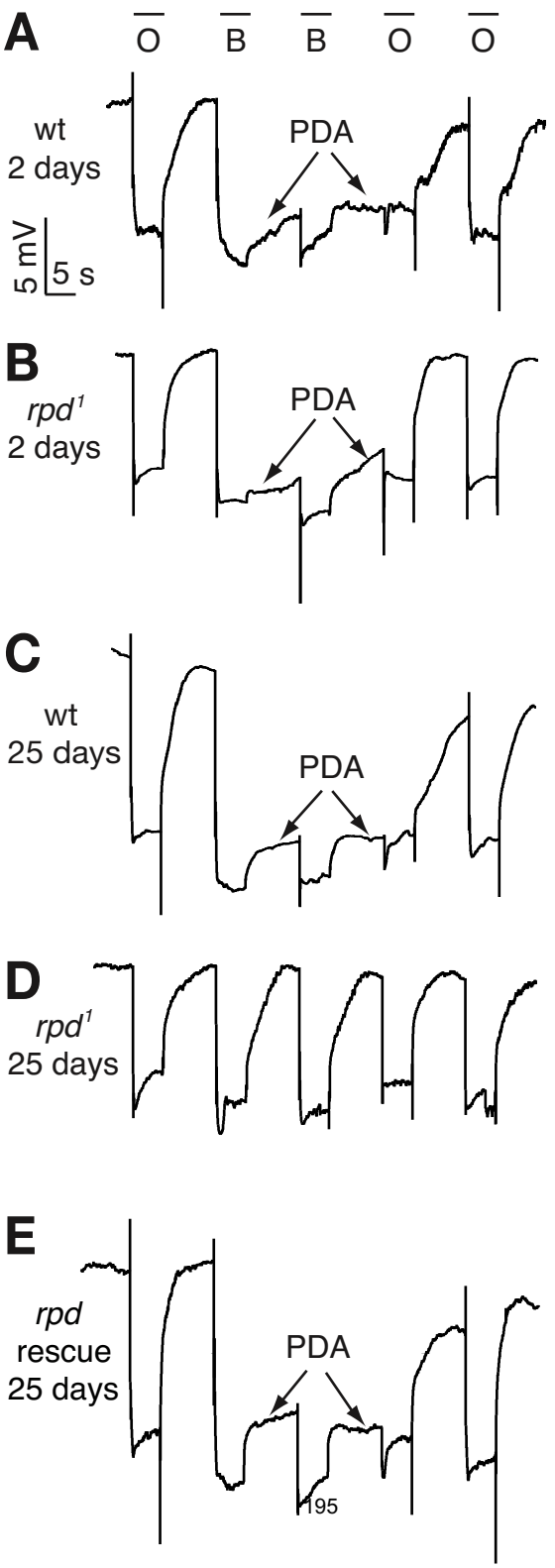
A
O
B
B
O
O
wt
2 days
PDA
5 mV
5 s
B
rpd1
2 days
PDA
C
wt
25 days
PDA
D
rpd1
25 days
E
rpd
rescue
25 days
PDA

Figure 5. Testing for a PDA in *rdhB*^{1} flies by performing ERG recordings. Flies of the indicated genotypes and ages were dark-adapted for 1 minute and subsequently exposed to 5 second pulses of orange (580 nm) light (O) or blue (480 nm) light (B) interspersed by 7 seconds. Arrows indicate the PDAs induced by blue light. The PDAs were terminated by orange light. ***A,*** Wild-type (wt), 2 days old. ***B,*** *rdhB*^{1}, 2 days old. ***C,*** wt, 25 days old. ***D,*** *rdhB*^{1}, 25 days old. ***E,*** *rdhB*^{1}, 25-day old, expressing a *rdhB*$^{+}$ transgene: *rdhB -gal4*;*rdhB*^{1}, *UAS-rdhB -myc*.

Figure 6

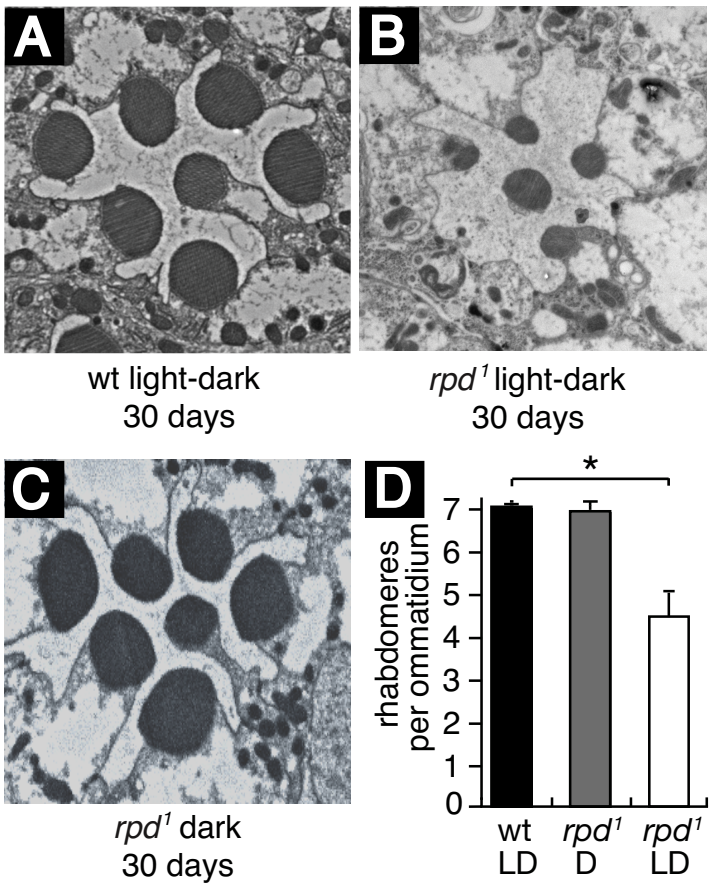
A
B
wt light-dark
30 days
rpd1 light-dark
30 days
C
D
rpd1 dark
30 days
*
rhabdomeres
per ommatidium
0
1
2
3
4
5
6
7
wt
LD
rpd1
D
rpd1
LD

Figure 6. Transmission EM images of cross-sections from adult retinas. The age in days and the light conditions are indicated. The light-dark cycles were 12 hours each. ***A,*** wt, 30 days under light/dark cycles. ***B,*** *rdhB*^{1}, 30 days under a light/dark cycle. ***C,*** *rdhB*^{1}, 30 days under constant darkness. ***D,*** Quantification of the numbers of rhabdomeres per ommatidia based on analyses of thin EM sections after 30 days under a light-dark cycle, or in the dark. 60 ommatidia from 3 flies were counted for each condition. Error bars represent $^{\pm}$SEMs. *p<0.05. ANOVA.

CURRICULUM VITAE FOR Ph.D. CANDIDATES

The Johns Hopkins University School of Medicine

Name: Jinfei Ni **Date: April 25, 2017**

Ph.D.expected 2017

Program in Biological Chemistry The Johns Hopkins University School of Medicine, Baltimore, MD. Mentor Craig Montell Ph.D.

M.S. 2009 Biomedical Sciences

University of Connecticut Health Center, Farmington, CT.

B.S. 2005 Biological Sciences

School of Life Sciences, Fudan University, Shanghai, China.

Other Academic Experience

2013-2016 Associate faculty member. Faculty 1000.

2012 Teaching assistant for medical biochemistry. The Johns Hopkins University School of Medicine, Baltimore, MD.

Publications

Ni JD, Baik L, Holmes T and Montell C. A rhodopsin in the brain functions in circadian photoentrainment in *Drosophila*. *Nature* (in press).

Ni JD, Ogunmowo TH, Hackbart H and Montell C. Coordinated activity of sleep and arousal neurons for stabilizing sleep/wake states in Drosophila. In preparation.

Akitake B, Ren Q, Boiko N, **Ni J**, Sokabe T, Stockand JD, Eaton BA, Montell C. Coordination and fine motor control depend on *Drosophila* TRPγ. *Nat. Commun.* 6(7288), 2015.

Li Z, **Ni JD**, Huang J, Montell C. Requirement for *Drosophila* SNMP1 for rapid activation and termination of pheromone-induced activity. *PLoS Genet.* 10(9), 2014.

Zhang YV, **Ni J**, Montell C. The molecular basis for attractive salt-taste coding in *Drosophila*. *Science* 340, 1334-8, 2013.

Wang X*, Wang T*, **Ni JD***, von Lintig J, Montell C. The *Drosophila* visual

cycle and *de novo* chromophore synthesis depends on *rdhB*. *J Neurosci*. 32, 3485-91, 2012. * Co-first authorship.

Conference presentation

Poster presentation: A sleep-promoting peptidergic network in *Drosophila*. Hypothalamic Circuits for Control of Survival Behaviors. Janelia conference 2015.